Molecular and Functional Analysis of Resistance Expansion and Suppression for Alleles of the Powdery Mildew Resistance Gene *Pm3* in Wheat

---

Dissertation

zur

Erlangung der naturwissenschaftlichen Doktorwürde

(Dr. sc. nat.)

vorgelegt der

Mathematisch-naturwissenschaftlichen Fakultät

der

Universität Zürich

von

Daniel Fabian Stirnweis

aus

Deutschland

Promotionskomitee

Prof. Dr. Beat Keller (Vorsitz und Leitung der Dissertation)

Prof. Dr. Christoph Ringli

Prof. Dr. Wilhelm Gruissem

Zürich, 2014

Contents

Abstract

Developing high yielding and high quality varieties with broad-spectrum and durable disease resistance is the ultimate goal of crop breeding. Resistance (*R*) genes encoding proteins with nucleotide-binding site (NBS) and leucine-rich repeat (LRR) domains provide high levels of resistance, but this type of *R* genes usually only confers resistance to a subset of pathogen races. In addition, major *R*-gene resistance is often rapidly overcome by newly adapted pathogen races when employed in agriculture. In this thesis the allelic series of the NBS-LRR-encoding powdery-mildew resistance gene *Pm3* of wheat was analyzed in two projects.

In the first project, *Pm3* alleles with a broad and a narrow resistance spectrum were investigated. It was found that *Pm3* alleles with a broad resistance spectrum can induce a fast and intense hypersensitive response (HR) in a *Nicotiana* transient-expression system and this activity could be attributed to two particular amino acids in the ARC2 subdomain of the NBS. The combined substitution of these amino acids in narrow-spectrum PM3 proteins enhanced their capacity to induce an HR in *Nicotiana benthamiana*, and it was found that these substitutions also enlarge the resistance spectrum of the *Pm3f* allele in wheat. Using the rice gene *Bph14*, it was confirmed that the region carrying the two relevant amino acids also plays a role in the HR regulation of another coiled-coil NBS-LRR resistance protein. These results improve the mechanistic understanding of NBS-LRR-protein function and suggest an approach to extend the effectiveness of resistance genes via minimal targeted modifications in the NBS domain.

In the second project, the pyramidization of alleles, a recommended strategy for more durable resistance, was investigated for *Pm3*. Here, a molecular mechanism was found which can negatively interfere with the allele-pyramiding approach. It is shown that pairwise combinations of different alleles in F1 hybrids and stacked transgenic wheat lines can result in suppression of *Pm3*-based resistance. This effect is independent of the genetic background and occurs at the post-translational level. Using a transient-expression system in *N. benthamiana*, the LRR domain was identified as the suppression-conferring domain. The results of this study suggest that the expression of closely related NBS-LRR resistance genes or alleles in the same genotype can lead to dominant-negative interactions. These findings provide a molecular explanation for frequently observed limitations in crop breeding, especially with polyploid species.

Zusammenfassung

Die Entwicklung von ertragreichen und qualitativ hochwertigen Sorten mit breitem Resistenzspektrum und dauerhaften Resistenzeigenschaften ist das ultimative Ziel der Nutzpflanzenzüchtung. Resistenzgene (*R*-Gene) welche für Proteine mit Nukleotidbindestelle- (NBS) und Leucin-reiche-Repeat (LRR)-Domäne kodieren, bieten ein hohes Mass an Resistenz, allerdings verleihen *R*-Gene dieser Art normalerweise nur Resistenz gegenüber einem Teil der Pathogenrassen. Wenn sie in der Landwirtschaft Verwendung findet, wird Hauptgenresistenz außerdem oft schnell von neuangepassten Pathogenrassen durchbrochen. In der vorliegenden Arbeit wurde die allelische Serie des NBS-LRR-kodierenden Mehltauresistenzgens *Pm3* aus Weizen innerhalb zweier Projekte analysiert.

Im Rahmen des ersten Projekts wurden *Pm3*-Allele mit einem breiten, beziehungsweise engen Resistenzspektrum untersucht. Es wurde herausgefunden, dass *Pm3*-Allele mit einem breiten Resistenzspektrum in einem transienten Expressionssystem in *Nicotiana* eine schnelle und intensive hypersensitive Antwort (HR) induzieren können und diese Aktivität konnte zwei speziellen Aminosäuren in der ARC2-Subdomäne der NBS zugerechnet werden. Durch den kombinierten Austausch dieser beiden Aminosäuren in einem PM3-Protein mit engem Resistenzspektrum konnte dessen Kapazität zur HR-Induktion in *Nicotiana benthamiana* erhöht werden und desweiteren wurde herausgefunden, dass diese Austausche auch das Resistenzspektrum des *Pm3f*-Allels in Weizen erweitern. Unter Verwendung des Reisgens *Bph14* wurde bestätigt, dass die Region, welche die beiden relevanten Aminosäurenbeinhaltet, auch bei anderen „Coiled-coil“ NBS-LRR Resistenzproteinen in der HR-Regulation eine Rolle spielt. Diese Resultate verbessern das mechanistische Verständnis über die Funktionsweise von NBS-LRR-Proteinen und sie schlagen einen Ansatz zur Effektivitätserweiterung von Resistenzgenen mittels minimaler, gezielter Modifikationen in der NBS-Domäne vor.

Im Rahmen des zweiten Projekts wurde die Pyramidisierung von Allelen, eine empfohlene Strategie zur Erzielung einer dauerhafteren Resistenz, für *Pm3* untersucht. Hierbei wurde ein molekularer Mechanismus gefunden, der negativ mit dem Allelpyramidisierungsansatz interferieren kann. Es wird gezeigt, dass paarweise Kombinationen von verschiedenen Allelen in F1-Hybriden und gestapelten transgenen Weizenlinien in der Suppression von *Pm3*-basierter Resistenz resultieren können. Dieser Effekt ist unabhängig vom genetischen Hintergrund und findet auf post-translationaler Ebene statt. Unter Verwendung eines transienten Expressionssystems in *N. benthamiana* wurde die LRR-Domäne als suppressionsvermittelnde Domäne identifiziert. Die Resultate aus dieser Studie legen nahe, dass die Expression von nahe verwandten NBS-LRR-Resistenzgenen oder -allelen im selben

Genotyp zu dominant-negativen Interaktionen führen kann. Diese Erkenntnisse liefern eine molekulare Erklärung für häufig beobachtete Limitierungen im Bereich der Nutzpflanzenzüchtung, speziell bei polyploiden Spezies.

1 General introduction

1.1 The plant immune system

Plants are primary producers and as such they represent an attractive energy source for insects, nematodes, microbial pathogens and viruses, all seeking access to the plant`s nutrients for their proliferation. To establish infestation these potentially pathogenic organisms have to overcome several barriers preventing successful penetration of plant tissues and cells. These include preformed chemical and physical barriers like trichomes, closed stomata, the cuticle wax layer, or the lignified cell wall. To counteract harmful organisms that are able to break these initial barriers plants have evolved a cell-autonomous innate immunity system. This disease resistance system relies on the detection of non-self molecules by immune receptors and the subsequent activation of immune responses preventing the pathogen entry or spread. These resistance reactions include the fortification of the cell wall by callose deposition, the formation of reactive oxygen species, the release of antimicrobial or insecticidal compounds, or the induction of localized cell death.

Current scientific consensus is that plant non-adaptive immunity systems are mainly based on two interconnected forms of resistance mechanisms. The first layer relies on cell-surface-localized transmembrane receptors, referred to as pattern recognition receptors (PRRs). They are responsible for the detection of pathogen-associated molecular patterns (PAMPs) conserved among multiple classes of pathogens (e.g., flagellin, chitin, bacterial elongation factors), or damage-associated molecular patterns (DAMPs) linked to enzymatic activities endangering the plant-cell integrity (Boller and Felix 2009). Accordingly, resistance conferred by PRRs is referred to as PAMP-triggered immunity, or PTI. This system prevents the colonization of the host plants by the majority of attacking microbes. It is evolutionarily ancient (Boller and Felix 2009; Thomma et al. 2011; Lopez-Gomez et al. 2012). Pathogens successfully invading plants have to avoid recognition by PRRs or suppress the PTI activity and signaling. In addition, they eventually have to manipulate the host plant to efficiently gain access to its nutrients. For all these purposes pathogens evolved specific mechanisms involving so called ‘effector’ proteins (Hogenhout et al. 2009) and small RNAs (Weiberg et al. 2013) that collectively enable a successful proliferation on the host plants. During host-pathogen coevolution plants evolved a second layer of immunity against pathogens that can escape the basal PTI. Here, the resistance mechanism usually relies on the detection of specific elicitor or effector proteins from the pathogen by highly-specific resistance (R) proteins and, hence, it is called effector-triggered immunity (ETI). The genetic loci of the recognized gene products are often polymorphic between different pathogen strains

displaying either immunity-activating avirulent (*Avr*) variants, or non-activating virulent (*avr*) or missing variants. Consequently, *R*-gene mediated ETI is often race-specific and a single R-gene is only effective towards a subset of the pathogen population. In most cases, the resistance level provided by R proteins against avirulent strains is very high, leading to complete resistance. ETI is frequently associated with a hypersensitive response (HR), a form of programmed cell death and a characteristic resistance reaction especially against biotrophic pathogens.

1.2 Structure and function of NB-LRR resistance proteins

Among the R proteins molecularly identified to date the majority are nucleotide-binding-site leucine-rich repeat domain-containing proteins that belong to a subgroup within the STAND (signal transduction ATPases with numerous domains) protein family. In this thesis the abbreviations NB-LRR, NBS-LRR, or NLR will be used redundantly for these nucleotide-binding-site- and leucine-rich repeat-containing proteins. Almost all of these R proteins can be categorized into two major classes depending on the presence of an N-terminal Toll/interleukin-1 receptor (TIR) domain or a domain with a coiled-coil (CC) structure. The TIR class is absent in grasses (Pan et al. 2000; Collier et al. 2011).

1.2.1 The N-terminal TIR or CC domain

The N-terminal TIR or CC domain is proposed to be the main platform for the activation of downstream signaling components. This conclusion is based on the observation that the expression of these domains alone or with only 39-45 extra amino acids can trigger an HR. This was demonstrated for the TIR domains of the resistance proteins RPS4, RPP1, N, AT4G19530.1, and L2/6/7/10 (Frost et al. 2004; Weaver et al. 2006; Swiderski et al. 2009; Krasileva et al. 2010; Bernoux et al. 2011b). Maekawa and associates (2011) showed HR induction by transient expression of only the CC domain of MLA10 in *N. benthamiana*. Similar experiments with the CC domains of the NB-LRR resistance proteins RPS2, RPS5, RPM1 I2, R3a, Bs2, and RB did not result in cell death induction (Tao et al. 2000; Ade et al. 2007; Tornero et al. 2002; Collier et al. 2011). Intermolecular interactions of the TIR or CC domains with numerous potential guarded host or downstream signaling proteins have been shown (e.g., Mackey et al. 2002; Ade et al. 2007; Shen et al. 2007; Sacco et al. 2007; Tameling and Baulcombe 2007; Caplan et al. 2008; Zhu et al. 2010; Chang et al. 2013). Besides, also intramolecular interactions with the NB-ARC or LRR domains have also been demonstrated (Moffett et al. 2002). On the one hand, these interactions have been implicated

in the inactivation of the immune receptors in the absence the Avr protein (Moffett et al. 2002). On the other hand, transcomplementation experiment involving separated CC and NB-LRR fragments have shown functional importance of these interactions for the immune response activation (Moffett et al. 2002; Rairdan et al. 2008). In a large subset of CC-NB-LRR resistance proteins a conserved EDVID motif can be found in the CC domain (Bai et al. 2002; Rairdan et al. 2008). This motif has been shown to be involved in intramolecular interactions with the NB-LRR domains and these interactions in turn are essential for the resistance function of the full-length *Potato virus X* resistance protein Rx1 (Rairdan et al. 2008). It is also required for the HR activity of the full-length powdery mildew resistance protein MLA10, but not for the HR activity of its separated CC domain (Bai et al. 2012), indicating an important role of this motif in the CC-NB-LRR protein activation mechanism, but not in downstream signaling processes.

The crystal structure of the TIR domain of the flax rust resistance protein L6 and the CC domain of MLA10 have recently been solved (Bernoux et al. 2011b; Maekawa et al. 2011). Both crystal structures revealed interfaces for self-association implicating that homodimerization of these domains might be a common prerequisite for the activation of NB-LRR immune receptors. Additional experimental data for these and other NB-LRR resistance proteins support this hypothesis (Mestre and Baulcombe 2006; Ade et al. 2007; Gutierrez et al. 2010; Bernoux et al. 2011b; Maekawa et al. 2011).

1.2.2 NB-ARC – the 'molecular switch' domain

The central nucleotide-binding domain of plant NB-LRR resistance proteins shows regions of homology to metazoan apoptosis regulating proteins: the human apoptotic protease-activating factor 1 (APAF-1) and *Caenorhabditis elegans* Death-4 (CED-4). Accordingly, this domain is often referred to as NB-ARC (nucleotide-binding adaptor shared by APAF-1, certain *R*-gene products and CED-4) (van der Biezen and Jones 1998). Crystal structures of NB-ARC domains from plant R proteins are not available, but structural models can be created based on crystal structures of APAF-1 and CED-4 (e.g., van Ooijen et al. 2008b, 2008a; Brunner et al. 2010; Slootweg et al. 2013). The NB-ARC domain is formed by three subdomains, the nucleotide binding (NB) module, the ARC1 and ARC2 subdomains. All three are involved in the formation of a central nucleotide binding pocket with hydrolytic activity. Many conserved sequence motifs like the hhGRExE, P-loop (Walker A), Walker B, RNBS-A to –D, GLPL, or MHD motif are present in the NB-ARC. Mutations of these conserved sequences frequently lead to loss-of-function phenotypes or constitutively active (autoactivated) proteins (van Ooijen et al. 2008b; Brunner et al. 2010). Binding assays

revealed that inactive NB-LRR proteins typically bind ADP, whereas the active state as in autoactivated variants is usually associated with the binding of ATP (Tameling et al. 2002; Ueda et al. 2006; Williams et al. 2011). Therefore, nucleotide exchange and ATP hydrolysis are thought to be crucial steps to switch NB-LRR proteins "on" or back "off". Models of ADP- and ATP-bound NB-ARC domains indicate major structural rearrangements between the two states (Takken and Goverse 2012).

Rairdan and associates (2008) showed that the overexpression of the NB subdomain of Rx1 fused to green-fluorescent protein (GFP) is sufficient to initiate cell death in *N. benthamiana*. A possible interpretation of these data is that not the CC domain, but the NB subdomain is responsible for the signal transduction to downstream components. Transcomplementation, coimmunoprecipitation and domain swap experiments demonstrated that functional and physical interactions of the NB-ARC with the N-terminal and LRR domains exist and that they are important for the proper activity regulation of NB-LRR resistance proteins (Moffett et al. 2002; Rairdan and Moffett 2006; van Ooijen et al. 2008a; Slootweg et al. 2013). A structural model for the docking between the Rx1/Gpa2 NB-ARC and LRR domains was recently published (Slootweg et al. 2013).

1.2.3 The C-terminal LRR domain

Leucine-rich repeat domains can be found in a vast number of prokaryotic, eukaryotic, and viral proteins. The repeat motif provides "a versatile structural framework for the formation of protein–protein interactions" (Kobe and Kajava 2001). Therefore, the LRR domain seems ideally suited for the direct recognition of Avr proteins. Sequence patterns of diversifying selection (McDowell et al. 1998; Meyers et al. 1998; Ellis et al. 2000) and gene-for-gene specific interactions of *L5*/*L6*- and *Rpp1*-LRR-gene products with the corresponding Avr proteins (Dodds et al. 2006; Krasileva et al. 2010; Steinbrenner et al. 2012) support this model. For multiple NB-LRR R proteins intramolecular interactions of the LRR domain with the N-terminal domains have been shown (Moffett et al. 2002; Rairdan and Moffett 2006; Leister et al. 2005; Ueda et al. 2006; van Ooijen et al. 2008a; Slootweg et al. 2013). Here, the LRR domain displays a bifunctional role: keeping the protein inactive in the absence of an Avr protein (Rairdan and Moffett 2006; Ade et al. 2007; Tameling et al. 2010; Qi et al. 2012; Slootweg et al. 2013) and contributing to the activation of immune receptor signaling after non-self molecule recognition (Moffett et al. 2002; Leister et al. 2005; van Ooijen et al. 2008a; Slootweg et al. 2013).

Although many LRR crystal structures have been solved, no LRR crystal structure of a plant NB-LRR R protein is available. However, well-understood structural principles and homology modeling allow inferring structural features of LRR domains (Bella et al. 2008): The overall structure is a horseshoe or curved solenoid where the "concave side of the LRR domains is defined by a parallel β-sheet to which each LRR contributes one strand" (Bella et al. 2008). Solvent exposed residues at the concave side are generally thought to form the ligand-binding surface.

1.2.4 Models for NB-LRR resistance protein activation

There are mostly three major concepts of how NB-LRR-type R proteins may perceive the presence of an Avr protein (van der Hoorn and Kamoun 2008). The simplest concept is based on direct R-Avr-protein interactions, potentially mediated by the LRR domain. Experimental data suggests this mechanism for flax L5/L6-AvrL5/6/7 and *Arabidopsis thaliana* RPP1-ATR1 interactions (Dodds et al. 2006; Krasileva et al. 2010). Patterns of diversifying selection in the LRR domain are considered as indicative for this mode of action. The concept of indirect Avr protein recognition implicates that the R protein surveys the integrity or modification status of another host protein. By sensing Avr protein-induced alterations of the guarded host protein the R protein may get activated and induces an immune response. If the guarded host protein has a function in host defense or susceptibility, the concept is called the guard model. If the guarded host protein has no direct function in host defense or susceptibility but rather mimics another effector-target protein, the concept is called the decoy model. Both these concepts provide an explanation of how a limited number of R proteins can sense the abundance of an exceeding number of different avirulence molecules from all sorts of potential pathogens. It is not easy to experimentally distinguish between the two cases and, hence, a categorization is not straight forward. Prominent examples for indirect modes of Avr recognition are the RIN4/RPS2/RPM1 system in *A. thaliana* (Mackey et al. 2002; Luo et al. 2009) or the Pto/Prf complex in tomato (*Solanum lycopersicum*)(Mucyn et al. 2006; Gutierrez et al. 2010; Oh and Martin 2011). As a consequence of the initial recognition event described above, conformational changes could lead to NB-LRR oligomerization, nucleotide exchange, translocation, and other critical downstream events in triggering immunity (Steinbrenner et al. 2012).

Besides the above introduced concepts, there are more and more indications that the cooperative action of two different NB-LRR proteins might be a widespread mechanism for NB-LRR resistance activation, but mechanistic details remain elusive (Ashikawa et al. 2008; Loutre et al. 2009; Narusaka et al. 2009; Cesari et al. 2013; Eitas and Dangl 2010). In

addition, the subcellular localization of R proteins was also shown to be important for their functionality and it was demonstrated that HR and other resistance reactions can be uncoupled by forced subcellular protein localizations (Bernoux et al. 2011a; Qi and Innes 2013 and references therein).

1.3 Sustainable employment of major resistance genes in crop plants

NB-LRR R proteins usually mediate a high level of resistance and, therefore, are an attractive source to be employed in crop breeding as major resistance genes. But the use of *R*-gene based resistance in crop plants may have the drawback of rapid loss of effectiveness. This is especially true for genetically uniform agricultural ecosystems that create a high selection pressure on pathogen populations (McDonald and Linde 2002; Stukenbrock and McDonald 2008). The breakdown of resistance of wheat against Ug99 races of stem rust (*Puccinia graminis* f. sp. *tritici*) is a recent prominent example (Singh et al. 2011).

The sustainable and more durable employment of major resistance genes in crops is an important task for reliable food production, especially since plant diseases pose an ever higher risk for a fast growing world population (Strange and Scott 2005). Good agricultural practices like crop rotation systems and adapted planting regimes as well as resistance management including virulence screenings in pathogen populations and selected pesticide applications are general measures to prevent or slow down resistance breakdowns. The sowing of cultivar mixtures/multilines (Mundt 2002), the transfer of *R* genes to other crop species (Wulff et al. 2011), or the design of new resistance genes (Dangl et al. 2013) are strategies for improved genetic resistance on the plant side. Resistance gene pyramiding, the combination of different *R* genes in a single genotype, is another widely recommended strategy for more durable pathogen resistance (Dangl et al. 2013).

1.3.1 Resistance-gene pyramiding

The pyramidization or stacking of disease resistance genes is widely considered a valid strategy to enlarge the resistance spectrum and to make *R*-gene-mediated resistance more durable. The first aspect relies on the additivity of the resistance spectra of different race-specific R proteins. The desired enhancement of durability depends on the redundancy in the recognition of the pathogen (Roush 1998; Manyangarirwa et al. 2006): If the same pathogen was detected by multiple different R proteins that detect independent Avr proteins, in theory, the pathogen would have to mutate all matching Avr proteins simultaneously since the

adaptation of only a single Avr protein would not lead to a gain of virulence (see Introductory Figure 1). This simultaneous mutation event is considered very unlikely.

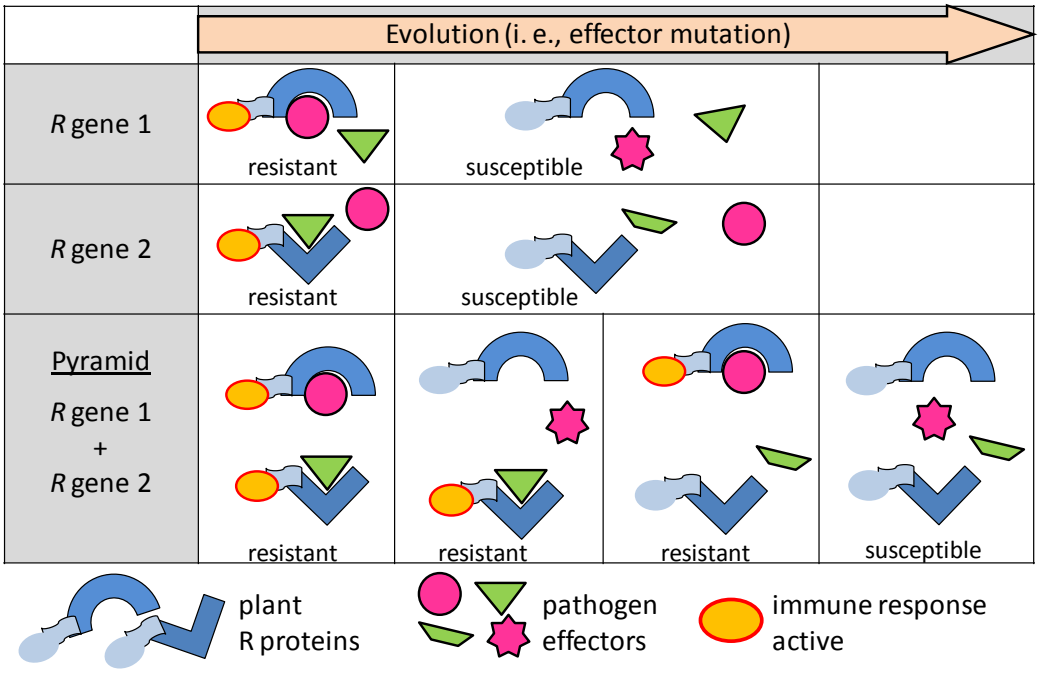

Introductory Figure 1. Theoretical concept for the enhancement of the resistance durability through *R* gene pyramiding: At the beginning of the evolutionary process the R proteins 1 and 2 detect different effectors from the same pathogen. Whereas the mutation of only one recognized effector is sufficient for the pathogen to overcome the resistance mediated by a single R protein, it would be necessary to mutate both recognized effectors simultaneously to overcome the resistance of the pyramided plants. This event is much more unlikely and, hence, pyramiding leads to an expanded resistance durability.

As an alternative the pathogen could for example evolve a new effector able to suppress the resistance signaling of all relevant immune sensors. This adaptation becomes less likely if R proteins with diverse resistance pathways are combined. The pyramiding strategy would be less effective if only a subset of races of the pathogen population was redundantly detected. It would also be diminished if plants expressing only one of the pyramided *R* genes were cultivated in parallel to the pyramided plants. Including all these recommendations, an optimal pyramiding strategy for R proteins would be the combination of diverse, exclusively employed, highly efficient, broad-spectrum R proteins directed against core effectors of the pathogen that are potentially essential for virulence. Integration of all pyramided genes in a single genetic locus could prevent recombination between the genes and, thereby, prevent the occurrence of plants with only a single *R* gene. The pyramiding strategy is especially recommended as disease control strategy against pathogen populations with low gene/genotype diversity and high gene/genotype flow (McDonald and Linde 2002).

With more and more cloned *R* genes the pyramiding strategy becomes more feasible since the stacking can be monitored with genetic markers or the genes can be transformed in parallel. A prerequisite for the success of gene pyramiding is the functional compatibility between the stacked genes.

1.3.2 Allele pyramiding

While the *R*-gene pyramiding approach relies on the diversity of different *R* genes, allele pyramiding, the combination of multiple alleles of the same gene in one genotype, makes use of the allelic diversity of *R* genes. In contrast to the gene stacking, the combination of different alleles in a single genotype by classical genetics is only possible in a genetically heterozygous situation, for example in F1 hybrids. Transgenic techniques now enable the genetically stable combination of different allelic variants of a gene.

The basic concept and constraints for the allele pyramiding approach remain the same as for the gene-pyramiding strategy. It seems likely that different alleles of the same *R* gene are responsible for the recognition of different alleles of the same *Avr* gene. In terms of durability this would make the allele pyramiding less effective since the recognition of different pathogen races might not always be redundant and the pathogen might be able to escape recognition by multiple allele by mutating just one gene. Nevertheless, it was already shown for alleles of NB-LRR *R* genes that they recognize different *Avr* genes (e.g., eleven alleles of flax rust resistance gene *L* have eight corresponding *Avr* loci in the genetic map of *Melampsora lini*, Dodds et al. 2004). The presumably common resistance pathway shared by different allelic *R*-gene products is potentially an unfavourable aspect for the durability of such allele pyramids.

1.4 The wheat – powdery mildew pathosystem

1.4.1 Wheat – the host

Wheat (*Triticum* spp.) is one the most important crops for human food and animal feed production. It was harvested worldwide from over 215 million hectares yielding more than 670 million tonnes in 2012 (www.faostat.fao.org). Wheat, like many major crop species (maize, rice, sugarcane, sorghum, millet, rye, and barley), belongs to the *Poaceae* family and therein is part of the *Triticeae* tribe. “For diploid einkorn and tetraploid durum wheat, a single domestication event has likely occurred in the Karacadag Mountains, Turkey” (Charmet 2011) more than 10’000 years ago. Bread wheat (*Triticum aestivum*) - a self-fertile species -

first appeared around 8'000 years ago after a cross between tetraploid durum and diploid *Aegilops tauschii*. It has an allohexaploid genome (2n=6x=42, AABBDD) with the A- and B-genomes contributed by the progenitor *Triticum turgidum* ssp *dicoccum* (or *T. dicoccum*) and the D-genome from diploid *Ae. tauschii* (Charmet 2011). The wheat genome is highly repetitive and has an approximate size of 17 Gb; more than five times larger than the human genome. The International Wheat Genome Sequencing Consortium is currently working on a high quality annotated, physical map-based genome sequence (www.wheatgenome.org).

Due to the complex genetic conditions only relatively few genes have been cloned from hexaploid wheat, among them only four genes involved in powdery mildew resistance: The two NB-LRR-encoding genes *Pm3* (Yahiaoui et al. 2004) and its ortholog *Pm8* from the 1BL.1RS wheat-rye-translocation (Hurni et al. 2013), as well as *Lr34/Yr18/Pm38* (Krattinger et al. 2009), and a "key gene" from the *Pm21* locus transferred from *Haynaldia villosa* to bread wheat (Cao et al. 2011). At least 43 loci for resistance to powdery mildew (Pm) have been genetically described in the wheat gene pool so far (http://www.shigen.nig.ac.jp/wheat/komugi/genes/download.jsp; McIntosh 2013). Crop losses caused by pathogens have been estimated to be around 10% for wheat, with powdery mildew, *Septoria* spp. and rust fungi being the most devastating diseases in areas with high productivity (Oerke 2006).

1.4.2 Powdery mildew – the pathogen

Powdery mildew is a collective term for about 820 species classified into the order Erysiphales within the Ascomycete phylum (Braun 2011). These fungal pathogens infect a wide range of angiosperm plants including economically and nutritionally important crop species. They are conspicuous with the formation of huge amounts of spores on the plant surface usually appearing as a white powder; therefore the name powdery mildew (Glawe 2008).

Powdery mildew of cereals is caused by the species *Blumeria graminis (*teleomorph; anamorph: *Oidium monilioides*). Due to a strict host specialization the species can be further classified into eight so-called *formae speciales* (f. sp.), each infecting only particular cereal species. Wheat-infecting powdery mildew, *Blumeria graminis* f. sp. *tritici* (*Bgt*), is infecting all aerial parts of the wheat plants, mainly the leaves. As a strict obligate biotrophic parasite it relies on living host tissue for its propagation. It exclusively infects the epidermal cell layer and mainly reproduces asexually by wind-dispersed, haploid spores (conidia) during the growth season (Zhang et al. 2005). Sexual reproduction takes place under unfavourable

conditions when hyphae of different mating types fuse to form chasmothecia. They can survive and overwinter on non-living tissue and release ascospores next spring (Glawe 2008).

The asexual life cycle of *Bgt* starts with the germination of a spore, formation of a primary germ tube that attaches the spore to the host cell surface, a subsequent outgrowth of a secondary germ tube, and the formation of an appressorium. To penetrate through the cuticle and the rigid plant cell wall, a penetration peg is formed beneath the appressorium. It is able to pierce the cell wall using high turgor pressure and the activity of hydrolytic enzymes. Later, the plant`s plasma membrane is invaginated but kept intact and a hand-like structure, a so-called haustorium, is formed by the fungus. It has a large surface area that is in close proximity to the host plasma membrane and is potentially the site of nutrient uptake for the fungus. After the establishment of a haustorium the fungus can form secondary hyphae at the host surface, and similarly infect neighboring cells. Finally, the fungus will produce conidiophores carrying conidia that can be released for dispersal. This life cycle may only take about 7 days under optimal condition (Zhang et al. 2005).

Severe infections with powdery mildew may result in smaller sized and fewer kernel on the spikes (Bowen et al. 1991; Everts et al. 2001), a high number of tillers without grain head (Everts and Leath 1992), and a reduced plant productivity due to reductions in transpiration and photosynthesis rate (Shtienberg 1992).

1.5 Aim of this thesis

In 2004, the NB-LRR-encoding gene *Pm3* was cloned (Yahiaoui et al. 2004). It was the first powdery mildew resistance gene from wheat to be molecularly identified. Since that time 54 different haplotypes for the coding region of this gene have been identified by allele mining approaches and for 17 of them there is experimental evidence for functionality as a race-specific powdery mildew resistance gene (Srichumpa et al. 2005; Yahiaoui et al. 2006, 2009; Bhullar et al. 2009, 2010). This makes *Pm3* one of *R* genes with the largest number of known allelic variants. The known allelic diversity of *Pm3* makes it an interesting system to study genetic determinants of resistance specificity. Previous work by Brunner and associates (2010) has shown that it is possible to combine the resistance specificity of two alleles in one artificial *Pm3* variant. It was also demonstrated that related *Pm3* alleles with a narrow or broad resistance spectrum exist and that polymorphic NB-ARC domains are influencing this property.

This thesis was initiated to address two different research questions concerning *Pm3*-based resistance. First, the molecular basis of the broad or narrow resistance-spectrum properties of

PM3 proteins encoded by different alleles should be further investigated. During these studies, the question arose whether it is possible to apply the gained knowledge to artificially modify a *Pm3* allele to enlarge its resistance spectrum and whether the results can be extrapolated to other NB-LRR R proteins. The second part of this thesis is dealing with the question whether different *Pm3* alleles can be successfully pyramided and if not, which molecular mechanism might be responsible for genetic interference.

2 Substitutions of two amino acids in the nucleotide-binding site domain of a resistance protein enhance the hypersensitive response and enlarge the PM3F resistance spectrum in wheat

Daniel Stirnweis, Samira Désiré Milani, Tina Jordan,
Beat Keller*, and Susanne Brunner

Molecular Plant-Microbe Interactions, Vol. 27, No. 3, 2014, pp. 265–276.

Submitted 2 October 2013. Accepted 6 December 2013.

* Author of correspondence

2.1 Abstract

Proteins with nucleotide-binding site (NBS) and leucine-rich repeat (LRR) domains are major components of the plant immune system. They usually mediate resistance against a subgroup of races of a specific pathogen. For the allelic series of the wheat powdery mildew resistance gene *Pm3*, alleles with a broad and a narrow resistance spectrum have been described. Here, we show that a broad *Pm3* spectrum range correlates with a fast and intense hypersensitive response (HR) in a *Nicotiana* transient-expression system and this activity can be attributed to two particular amino acids in the ARC2 subdomain of the NBS. The combined substitution of these amino acids in narrow-spectrum PM3 proteins enhances their capacity to induce an HR in *Nicotiana benthamiana*, and we demonstrate that these substitutions also enlarge the resistance spectrum of the *Pm3f* allele in wheat. Finally, using *Bph14*, we show that the region carrying the relevant amino acids also plays a role in the HR regulation of another coiled-coil NBS-LRR resistance protein. These results highlight the importance of an optimized NBS-'molecular switch' for the conversion of initial pathogen perception by the LRR into resistance-protein activation, and we describe a possible approach to extend the effectiveness of resistance genes via minimal targeted modifications in the NBS domain.

2.2 Introduction

In addition to physical and chemical barriers, plants have a nonadaptive, cell-autonomous immune system to protect themselves against potentially pathogenic organisms and viruses. This immune system comprises two layers of resistance that both involve receptors for nonself molecules or activities (Jones and Dangl 2006). The first layer is based on cell-surface receptors with extracellular sensor domains that detect conserved molecular patterns associated with multiple classes of microbes or with cell damage. To establish virulence, host-adapted pathogens have evolved mechanisms to either evade recognition by those pattern recognition receptors, employ so-called effectors to suppress immune responses of the host, or both. The second layer of plant immunity is mediated by resistance (R) proteins. They specifically recognize pathogen effectors and elicitors directly or indirectly via detection of an alteration of a guarded host protein. Accordingly, the *R* gene–activated resistance is referred to as effector-triggered immunity and the recognized gene products of the pathogens are named avirulence (Avr) proteins (Dodds and Rathjen 2010).

During coevolution of host and pathogen populations, new variants of *R* and *Avr* genes rapidly evolve, leading to a large diversity or fast turnover at the respective genomic loci. Consequently, a particular *R* gene usually only prevents disease instigated by a subset of

pathogen races. *R* genes have been extensively employed in crop breeding programs, due to the high level of resistance provided by most of them and the resulting ease in phenotypic selection. However, the drawback of their use, especially in modern agricultural cropping systems, is their rapid loss of effectiveness. They are overcome by newly emerging or spreading pathogen strains with mutated or lost *Avr* genes. The majority of *R* genes code for proteins with a central nucleotide-binding site (NBS) and a C-terminally linked leucine-rich repeat (LRR) domain (Marone et al. 2013). The two most prominent classes of NBS-LRR resistance proteins are defined by their N-terminus, either a toll-interleukin-1 receptor (TIR) domain or a domain with a coiled-coil (CC) structure. The TIR and CC domains were shown to provide an interface for oligomerization (Bernoux et al. 2011b; Chang et al. 2013; Maekawa et al. 2011) or to interact with guardee and signaling proteins (Ade et al. 2007; Mackey et al. 2002; Sacco et al. 2007; Shen et al. 2007; Tameling and Baulcombe 2007). The LRR domain is often considered the major determinant of recognition specificity (Padmanabhan et al. 2009). It was shown, for example, for the resistance genes *L5/L6* (Dodds et al. 2006) and *Rpp1* (Krasileva et al. 2010), that their gene products interact directly with the corresponding avirulence proteins via the LRR domain in a gene-for-gene specific manner.

The central ATPase part of many R proteins, the NBS domain, can be further subdivided into three subdomains, a nucleotidebinding (NB) module and the ARC1 and ARC2 subdomains designated according to their presence in the human apoptotic protease activating factor 1 (APAF-1), R proteins, and the *Caenorhabditis elegans* death-4 (CED-4) protein. All three subdomains are important for the ATPase activity that enables the NBS domain to act as a ‘molecular switch’ (Takken et al. 2006) controlling transition of the R protein between an ATP- and ADP-bound state. The two states usually correspond to an active and inactive structural conformation, respectively. Current mechanistic models for NBS-LRR proteins predict that an initial detection of nonself molecules or non–self-modified host proteins leads to small structural changes in the receptor. Those are subsequently amplified into major conformational changes that are accompanied by a nucleotide exchange (Rafiqi et al. 2009; Takken and Goverse 2012). The shift of the equilibrium to the activated form enables the resistance receptor to oligomerize or mobilize downstream signaling components or both (Bernoux et al. 2011a).

For the PM3 resistance protein, domain-swap experiments in a transient resistance assay have shown that blocks of 19 or 40 polymorphic amino acids in the NBS domain of the proteins PM3A or PM3B, respectively, contribute to a quantitatively higher resistance level against wheat powdery mildew (*Blumeria graminis* f. sp. *tritici*) (Brunner et al. 2010). Interestingly, these two alleles exhibit an extended resistance spectrum compared with *Pm3f*

or *Pm3c* (Brunner et al. 2010). In a large set of tested *B. graminis* f. sp. *tritici* isolates, *Pm3a* mediated resistance against 454 *B. graminis* f. sp. *tritici* isolates, including all 173 races that also displayed avirulence on *Pm3f*, thus exhibiting an extended resistance spectrum of *Pm3f*. A similar pattern was observed for the broad-spectrum *Pm3b* allele compared with the narrow-spectrum *Pm3c* allele.

A deeper understanding of the underlying mechanisms of such resistance-spectrum extensions can potentially be important for enhancing crop resistance with rationally designed resistance genes. To our knowledge, such approaches to artificially improve resistance genes have only been achieved, so far, by modifications in the LRR domain, once via random mutagenesis (Farnham and Baulcombe 2006), and once via intragenic pyramiding of polymorphisms from two alleles (Brunner et al. 2010).

In this study, we were able to show that the property of an extended *Pm3* resistance spectrum correlates with the intensity of hypersensitive response (HR) induction in a transient expression system. Based on *Nicotiana* infiltrations, we identified two amino acid polymorphisms in the ARC2 domain of PM3A/B/S that explain the enhanced HR and applied this knowledge to extend the resistance of the narrow-spectrum *Pm3f* allele in wheat. The importance of the identified region in the fine tuning of HR is demonstrated in an additional R protein of the CC-NBS-LRR class. The presented study suggests a possible approach for the optimization of plant resistance via minimal targeted gene modifications.

2.3 Results

2.3.1 An extended resistance spectrum correlates with an enhanced HR of *Pm3* alleles in an autoactivated form.

The two *Pm3* alleles *Pm3a* and *Pm3b* exhibit an extended resistance spectrum in comparison with the *Pm3* alleles *Pm3f* and *Pm3c*, respectively (Brunner et al. 2010). Polymorphic sequence blocks in the NBS domain, unique to *Pm3a* and *Pm3b* (Fig. 1A) (Bhullar et al. 2010), were shown to contribute to the enhanced resistance. Since the NBS domain is known to modulate R protein activity, it was speculated that the ability of *Pm3a* and *Pm3b* to recognize additional isolates, as compared with *Pm3f* and *Pm3c* might be due to a more intense signaling activity and not due to different recognition specificities in the LRR domain of these alleles.

To investigate this further, we conducted *Agrobacterium tumefaciens*– mediated transient expression experiments in *Nicotiana benthamiana*. This agroinfiltration system was widely

used previously to investigate *R* gene responses (Bendahmane et al. 2000; Houterman et al. 2009; Ma et al. 2012; Tang et al. 1996; Van den Ackerveken et al. 1996; Van der Hoorn et al. 2000; van Ooijen et al. 2008b). Usually coexpression of the matching *Avr* gene is employed to induce R protein activity, but in the absence of a cloned *AvrPm3* gene, it was necessary to activate the PM3 proteins via an autoactivating mutation. Therefore, we introduced into *Pm3a*, *Pm3b*, *Pm3c*, and *Pm3f* an aspartate-to-valine-substitution in the MHD motif (IHD in PM3) that has been shown to render many NBS-LRR proteins autoactive (Bendahmane et al. 2002; van Ooijen et al. 2008b; Williams et al. 2011). Indeed, this mutation (D502V in PM3A/B and D501V in PM3C/F) resulted in cell-death induction upon transient expression (Fig. 1B through E). This effect was not visible when nonmutated *Pm3* genes were overexpressed in *Nicotiana benthamiana* (Fig. 1D and E). Hereafter, these MHD mutant variants are designated by a superscript HR (e.g., $Pm3a^{HR}$), since the programmed cell-death response is reminiscent of the HR, a characteristic resistance reaction of plant cells against biotrophic pathogens. When different autoactive $Pm3^{HR}$ alleles were agroinfiltrated into *Nicotiana benthamiana*, a striking difference in the timing and intensity of the HR was observed. Infiltration of alleles with an extended resistance spectrum, $Pm3a^{HR}$ and $Pm3b^{HR}$, resulted in a completely necrotic spot within 45 h postinfiltration (hpi), whereas the respective $Pm3^{HR}$ alleles with narrow resistance spectra triggered only a moderate ($Pm3c^{HR}$) or delayed ($Pm3f^{HR}$) HR (Fig. 1B through E). Thus, we conclude that a narrow (*Pm3f* or *Pm3c)* or a broad (*Pm3a* or *Pm3b*) resistance spectrum correlates with a mild or slow or an intense and fast HR, respectively, of autoactivated $Pm3^{HR}$ alleles in the *Nicotiana* transient expression system. We will refer to *Pm3* variants with a fast and intense HR after agroinfiltration as ‘strong’ alleles and to those with a slower or milder HR as ‘weak’ alleles.

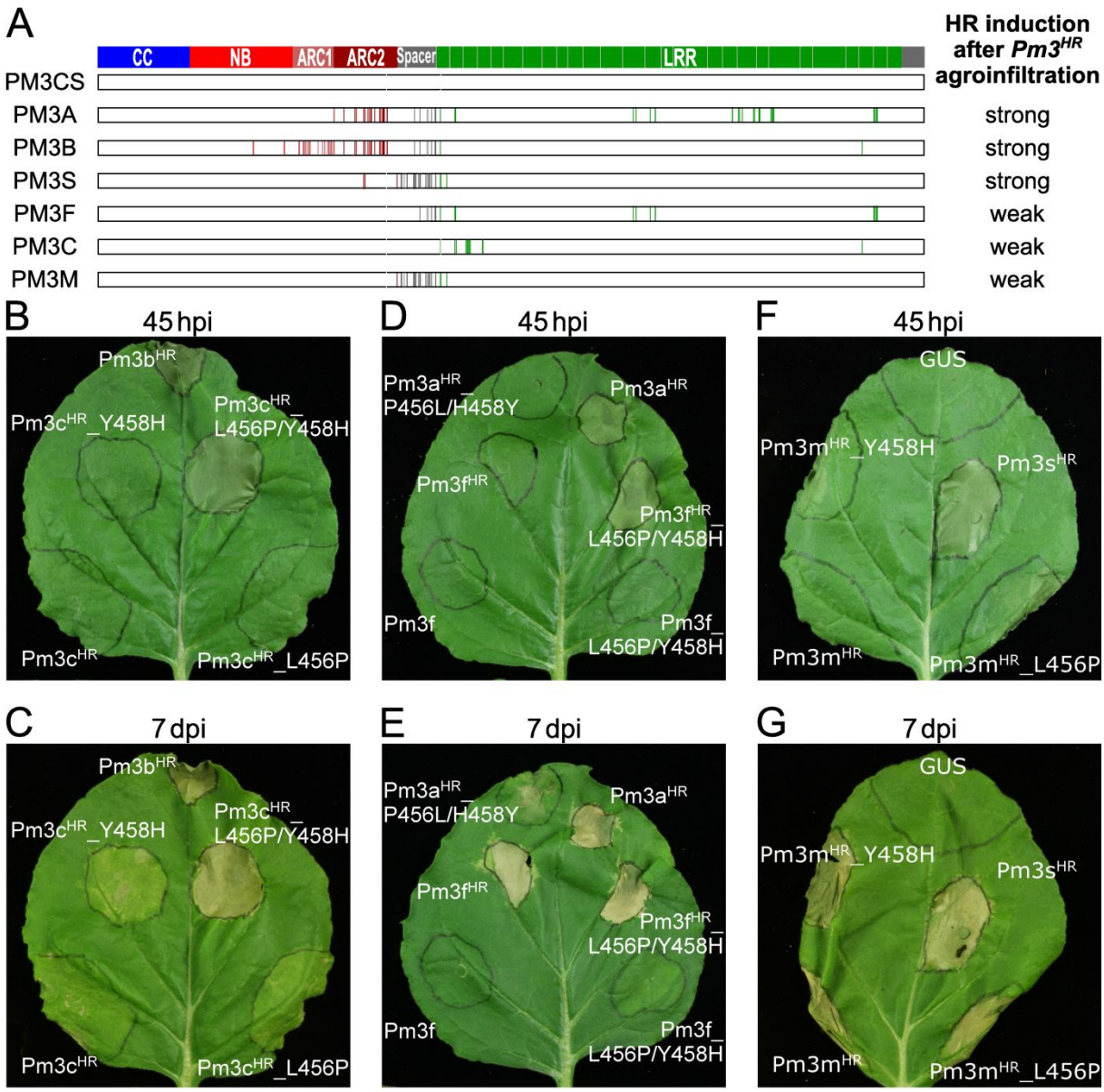

Fig. 1 PM3^{HR} proteins autoactivated by D-to-V mutations in the MHD motif differ in their ability to induce a hypersensitive response (HR) in a *Nicotiana* transient expression system. **A,** Schematic representations of the wild-type PM3 proteins used in this study. The top row shows the PM3 domain structure with the coiled-coil (CC) (blue), nuceotide-binding (NB) (red), ARC1 (salmon), ARC2 (dark red), spacer (gray), and leucine-rich repeat (LRR) (green) (sub)domains. Vertical bars are colored according to the domain affiliation and indicate polymorphic amino acids in comparison with PM3CS, the consensus sequence of all known PM3 proteins (Yahiaoui et al. 2006). Different Pm3 expression constructs were delivered into *N. benthamiana* leaves via *Agrobacterium tumefaciens* infiltration. Strength of the resulting HR after *Pm3^{HR}* infiltration is indicated. **B** and **C,** Introduction of the L456P/Y458H double substitution renders the narrow-spectrum allele *Pm3c^{HR}* nearly as effective in HR induction as the broad-spectrum allele *Pm3b^{HR}*. The respective single substitutions display only a minimally enhanced HR. **D** and **E,** Infiltrated spots with *Pm3a^{HR}* and double-mutated *Pm3f^{HR}_L456P/Y458H* display extensive cell death at 45 h postinfiltration (hpi), whereas *Pm3f^{HR}*–cell death symptoms develop more slowly, and *Pm3a^{HR}_P456L/H458Y* symptoms are even less pronounced by 7 days postinfiltration (dpi). Without the autoactivating mutation in the MHD motif, L456P/Y458H substitutions in *Pm3f* do not cause HR symptoms within 7 dpi. **F** and **G,** Cell-death induction by *Pm3s^{HR}* (equal to *Pm3m^{HR}_L456P/Y458H*) causes a complete tissue collapse in the infiltration spot within 45 hpi, whereas HR induction by *Pm3mHR* and its single substitution variants is slower. The negative control β-glucuronidase (GUS, *uidA*) does not induce cell death. B to G, Pictures of infiltrated leaves were taken at 45 hpi and 7 dpi and representative examples are shown.

2.3.2 HR is modulated by the combination of two amino acids in the ARC2 subdomain.

As the strong alleles *Pm3a* and *Pm3b* specifically share the same ARC2 sequence, we checked whether any amino acids in this subdomain are polymorphic to the consensus sequence PM3CS in any of the other known 15 functional PM3 proteins. Two polymorphic amino acids identical to the *Pm3a/b* haplotype were found in PM3S. Interestingly, the polymorphic proline 456 and histidine 458 residues are exclusively shared by PM3S and the strong PM3A and PM3B proteins, but all other *Pm3* alleles encode for leucine 456 and tyrosine 458 (Bhullar et al. 2010). Additionally, the amino acids 456 and 458 are the only two polymorphic amino acids between PM3M and PM3S (Bhullar et al. 2009, 2010) (Fig. 1A; Supplementary Fig. S1). These two alleles were, therefore, used to initially test whether P456 and H458 have an influence on HR in the *Nicotiana* expression system.

Autoactivated versions of *Pm3s* and *Pm3m* were produced via the MHD mutation (D501V) and, indeed, $Pm3s^{HR}$-infiltrated spots showed a completely collapsed plant tissue at 45 hpi that was not observed with $Pm3m^{HR}$ (Fig. 1F). $Pm3m^{HR}$-mediated HR developed more slowly but was often indistinguishable from $Pm3s^{HR}$ at 7 days postinfiltration (dpi) (Fig. 1G). We also introduced P456 and Y458 in $Pm3c^{HR}$. The PM3C protein does not share a polymorphic sequence block in the spacer and first LRR with the PM3A, PM3B, and PM3S proteins that have been described above to exhibit a strong HR phenotype in *Nicotiana* (Fig. 1A). Infiltrations with the double- mutated $Pm3c^{HR}$*_L456P/Y458H* led to entirely collapsed spots within 45 hpi (Fig. 1B). In contrast, $Pm3c^{HR}$ elicited no HR within 45 hpi and only mild cell-death symptoms, even within 7 dpi (Fig. 1B and C). Based on this result we can conclude that the HR-enhancing effect of P456 and H458 is independent of those amino acids in the spacer and first LRR that are shared by the PM3A, PM3B, PM3M, and PM3S proteins (Fig. 1A).

As for $Pm3m^{HR}$ and $Pm3c^{HR}$, the double substitution L456P/ Y458H also intensified the HR of $Pm3f^{HR}$ (Fig. 1D and E). Remarkably, the *Pm3f_L456P/Y458H* construct without the MHD mutation did not show any signs of cell-death induction, even at 7 dpi (Fig. 1E). This shows that it is possible to modify PM3F by the two amino acid changes to exhibit a faster and more intense HR but without rendering the protein autoactive.

To test whether a single amino acid substitution is sufficient for enhancing the HR, we performed infiltrations with L456P or Y458H variants of $Pm3c^{HR}$ and $Pm3m^{HR}$. The effect of these single substitutions on $Pm3c^{HR}$ appears negligible (Fig. 1B and C). For the $Pm3m^{HR}$*_L456P* and *_Y458H* variants, a slightly intensified HR could be observed at 45 hpi in comparison with $Pm3m^{HR}$ (Fig. 1F). But the combination of both substitutions, as present in $Pm3s^{HR}$ and $Pm3c^{HR}$*_L456P/Y458H*, led to an exceedingly stronger HR (Fig. 1B, C, F, and G).

To more sensitively detect possible differences within the *Pm3m*/*Pm3s* or *Pm3b*/*Pm3c* infiltration sets in the very early phase of HR induction (17 to 30 hpi), we performed measurements of electrolyte efflux from leaf discs, a frequently used proxy for cell-death quantification (Baker et al. 1991; Gao et al. 2011; Mackey et al. 2002; Maekawa et al. 2011). Here, a significant increase, in comparison with the negative control (β-glucuronidase [GUS]), could be measured 23 to 30 hpi only for $Pm3s^{HR}$ but not for $Pm3m^{HR}$ or its single-substitution versions (Fig. 2A). Similar to $Pm3s^{HR}$, $Pm3b^{HR}$ also showed a fast increase in electrolyte leakage. However, no measurable deviation of electrolyte leakage between $Pm3c^{HR}$*_L456P/Y458H* and $Pm3c^{HR}$ could be detected within the first 30 hpi and also, consistently, not with the two single-mutant variants of $Pm3c^{HR}$ (Fig. 2B). The strong HR mediated by $Pm3c^{HR}$*_L456P/Y458H*, therefore, predominantly developed between 30 and 45 hpi. The results of the *Pm3m* and *Pm3s* variants again suggest that both amino acid substitutions are necessary for the enhanced HR.

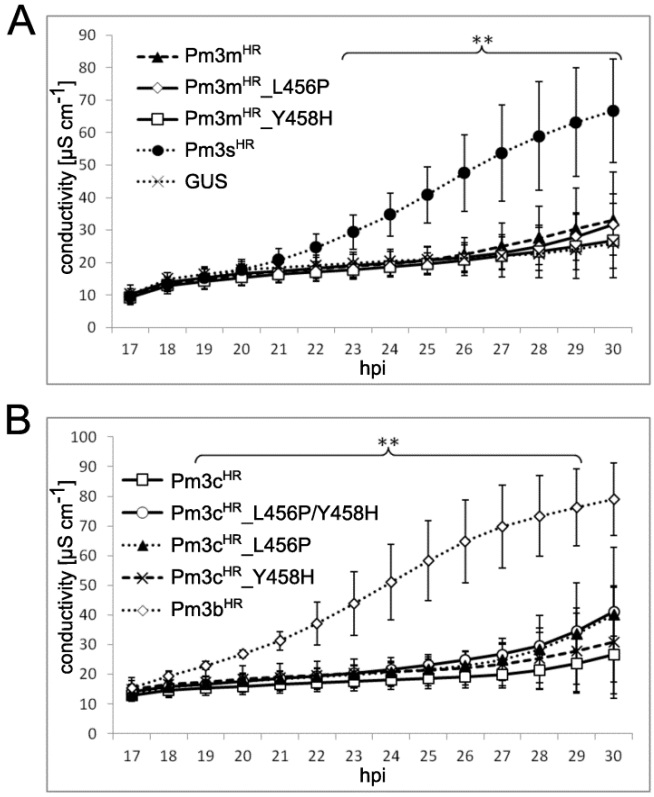

Fig. 2 Measurement of ion leakage in the early phase of hypersensitive response (HR) induction (17 to 30 h postinfiltration [hpi]) detects differences for the *Pm3m/Pm3s* and *Pm3b/Pm3c* infiltration sets. **A,** Within the first 30 hpi, increased electrolyte leakage from infiltrated leaf discs harvested 17 hpi can only be measured for $Pm3s^{HR}$ in the *Pm3m/Pm3s* infiltration set. β-glucuronidase (*uidA*)-infiltrated leaf discs represent a negative control for HR induction. **B,** Within the first 30 hpi, significantly increased electrolyte leakage can only be measured for $Pm3b^{HR}$ in the *Pm3b/Pm3c* infiltration set. Conductivity was measured in 1.5 ml of H2O with one 7-mm diameter leaf disc and is illustrated as mean ± standard deviation ($n = 8$). Relevant significant differences between $Pm3s^{HR}$ (A) or $Pm3b^{HR}$ (B) and all other samples in the respective infiltration set are reported (**$P < 0.01$, paired Student's *t*-test, same leaf as pairing criteria).

We conclude that the combined substitution of leucine 456 to proline and tyrosine 458 to histidine can convert weak into strong HR-inducing *Pm3* alleles in the *Nicotiana* transient assay without rendering them autoactive.

2.3.3 *Pm3b*-mediated HR is also modulated by polymorphism outside the ARC2 subdomain.

The previous ion-efflux experiment with the *Pm3b* and *Pm3c* constructs showed that *Pm3b*^{HR}-mediated, HR-related ion leakage started around 19 hpi, earlier, therefore, than the HR induced by the strong *Pm3c*^{HR}*_L456P/Y458H*. This suggests that additional HR-enhancing polymorphisms are present in *Pm3b* (Fig. 2B). The observation that the double mutated *Pm3b*^{HR}*_P456L/H458Y* is not significantly compromised in its HR activity strongly supports this hypothesis (Fig. 3).

Interestingly, introduction of the same P456L/H458Y mutations in the strong *Pm3a*^{HR} allele almost completely abolished cell-death signaling and made *Pm3a*^{HR}*_P456L/H458Y* even less active than the respective weak allele *Pm3f*^{HR} (Fig. 1D and E). This highlights the importance of the two amino acids for PM3A-mediated signaling and allows the inference that the additional HR-enhancing polymorphisms in PM3B are located outside the ARC2, presumably in the NB-ARC1.

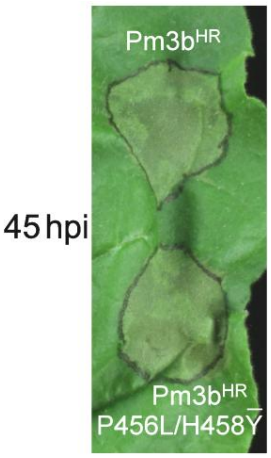

Fig. 3 Polymorphic amino acids distinct from P456 and H458 are also responsible for the fast and intense hypersensitive response (HR) mediated by *Pm3b*^{HR}. Double-mutated *Pm3b*^{HR}*_P456L/H458Y* was not affected in HR induction compared with its wild-type version. A representative picture of an infiltrated leaf at 45 h postinfiltration is shown.

2.3.4 The HR enhancing effect is not caused by modified protein stability and is independent of particular autoactivating mutations.

To verify whether a higher PM3^{HR} protein abundance might be responsible for the more intense HR of the strong PM3^{HR} variants, we performed a Western blot analysis making use of a hemagglutinin (HA) epitope tag that was C-terminally fused to all PM3 proteins. We compared the PM3^{HR}–protein levels in extracts from infiltrated spots from the same leaf, harvested shortly before the onset of cell death (15 hpi). Similar band intensities for the weak and the strong PM3^{HR} variants in the *Pm3m/Pm3s* and *Pm3b/Pm3c* infiltration sets were found. This shows that the strong HR of the *Pm3b*^{HR}, *Pm3s*^{HR}, and *Pm3c*^{HR}*_L456P/Y458H* alleles was not caused by higher protein abundance (Supplementary Fig. S2).

To test whether the enhancing effect of P456/H458 (proline 456/histidine 458) is specific for the MHD-mutant versions, we developed *Pm3m* and *Pm3s* genes mutated in the Walker B (*Pm3_D284E*) or RNBS-A motif (*Pm3_S238F*). They were designed based on described autoactive variants of the *R* genes *I-2* (Tameling et al. 2006) or *Rps5* (Ade et al. 2007). While the D284E mutation did not lead to cell-death symptoms, the S238F substitution rendered *Pm3* autoactive. The HR of *Pm3s_S238F* was clearly more pronounced than the *Pm3m_S238F* induced HR (Supplementary Fig. S3), showing that the enhancing effect is independent of a particular autoactivating mutation.

2.3.5 Modifications of two amino acids in the ARC2 domain result in an extended resistance spectrum of *Pm3f* in wheat.

We performed a transient resistance assay (Schweizer et al. 1999) in leaf epidermal cells of wheat, to explore whether the exchange of L456P/Y458H may also result in an extended resistance spectrum of *Pm3f_L456P/Y458H* in comparison with *Pm3f*. Here, the constructs were biolistically delivered into epidermal cells of the susceptible wheat line ‘Chancellor’ and the leaves were subsequently infected with powdery mildew spores. The interaction of transformed cells with the fungus was quantified as a haustorium index (HI) that gives the percentage of attacked cells with a successfully established fungal haustorium (Fig. 4).

The *B. graminis* f. sp. *tritici* isolate 97028 differentiates the resistance reaction of *Pm3a* and *Pm3f* in seedling infection tests of wheat differential lines; it is avirulent on *Pm3a* and virulent on *Pm3f*. Whereas the HI of *Pm3f* for this isolate was 50% ± 5%, the construct *Pm3f_L456P/Y458H* (16% ± 5% HI; Student’s *t*-test for comparison with *Pm3f*, $P < 0.001$) showed a resistance level as high as the resistant *Pm3a* allele (18% ± 3% HI; Student’s *t*-test for comparison with *Pm3f_L456P/Y458H*, $P = 0.579$). We included in this assay the construct *Pm3f-aARC*, which encodes for a chimera of the CC-NBS domains of *Pm3a* and the spacer-

LRR region of *Pm3f*. It resembles a construct tested by Brunner and associates (2010) (same chimera but different plasmid vector and without the HA-epitope tag) that was employed to show an enhancing effect of the *Pm3a*-ARC2 subdomain on the *Pm3f* resistance. Since the HI of *Pm3f-aARC* (15% ± 3% HI) for *B. graminis* f. sp. *tritici* isolate 97028 was not significantly different from the HI of *Pm3f_L456P/Y458H* (Student's *t*-test, $P = 0.842$), we conclude that the other 17 polymorphic amino acids between PM3A and PM3F in the ARC2 domain do not further enhance the effectiveness of the modified *Pm3f* version. As a susceptible control, we also included *Pm3CS* throughout the assay. A comparison of the HI of *Pm3f* and *Pm3CS* for the isolate 97028—50% ± 5% compared with 73% ± 6%, respectively (Student's *t*-test, $P < 0.01$)—indicates that *Pm3f* carries some residual recognition activity against the isolate 97028, but this is not sufficient to trigger an efficient resistance response against this virulent race in the leaf segment assay (Fig. 4).

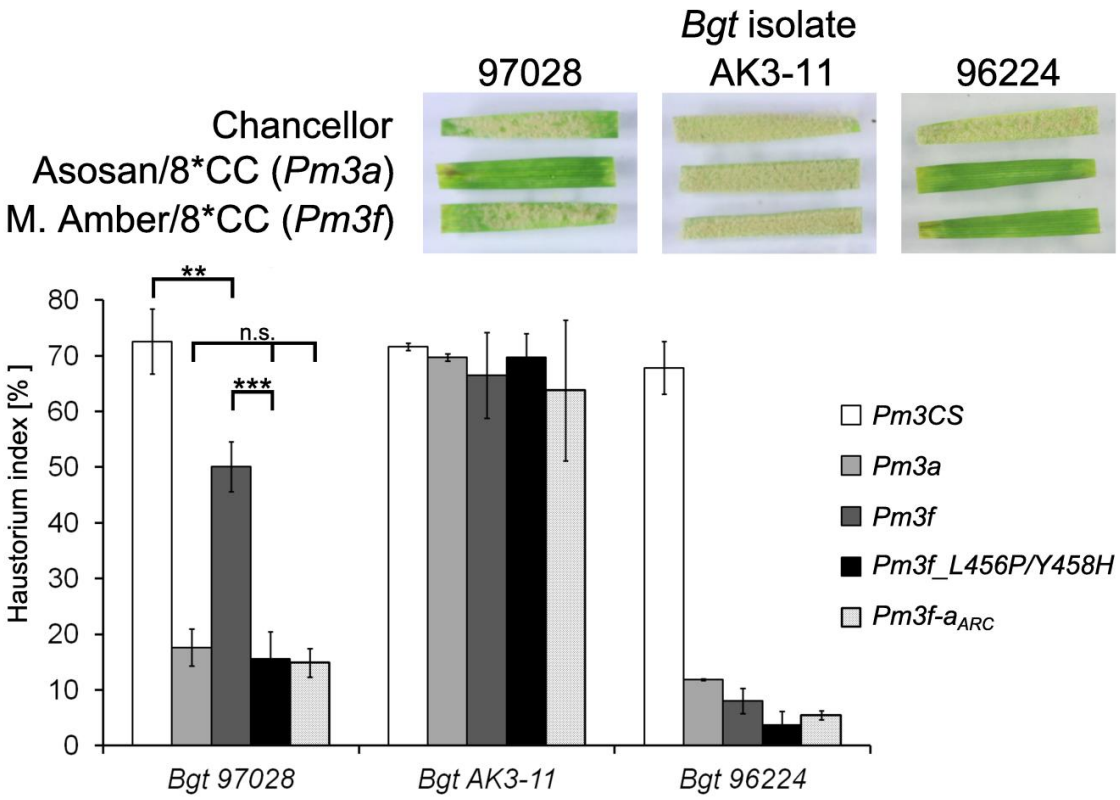

Fig. 4 Transient resistance assay in wheat reveals an enlarged powdery mildew resistance spectrum for the double-substituted *Pm3f_L456P/Y458H* compared with *Pm3f*. In the top panel, results of a seedling infection test with the susceptible cultivar Chancellor, which was used for the transient resistance assay, and with wheat differential lines for *Pm3a* and *Pm3f* are shown. The lower panel gives the results of the transient resistance experiments with the susceptible control *Pm3CS*, the wild-type alleles *Pm3a* and *Pm3f*, the double-substituted *Pm3f_L456P/Y458H*, and the *Pm3f-aARC* chimera (coiled-coil and nucleotide-binding site of *Pm3a* and leucine-rich repeat domain of *Pm3f*). Haustorium index values (in percent) are reported as means (± standard deviation) of three (*Blumeria graminis* f. sp. *tritici* [*Bgt*] isolate 97028) or two (*B. graminis* f. sp. *tritici* isolates AK3-11 and 96224) independent experiments. Relevant (non-) significant differences are indicated (Student's *t*-test: n.s. = nonsignificant, $^{**}P < 0.01$, and $^{***}P < 0.001$).

High HI values were obtained with all tested constructs in combination with the isolate AK3-11 (64 to 72% HI), which is virulent on *Pm3a* as well as *Pm3f*. This shows that none of the tested constructs activated unspecific resistance via autoactivation. As a further control, we used isolate 96224, which is avirulent on *Pm3f* and *Pm3a*. All constructs mediated high levels of resistance (4 to 12% HI), except for the susceptible control *Pm3CS* (68% HI).

Overall, these results demonstrate that the substitution of the two relevant amino acids in the ARC2 domain converts *Pm3f* from a susceptible into a resistant allele with regard to the tested isolate 97028, thus expanding its resistance spectrum without inducing unspecific resistance mechanisms.

2.3.6 The P456/H458 residues of broad-spectrum *Pm3* alleles represent an optimal amino acid combination for a strong HR.

A nucleotide sequence alignment of *Pm3* alleles revealed that the triplet coding for amino acid 456 differs between the strong alleles *Pm3a/b* and *Pm3s* and that polymorphisms in the close vicinity of this codon are not conserved between these alleles (Supplementary Fig. S4). This indicates that independent evolutionary events led to P456 (and presumably also to H458) in PM3A/B and in PM3S. Since the specific amino acid combination P456/H458 evolved twice, we wanted to test what effects other amino acids cause in the respective positions. Therefore, we used the *Pm3c*^{HR}-single-substitution constructs Pm3c^{HR}_L456P and Pm3c^{HR}_Y458H, which showed a very clear HR difference to the corresponding double-substituted gene (Fig. 1B and C) and exchanged the second relevant amino acid (Y458 and L456, respectively) with any other amino acid. *Nicotiana* infiltrations with these constructs showed that many substitutions led to a stronger HR but the P456/H458 combination always caused the fastest HR. Whereas, for many other constructs, the HR scoring showed some variability, strongly intensified HR compared with the single-substituted *Pm3c*^{HR} was consistently observed for arginine or aspartate at position 456 and for cysteine, arginine, glutamine, lysine, or serine at position 458 (Table 1; Supplementary Figs. S5 and S6). Loss-of-function was observed with tryptophan at position 456 and valine or glutamate at position 458, but in contrast to the constructs with W456 or V458, we did not detect PM3c^{HR}_L456P/Y458E protein, indicating that the P456/E458 combination renders the protein unstable. For the two positions, physico-chemical properties of the different amino acid residues did not correlate with the effect on HR. On the one hand, these results show that the very moderate HR related to the L456/Y458 combination in narrow-spectrum *Pm3* alleles is rather exceptional. On the other hand, the P456/H458 combination in strong *Pm3* alleles seems to be an optimized amino acid combination regarding HR capacity.

Table 1 Effects on the hypersensitive response (HR) observed in *Nicotiana* agroinfiltration assays for single amino acid substitutions of L456 or Y458 in autoactivated *Pm3c^{HR}_Y458H* or *Pm3c^{HR}_L456P*, respectively.

Category	Effect on HR[a]	Pm3c^{HR}_L456x/Y458H	Pm3c^{HR}_L456P/Y458x
A	Strongly intensified HR: strong HR within 45 hpi; nearly as strong as for Pm3c^{HR}_L456P/Y458H	Arg, Asp	Cys, Arg, Gln, Lys, Ser
	Variable phenotypes between categories A and B	Ser, Gly, Gln, Asn, Lys	Pro, Ala, Thr, Trp, Asn
B	Weakly intensified HR: no strong HR within 45 hpi, but within 7 dpi	Thr, His, Tyr, Glu, Ile	Leu, Met, Phe
	Variable phenotypes between categories B and C	Val, Ala, Cys	Gly, Ile
C	No change in HR: weak HR within 7 dpi; indistinguishable from Pm3c^{HR}_L456P and Pm3c^{HR}_Y458H	Phe, Met	Asp
D	Loss of function: no HR within 7 dpi	Trp	Val

[a] As compared with Pm3c^{HR}_Y458H and Pm3c^{HR}_L456P; hpi = h postinfiltration; dpi = d postinfiltration

2.3.7 The ARC2 loop region modulates HR of additional CC-NBS-LRR resistance genes.

According to a structural model of the NBS domain of PM3, the amino acids 456 and 458 are situated in an exposed loop (hereafter referred to as the ARC2 loop) connecting two α-helices at the outer surface (Brunner et al. 2010) (Supplementary Fig. S7). An alignment of the PM3 protein sequence with numerous other plant NBS-LRR proteins shows that this loop is located C-terminally of the RNBS-D/RNBS-V motif (Meyers et al. 2003; Zhou et al. 2004) and is absent in TIR-NBS-LRR proteins. The loop is highly diverse among CC-NBS-LRR proteins but well conserved in hPM3-1B, a *Pm3* homolog from wheat homologous chromosome 1B (Hurni et al. 2013), as well as in PM8, the *Pm3* ortholog from rye (*Secale cereale*) (Hurni et al. 2013) (Supplementary Fig. S8). They both share the amino acid combination P456/H458 with the *Pm3* alleles with extended resistance spectra. When autoactive MHD mutants of PM8 and hPM3-1B were infiltrated in *N. benthamiana*, both also exhibited a very fast and intense HR (Fig. 5A and C). The double substitution P455L/H457Y in the ARC2 loop residues corresponding to amino acids 456 and 458 in PM3 markedly dampened the HR induction of hPM3-1B^{HR} (Fig. 5A and B), as it was previously observed for PM3A^{HR}_P456L/H458Y (Fig. 1D and E). Agroinfiltrations with the respective single-substitution variants showed that the H457Y exchange is sufficient to explain the reduced HR of hPM3-1B^{HR}_P455L/H457Y (Fig. 5A). The strong HR mediated by hPM3-1B^{HR}_P455L is in contrast to PM3C^{HR}/PM3M^{HR}, in which the L456/H458 combination results in a weak HR (Fig. 1B, C, and F). These results demonstrate that, although the exact molecular details of HR modulation differ between PM3 and hPM3-1B, the ARC2 loop is also a key regulator of

HR induction in hPM3-1B. No reduced HR could be observed after agroinfiltration of *Pm8^{HR}_P456L/H458Y* compared with *Pm8^{HR}* (Fig. 5C and D). As suggested above for PM3B^{HR}_P456L/H458Y, additional HR-enhancing polymorphic amino acids might be present in PM8.

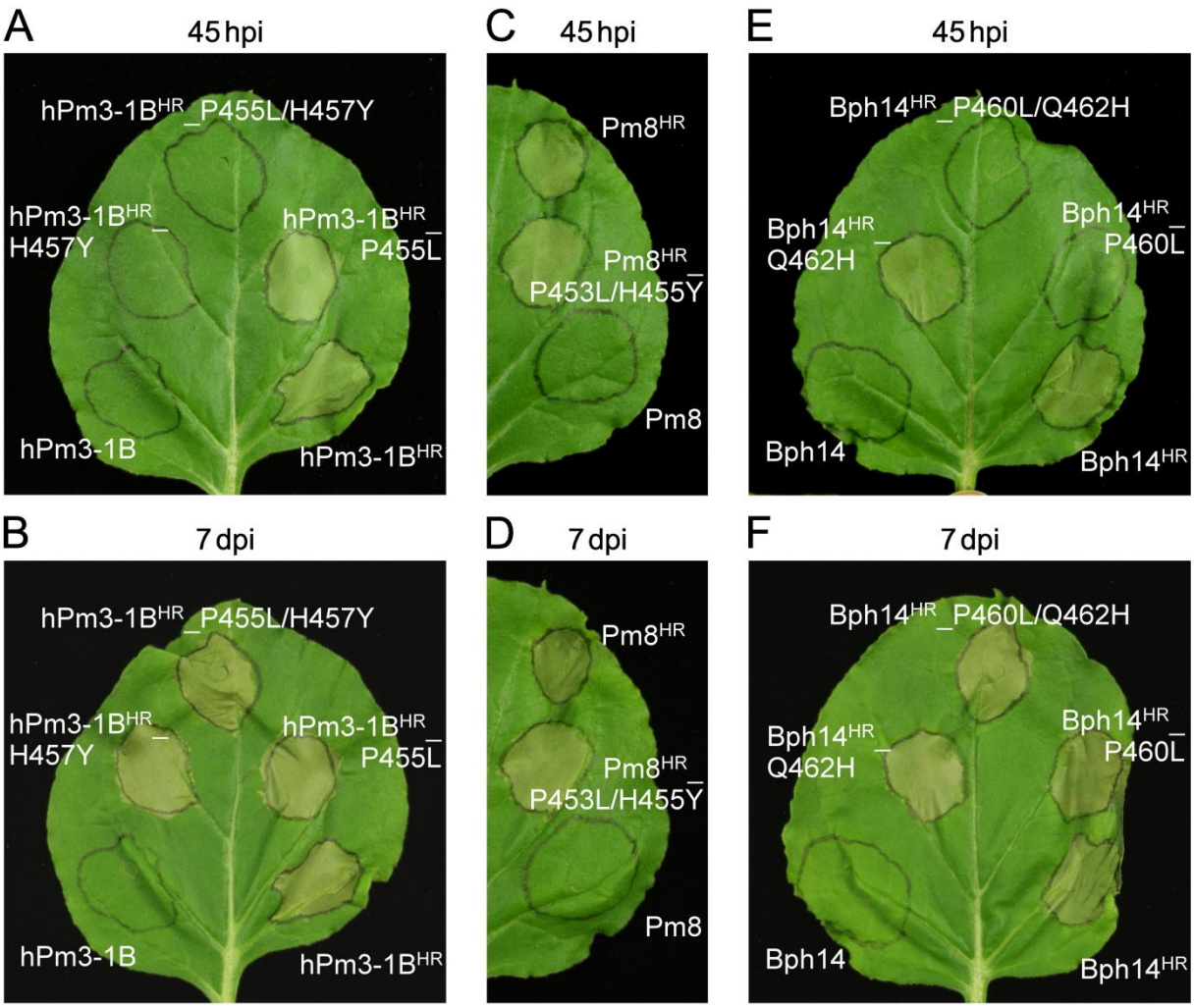

Fig. 5 Homologues of *Pm3* that share the P456/H458 haplotype with strong *Pm3* alleles (*hPm3-1B* and *Pm8*) also induce a rapid and intense hypersensitive response (HR) in *Nicotiana* infiltrations and substitutions in the ARC2 loop of the coiled-coil nucletide-binding site leucine-rich repeat genes *hPm3-1B* and *Bph14* can modulate their HR activity. **A** to **F,** The contribution of the amino acids corresponding to P456 and H458 in strong *Pm3* alleles to HR modulation is tested by single (*hPm3-1B^{HR}_P455L*, *hPm3-1B^{HR}_H457Y*, *Bph14^{HR}_P460L*, *Bph14^{HR}_Q462H*) and double (*hPm3-1B^{HR}_P455L/H457Y*, *Pm8^{HR}_P453L/H455Y*, *Bph14^{HR}_P460L/Q462H*) substitutions. HR development in *Nicotiana benthamiana* leaves agroinfiltrated with autoactivated variants of a *Pm3* homolog from wheat chromosome 1B (*hPm3-1B^{HR}*), *Pm8* (*Pm8^{HR}*), or *Bph14* (*Bph14^{HR}*) (A, C, E, respectively) is shown at 45 h postinfiltration and 7 days postinfiltration (B, D, F, respectively). Nonautoactivated *hPm3-1B*, *Pm8*, and *Bph14* do not induce cell death (B, D, F, respectively).

Apart from PM8 and hPM3-1B, the sequence most closely related to the ARC2 loop of the PM3 proteins is present in Bph14, a CC-NBS-LRR protein conferring resistance against brown planthopper in rice (Du et al. 2009). A mutation of the MHD motif (D508V) autoactivates *Bph14^{HR}*, leading to a strong HR after infiltration in *N. benthamiana*. This HR

activity could not be further enhanced by a substitution of glutamine 462 to histidine (Q462H; Fig. 5E and F), which corresponds to the weak-tostrong exchange Y458H in PM3. This is consistent with the observation that glutamine at position 458 in the Pm3c^{HR}_ L456P/Y458Q construct also causes a strong HR (Table 1). However, when proline 460, corresponding to proline 456 in strong PM3, was replaced by leucine (P460L), the occurrence of cell death induced by Bph14^{HR}_P460L was clearly delayed compared with Bph14HR, and consistently, the Bph14^{HR}_P460L/Q462H construct also displayed a delayed HR (Fig. 5E and F). This demonstrates that this ARC2 loop region is also involved in the fine tuning of a distantly related CC-NBS-LRR protein.

2.3.8 ARC2 loop substitutions that lead to a strong HR do not modify interdomain interactions between the CC-NBS and the LRR.

Slootweg and associates (2013) demonstrated that, for *Rx1*/ *Gpa2*, particular amino acid exchanges in the ARC2 loop region lead to a loss of HR activation in trans between the Gpa2 CCNBS and an autoactivating Rx1 LRR, most likely due to a reduction of the binding between the Gpa2 CC-NBS and the matching LRR fragment. This suggests that a stronger activation correlates with a more efficient binding of the ARC2 loop to the LRR.

To test whether the L456P/Y458H substitutions modify interdomain interactions of PM3, we split the PM3 protein into CC-NBS (PM3B: aa 1-524, PM3F: aa 1-523) and LRR parts (PM3B: aa 525-1415, PM3F: aa 524-1414). To test for in trans functionality of these fragments, we combined the CC-NBS carrying the D501V- or D502V-MHD mutation with the respective LRR in agroinfiltrations of *Nicotiana benthamiana* No macroscopic signs of HR were visible for the split PM3F, while a moderate HR was induced within 8 dpi by the split PM3B (Fig. 6A and B). Thus, the HR was severely reduced compared with the full-length PM3B^{HR} (Fig. 1B and C). To our knowledge, the in trans HR with corresponding fragments from Rx1 was not reported to be impaired compared with the full-length equivalent (Moffett et al. 2002). However, the weak HR induced by split PM3B and the lack of signs of transcomplementation of split PM3F may partially reflect observations with other CC-NBS-LRR that are not functional in trans with autoactivating mutations in the ARC2 subdomain (van Ooijen et al. 2008a). Nevertheless we could demonstrate that the chosen PM3B fragments are able to functionally interact to activate HR in trans. Therefore, we followed up the study on interdomain interactions of PM3.

Using the same CC-NBS and LRR fragments of PM3F, we performed a coimmunoprecipitation experiment to check for an altered CC-NBS-to-LRR affinity between the wild type and the L456P/Y458H-modified variant. Despite the lack of a transcomplementation phenotype, we were able to pull down the c-myc-tagged LRR domain

with agarose bead–coupled antibodies against the HA-tagged CC-NBS domain, indicating that these protein fragments interact. However, no obvious difference in the amount of coprecipitated LRR could be detected when comparing the two CC-NBS variants (Fig. 6C). We infer that the HR-enhancing modifications in the ARC2 loop have no major impact on interdomain interactions between CC-NBS and LRR, at least in the transient *Nicotiana* system.

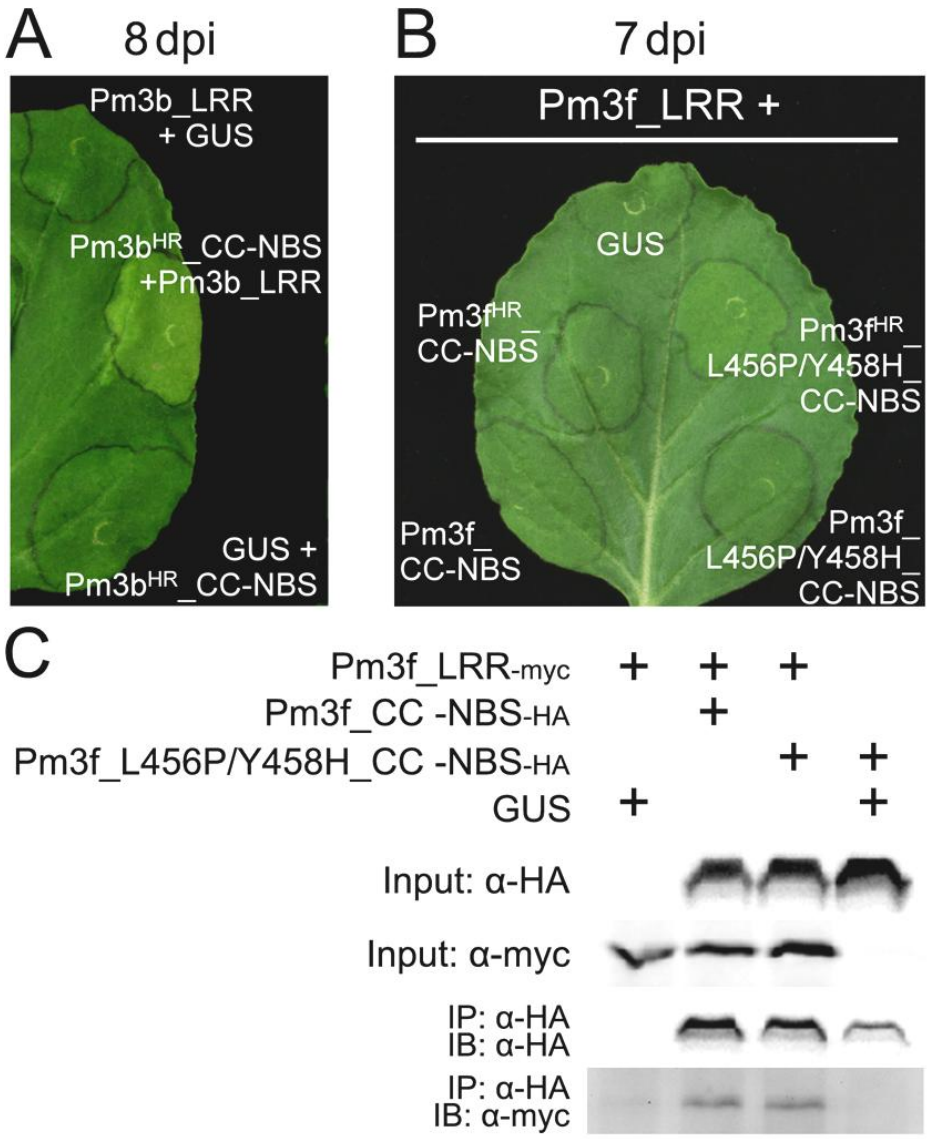

Fig. 6 Coimmunoprecipitation experiment reveals no modification of the PM3 coiled-coil nucleotide-binding site (CC-NBS) to leucine-rich repeat (LRR) domain interaction by the hypersensitive response (HR)-enhancing L456P/Y458H substitutions. **A,** Representative weak HR symptoms in *Nicotiana* leaves at 8 days after coinfiltation of PM3B CC-NBS and LRR fragments. **B,** Agroinfiltrations in *Nicotiana benthamiana* with the respective PM3F and PM3F_L456P/Y458H fragments are shown at 7 days postinfiltration. **C,** Coimmunoprecipitation of c-myc-tagged LRR with hemagglutinin (HA)-tagged CC-NBS fragments of PM3F. Immune blots (IB) before (two upper panels) and after (two lower panels) immunoprecipitation (IP) with anti-HA-coupled agarose beads are shown.

2.4 Discussion

For many NBS-LRR resistance proteins, it was shown that effector or elicitor perception, the first step in determining resistance specificity, is mediated by the LRR domain. Using comparative sequence analysis of alleles (Yahiaoui et al. 2006) and domain-swap experiments (Brunner et al. 2010), this was also demonstrated for the *Pm3* powdery mildew resistance gene. The translation of an initial detection into an efficient resistance response is attributed to the tightly regulated molecular switch function of the NBS domain, which consequently has to be considered as an important determinant of resistance specificity. In agreement with this model, it was shown that a polymorphic sequence block in the ARC2 subdomain of the NBS as present in the PM3A protein contributes to an expansion of the resistance spectrum in comparison with the PM3F protein (Brunner et al. 2010). In the study here, we were able to pinpoint two amino acids that completely explain this effect. Similar observations that the N-terminal domains modulate the resistance specificity of the LRR were made in other NBS-LRR. The flax rust TIR-NBS-LRR resistance protein L6 differs from the L7 allele only in the TIR domain but has a broader resistance spectrum than L7, indicating that the resistance is modulated by the TIR domain (Dodds et al. 2006; Ellis et al. 1999; Luck et al. 2000). Three amino acid changes are sufficient to explain this difference (L2/L6 recombinant, Luck et al. 2000). Tomita and associates (2011) were able to show that the CC-NBS domains influence the recognition spectrum of the *Tobamovirus* resistance protein L^3 from pepper. By combining the LRR of L^3 with the CC-NBS of its paralog PIH-X, they constructed a functional chimeric protein detecting P0 and P1 variants of the viral coat protein but not P1,2 variants that used to be recognized by full-length L^3 (chimera A, Tomita et al. 2011). Interestingly, PIH-X has an extended ARC2 loop sequence as compared with L3. Ashikawa (2012) analyzed the broad-spectrum *Pikm1-TS* gene and the narrow spectrum *Pik1-KA* gene from the rice blast *Pik* locus. A chimera with the CC-NBS of Pikm1-TS and the LRR of Pik1-KA kept resistance against a blast isolate that is avirulent on *Pikm1-TS* but virulent on *Pik1-KA*, demonstrating that one or more of the five polymorphic amino acids in the CC or of the three polymorphisms in the NBS domain determine the difference in recognition specificity (Ashikawa 2012). All these data for various NBS-LRR resistance proteins show that polymorphisms in the TIR, CC, or NBS domains that are not necessarily involved in the perception of the Avr protein or activity can be important for the outcome of the resistance specificity.

2.4.1 Putative function of the ARC2 loop.

In this study, we were able to attribute the effect of enhanced resistance activity of multiple PM3 proteins to two amino acid positions in a sequence that was modeled as a loop (Brunner et al. 2010) located C-terminally of the RNBS-D/RNBS-V motif (Meyers et al. 2003; Zhou et al. 2004). This motif is highly conserved, especially in non–TIR-NBS-LRR, but different consensus sequences for the RNBS-D motif are assigned for TIR (EDKDLFLHIACFFNG) and non-TIR (CFLYCALFPED YEIxKEKLIDYWIAEGFI) NBS-LRR proteins (Meyers et al. 2003). This suggests that there is a structural difference between the NBS of TIR and non-TIR proteins, and the identified effect of sequence polymorphisms in the ARC2 loop is possibly relevant only for non-TIR-NBS-LRR. The RNBS-D motif is conserved in neither APAF-1 nor CED-4 (van Ooijen et al. 2008b) and, therefore, is specific for R proteins. For CC-NBS-LRR, multiple gain- (autoactivity) and loss-of-function mutations have been described at the N-terminal end of the RNBS-D motif (Axtell et al. 2001; Bendahmane et al. 2002; Tornero et al. 2002), but the particular mechanistic function, especially of the conserved C-terminal part of the motif that is also part of the ARC2 loop, remains obscure.

Interestingly, loss-of-function mutations have been described for the loop region C-terminal of the RNBS-D motif in the resistance protein RPM1 (P464L, G467R; Tornero et al. 2002). Bearing in mind that the amino acid position does not align perfectly (shift of one position), the P464L substitution in the *rpm1-52* mutant allele may correspond to P456L that renders PM3 less active. Along with the results for hPM3-1B and Bph14 (Fig. 5A, B, E, and F), these observations demonstrate that the ARC2 loop is an important regulative element of CCNBS- LRR activity. Additionally, they also indicate that a proline- to-leucine substitution in the ARC2 loop dampens or blocks the activity of numerous CC-NBS-LRR.

The best-studied system in regard to the ARC2 loop is the resistance-gene homologues *Rx1* and *Gpa2* (Slootweg et al. 2013). Replacement of 419-EEE in Gpa2 by uncharged amino acids leaves the tested properties of the full-length protein unchanged but disrupts the capability of the CC-NBS fragment to bind its LRR and to be activated by a modified Rx1 LRR in trans (Slootweg et al. 2013). Based on these results in combination with a structural docking model, the authors of the corresponding study predict that the protruding negatively charged loop forms an interface for the interaction with positively charged residues at the N-terminal end of the LRR. This electrostatic attraction would be important for reassociation of the receptor after an activation cycle (Slootweg et al. 2013). In PM3, the loop region is also occupied by three acidic amino acids (E457, E459, D460), but the fact that a basic histidine at position 458 is present in strong PM3 proteins evidently stands against the hypothesis that a particular charge is the essential feature of the ARC2 loop for an efficient R protein activity in the PM3 context. The amino acid substitution study at positions 456 and 458 in PM3C (Table

1) also did not indicate that a positive or a negative charge enhances the HR. We were not able to finally elucidate whether an enhanced HR and an expanded recognition specificity caused by P456/H458 in PM3F correlates with a stronger interaction between the CC-NBS and LRR domains (Fig. 6C).

A PM3-NBS model (Brunner et al. 2010) places the solvent exposed amino acids 456 and 458 at the extremity of the ARC2 subdomain that is not in contact with other parts of the NBS. Whereas amino acids that are directly involved in the binding or hydrolysis of ADP/ATP in the NBS often cause autoactivity when being mutated (van Ooijen et al. 2008b), the central ARC2 loop amino acids are obviously not involved in the formation of the ADP/ATP binding pocket but remain accessible at the NBS surface in models for the ADP-bound as well as the ATP-bound conformation (Brunner et al. 2010; Maekawa et al. 2011; Slootweg et al. 2013; Takken and Goverse 2012; van Ooijen et al. 2008a, 2008b). Consequently, we suspect that NBS interactions either with the CC or the LRR domain, with a guarded host protein, or with downstream signaling components might be modified. We can also not exclude that the enhancing effects of the ARC2 modifications are due to slight changes in the conformation of the NBS itself that make this molecular switch more sensitive to be turned on.

2.4.2 Evolution of the strong ARC2 haplotype.

The activity-enhancing *Pm3a/b*-specific ARC2 haplotype has an interesting evolutionary history. It is also found in a PM3-like protein from *Aegilops tauschii* as well as in PM8, the *Pm3* ortholog from rye (*Secale cereale*), and is conserved in PM3-like proteins from wheat homologous chromosome 1B (hPM3-1B) and barley (*Hordeum vulgare*). This indicates an ancient origin of this sequence block (Hurni et al. 2013). Interestingly, the presence of the proline-histidine haplotype in the ARC2 loop of hPM3-1B and PM8 also correlates with a fast and intensive HR in the *Nicotiana* expression system (Fig. 5A and C), suggesting conserved functional properties, even in more diverse genes (64% similarity between hPM3-1B and PM3CS). *Pm3CS* is the consensus sequence of all isolated *Pm3* alleles, was identified in tetraploid wheat accessions (Yahiaoui et al. 2009), and is consequently regarded as the ancestral *Pm3* allele in hexaploid wheat (Yahiaoui et al. 2006). It encodes the same CC-NBS domains as the narrow-spectrum allele *Pm3c*/*f* with its L456/Y458 haplotype, which we only found in *Pm3* homologues of tetraploid and hexaploid wheat but not of other related grass species (Wicker et al. 2007a). Thus, the following evolutionary scenario can be proposed. The ancestral gene of *Pm3* in the Triticeae family possessed an ARC2 sequence block for fast and intensive activity, but by the time that tetraploid wheat was domesticated, the *Pm3CS* sequence was established as an A-genome copy that was later transmitted to hexaploid bread

wheat. After this genetic bottleneck new *Pm3* alleles evolved (Yahiaoui et al. 2006) and three of them regained an ARC2 loop for an enhanced resistance signaling, most likely independently through gene conversion (*Pm3a/b*; Wicker et al. 2007b) or point mutations (*Pm3s*). We can only speculate about the evolutionary pressure leading to the interim benefit of the *Pm3CS*-ARC2, but climatic changes (Alcázar and Parker 2011) and redundant gene function or hybrid necrosis effects (Bomblies and Weigel 2007) after the polyploidization event might have played a role.

2.4.3 ARC2 loop modifications for applied resistance optimization.

The fact that natural selection led independently at least twice to the reacquisition of P456/H458 in PM3 since the domestication of wheat highlights the importance of the ARC2 loop and indicates that no negative aspects of possible *Pm3_L456P/Y458H*–resistance gene modifications are to be expected. Accordingly the results of this study may have implications for applications. Most obvious is the optimization of narrow-spectrum *Pm3* alleles as demonstrated here for *Pm3f* or the possible (re)activation of *Pm3* alleles that are so far classified as nonfunctional. Besides a transgenic approach to introduce the modified genes, genome editing technologies based on TALEN (transcription-activator-like-effector nucleases) (Li et al. 2012; Mahfouz et al. 2011) or CRISPR (clustered regularly interspaced short palindromic repeats) (Cong et al. 2013; Mali et al. 2013) hold great promise for such 'minimally invasive,' two-nucleotide resistance enhancement. We think that targeted adaptations or random mutagenesis of the ARC2 loop in other CC-NBS-LRR could also render some of them more effective or extend their resistance spectra. Good candidates for such an approach might be cloned *R* genes that mediate an intermediate resistance, indicating a residual recognition activity, or *R* genes that have just recently been overcome. We consider the wheat resistance gene *Sr33*, which gives intermediate resistance towards the Ug99 race of stem rust (Periyannan et al. 2013), or the LRR-mutagenized M1 variant of *Rx1*, which detects the coat protein of *Poplar mosaic virus* but does not mediate resistance against the latter (Farnham and Baulcombe 2006), as just two possible target gene options.

It remains to be determined how efficient in terms of resistance-spectrum extension, enhancement of intermediate resistance, or evasion of negative side effects such ARC2 loop modifications in different plant-pathogen systems can be. We consider it possible that additional positive effects, like temperature insensitivity of resistance might be achieved by such approaches of *R* gene improvement. In summary, the results of this study represent an additional step toward rational design of resistance proteins, and we demonstrate how gene optimization in a model system can be translated into enhanced crop resistance.

2.5 Materials and methods

2.5.1 Construction of plasmid vectors.

Genes were amplified by polymerase chain reaction from existing plasmids and were cloned into Gateway system compatible entry vectors via Gateway BP Clonase II reactions (Life Technologies, Carlsbad, CA, U.S.A.) or pENTR Directional TOPO Cloning (Life Technologies). Introduction of modifications and cloning of fragments were achieved by Gibson Assembly (NEB, Ipswich, MA, U.S.A.) or by the principle of the QuikChange site-directed mutagenesis kit (Stratagene, La Jolla, CA, U.S.A.). All resulting pENTR plasmids were recombined to the binary vector pIPKb004 (Himmelbach et al. 2007) carrying the double-enhanced *Cauliflower mosaic virus 35S* promoter by Gateway LR reaction (Life Technologies). Detailed primer and cloning information is available in Supplementary Tables S1 and S2.

2.5.2 *Agrobacterium* infiltration procedure.

Binary plasmids were transformed via electroporation into *Agrobacterium tumefaciens* GV3101 (pMP90) (Koncz and Schell 1986). Bacteria were grown overnight in Luria Bertani medium supplemented with appropriate antibiotics, were harvested by centrifugation at 2,500 × *g* for 15 min, and were resuspended and diluted in infiltration medium (10 mM morpholineethanesulfonic acid, pH 5.6, 10 mM MgCl2, 150 µM acetosyringone) to an optimal density at 600 nm = 0.8. After 2 to 4 h of incubation at room temperature, one or more cultures were mixed in a 1:1 or 1:1:1 ratio with an equally treated *Agrobacterium* p19-silencing-suppressor strain (Voinnet et al. 2003) and were infiltrated with a needleless syringe into the abaxial side of leaves from 4- to 5-week-old *Nicotiana benthamiana*. Plants were subsequently kept at room temperature in a glasshouse.

2.5.3 Ion leakage measurements.

Ion leakage was measured with the CM100-2 multiple cell conductivity meter (Reid & Associates, Johannesburg, South Africa). Two leaf discs (7 mm diameter) were collected from an infiltrated spot at 17 hpi and were transferred separately into 1.5 ml of double distilled H2O, and conductivity was measured hourly. For better comparability among replicates, all constructs of a *Pm3* infiltration set were harvested from the same leaf. Two experiments, each with four individual plants or leaves per set were conducted.

2.5.4 Protein detection.

Protein detection from four pooled leaf discs (5 mm diameter) per infiltrated area was performed essentially as described by Brunner and associates (2012), except for not having polyvinylpolypyrrolidone (PVPP) in the extraction buffer and using the Chemidoc XRS system (Bio-Rad, Hercules, CA, U.S.A.) for blot development instead of X-ray film. Samples were collected 15 h after the *Agrobacterium* infiltration. Protein levels were compared between samples from the same leaf.

2.5.5 Transient resistance assay and leaf segment infection test.

Wheat seedling leaf infection tests as well as the transient resistance assay with leaves from 7-day-old plants of wheat cultivar Chancellor were performed as described by Brunner and associates (2010). pUbi-GUS reporter plasmid (1.5 µg) together with 1.5 µg of a tested pIPKb004-Pm3 construct were used per particle bombardment. At least 50 interactions per construct, isolate, and independent experiment were scored. The wheat powdery mildew *(B. graminis* f. sp. *tritici)* isolates 96224 and 97028 originate from the former mildew collection of Agroscope, Reckenholz-Tänikon, Switzerland and isolate AK3-11 is from USDA-ARS, North Carolina State University, Raleigh, NC, U.S.A.

2.5.6 Coimmunoprecipitation.

For coimmunoprecipitation experiments, protein extracts were prepared as described by Sacco and associates (2007) with a few modifications, i.e., 1 g of coinfiltrated *Nicotiana benthamiana* leaf material harvested 48 hpi was ground in liquid nitrogen, was resuspended in 3 ml of ice-cold extraction buffer (GTEN [10% {vol/vol} glycerol; 25 mM Tris-HCl, pH 7.5; 1 mM EDTA; 150 mM NaCl], 10 mM dithiothreitol [DTT], 2% [wt/vol] PVPP, and 1 tablet per 10 ml of complete mini protease inhibitor cocktail [Roche Diagnostics, Mannheim, Germany]) and was cleared by two centrifugation steps at 16,000 × *g* for 5 min each at 4°C. Nonidet P-40 (NP-40) in 100 µl of IP buffer (GTEN, 2 mM DTT, 1 tablet per 20 ml of complete mini protease inhibitor) was added to 1.9 ml of protein extract for a final concentration of 0.15% (vol/vol). HA epitope–tagged protein was immunoprecipitated with 35 µl of anti-HA affinity matrix (Roche Diagnostics) by end-over-end incubation for 1 h at 4°C. Agarose beads were washed four times with 1 ml of IP buffer containing 0.15% (vol/vol) NP-40 and were resuspended in 40 µl of 1× Laemmli buffer (Laemmli 1970). Subsequent protein detection was performed as described above. For detection of myc-tagged proteins, 1:4,000 dilutions of anti-c-myc primary antibodies (rat monoclonal, clone JAC6, sc-56633; Santa Cruz Biotechnology, Santa Cruz, CA, U.S.A.) were used.

2.5.7 Sequence alignments.

Nucleotide as well as protein sequence alignments were done with CLC Main Workbench version 6.8.4 (CLC Bio, Aarhus, Denmark), using the standard settings.

2.6 Acknowledgments

We thank D. Peditto for excellent substantial technical support with plasmid clonings, agroinfiltrations, ion leakage assays, and protein work. We are grateful to S. Hurni for providing the *Pm8* plasmids and *hPm3-1B* DNA and to J. Kumlehn for providing the pIPKb004 vector. This work was supported by an Advanced Investigator Grant from the European Research Council (ERC-2009-AdG 249996, Durable resistance) and Swiss National Science Foundation grant 310030B_144081/1.

D. Stirnweis, B. Keller, and S. Brunner designed the project. D. Stirnweis designed the experiments, performed protein work, wrote the manuscript, and prepared figures. D. Stirnweis and S. D. Milani performed cloning work, agroinfiltrations, and ion leakage assays. D. Stirnweis, T. Jordan, and S. Brunner performed the transient resistance assay and discussed results. D. Stirnweis, T. Jordan, B. Keller, and S. Brunner revised the manuscript.

2.7 Note added in proof

By random mutagenesis, Harris and associates (2013) recently discovered amino acid substitutions in the NB and ARC1 subdomains that enhance the HR and resistance activity of Rx1 in a similar manner as described for PM3 in this study. None of the identified substitution sites in Rx1 match with the polymorphic amino-acid positions in PM3B compared with other PM3 that might explain the strong HR of PM3B_P456L/H458Y.

2.8 Supplementary material

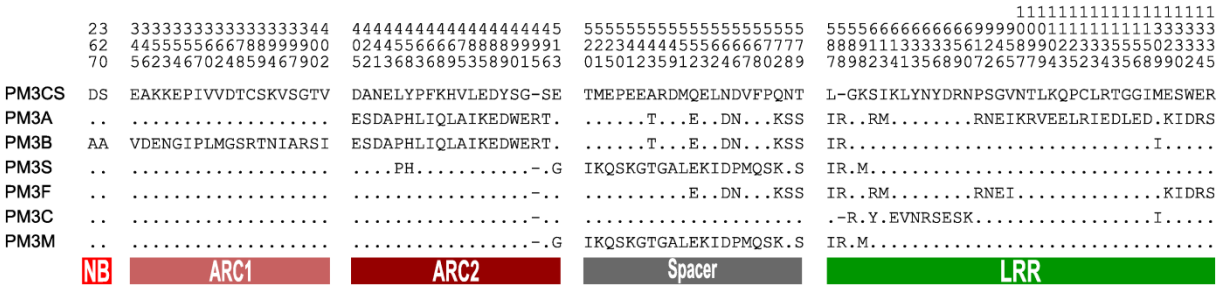

Supplementary Fig. S1 Amino acid polymorphisms in the PM3CS/A/B/S/F/C/M proteins. The first sequence lists the residues of PM3CS at the polymorphic sites (vertical numbers give the corresponding amino acid positions in the PM3A/B protein). Below the PM3CS sequence, the polymorphic residues in the additional PM3 proteins are indicated. Dots represent residues identical to those in PM3CS and deletions are shown as dashes. The alignment is arranged in blocks according to the PM3 domain structure with the NB (red), ARC1 (salmon), ARC2 (dark red), Spacer (gray) an d LRR (green) (sub)domains.

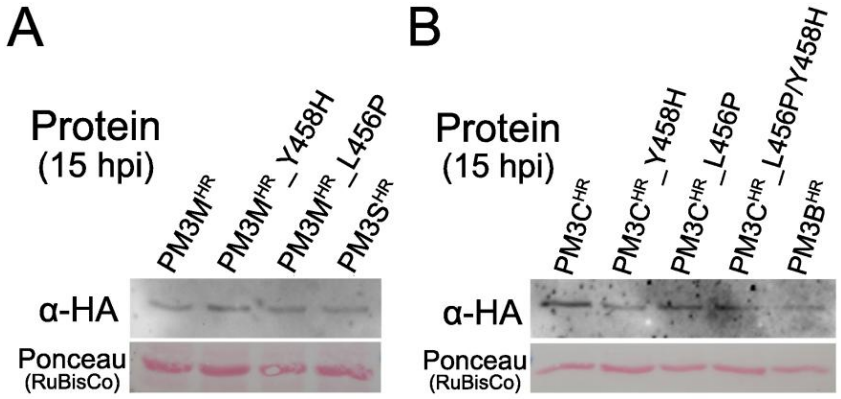

Supplementary Fig. S2 The faster and more intense hypersensitive response (HR) mediated by strong PM3 proteins is not due to a higher protein abundance. Similar protein levels were detected for all PM3 HR variants shortly before the first HR induction (15 hpi) within the PM3M/S (**A**) and the PM3B/C (**B**) infiltration sets. Western blot analysis of protein extracts from infiltrated regions expressing different hemagglutinin (HA) epitope-tagged PM3^{HR} constructs from one leaf. Ponceau S membrane staining of Ribulose-1,5-bis-phosphate carboxylase/oxygenase (Rubisco) is shown as control for equal loading of total protein.

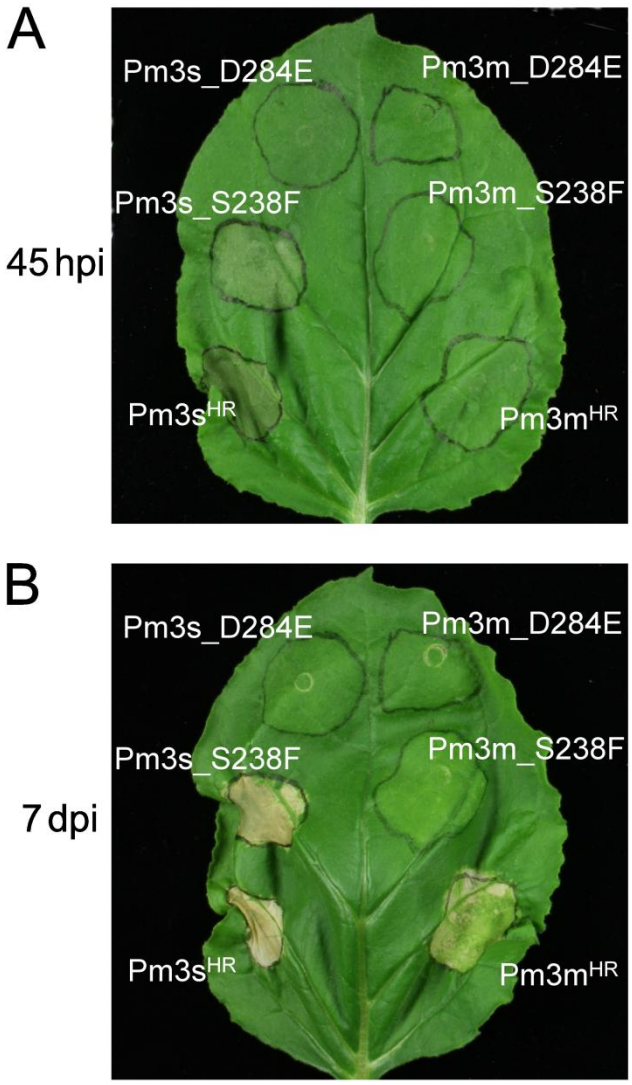

Supplementary Fig. S3 The enhanced hypersensitive response (HR) induction of *Pm3s* compared with *Pm3m* is independent of a particular autoactivating mutation. **A** and **B,** Autoactivating mutations in the MHD (D501V = ^{HR}) or the RNBS-A (S238F) motif both led to a HR induction by *Pm3s* that was faster and more intense than by *Pm3m*. The D284E mutation (Walker B motif) did not render *Pm3* autoactive. Representative pictures of an infiltrated leaf at 45 hpi (A) and 7 dpi (B) are shown.

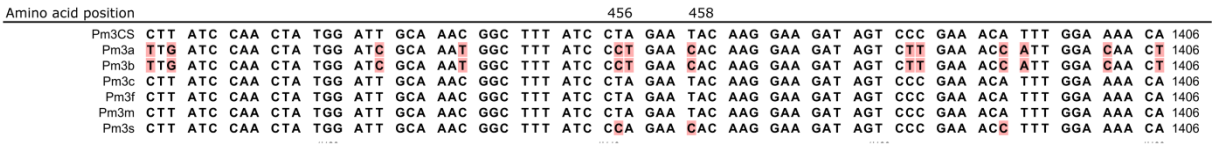

Supplementary Fig. S4 Independent evolutionary events led to the codons for proline 456 and histidine 458 in *Pm3a/b* in comparison with *Pm3s*. Nucleotide sequence alignment of *Pm3* alleles shows that the sequence for amino acid 456 differs between *Pm3a/b* and *Pm3s* and polymorphisms in the close vicinity of this codon are not conserved between these alleles. Nucleotide differences in comparison to *Pm3CS* are highlighted in red.

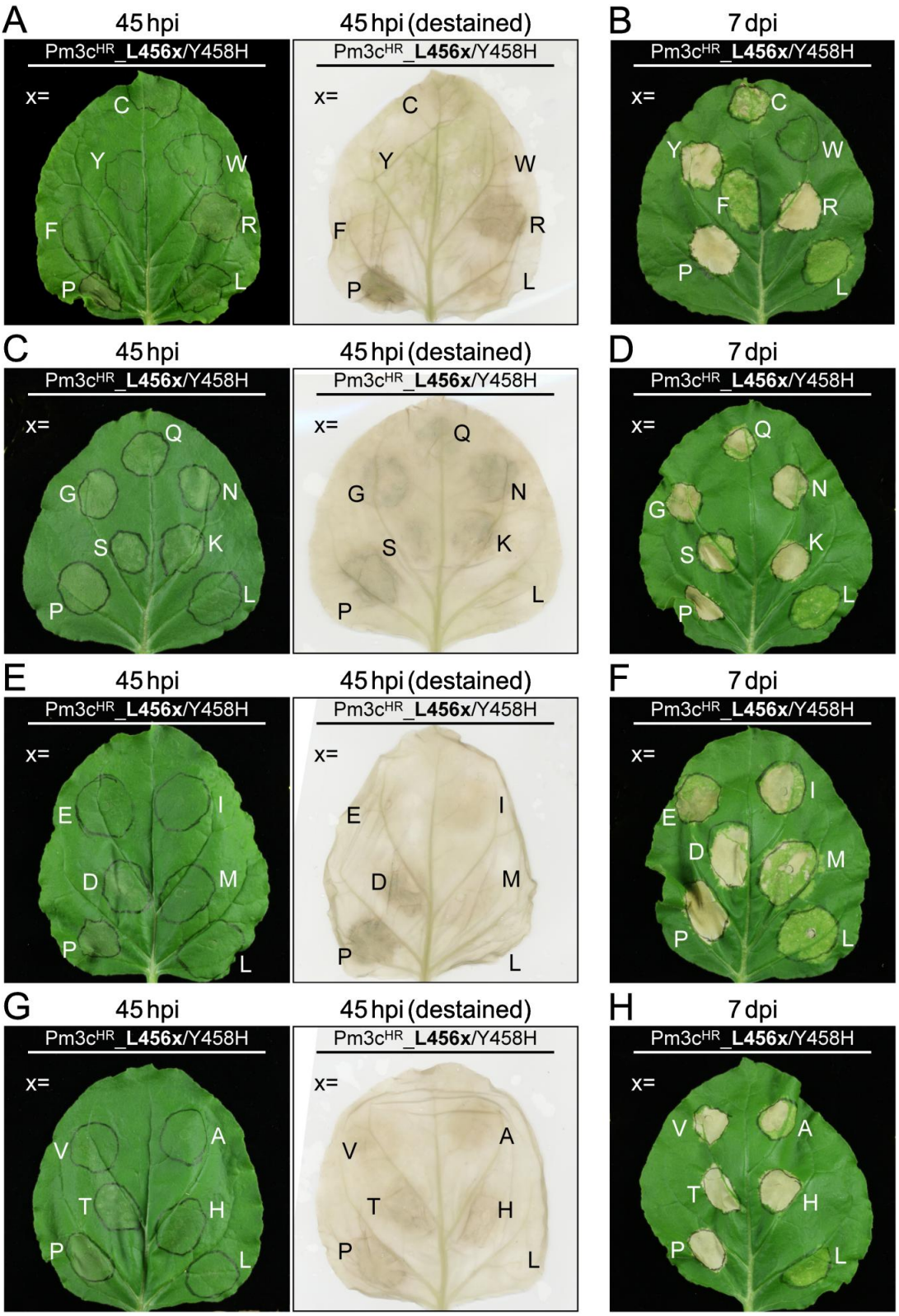

Supplementary Fig. S5 Effects of amino acid substitutions at position 456 on hypersensitive response (HR) in an autoactivated PM3C^{HR} variant carrying the Y458H substitution of the strong HR-inducing L456P/Y458H variant. Examplary pictures of agroinfiltrated *Nicotiana* leaves harvested at 45 hpi (also destanined in 100% ethanol) (**A/C/E/G**) and at 7 dpi (**B/D/F/H**) are shown. Infiltated areas with the weak HR-inducing initial construct Pm3c^{HR}_Y458H (x=L) and the strongest HR-inducing construct Pm3c^{HR}_L456P/Y458H (x=P) serve as references on each infiltrated leaf. Infiltrations were repeated 3 times. Due to variable phenotypes these pictures cannot be representative for all constructs. Detailed information is given in Table 1 in the main text.

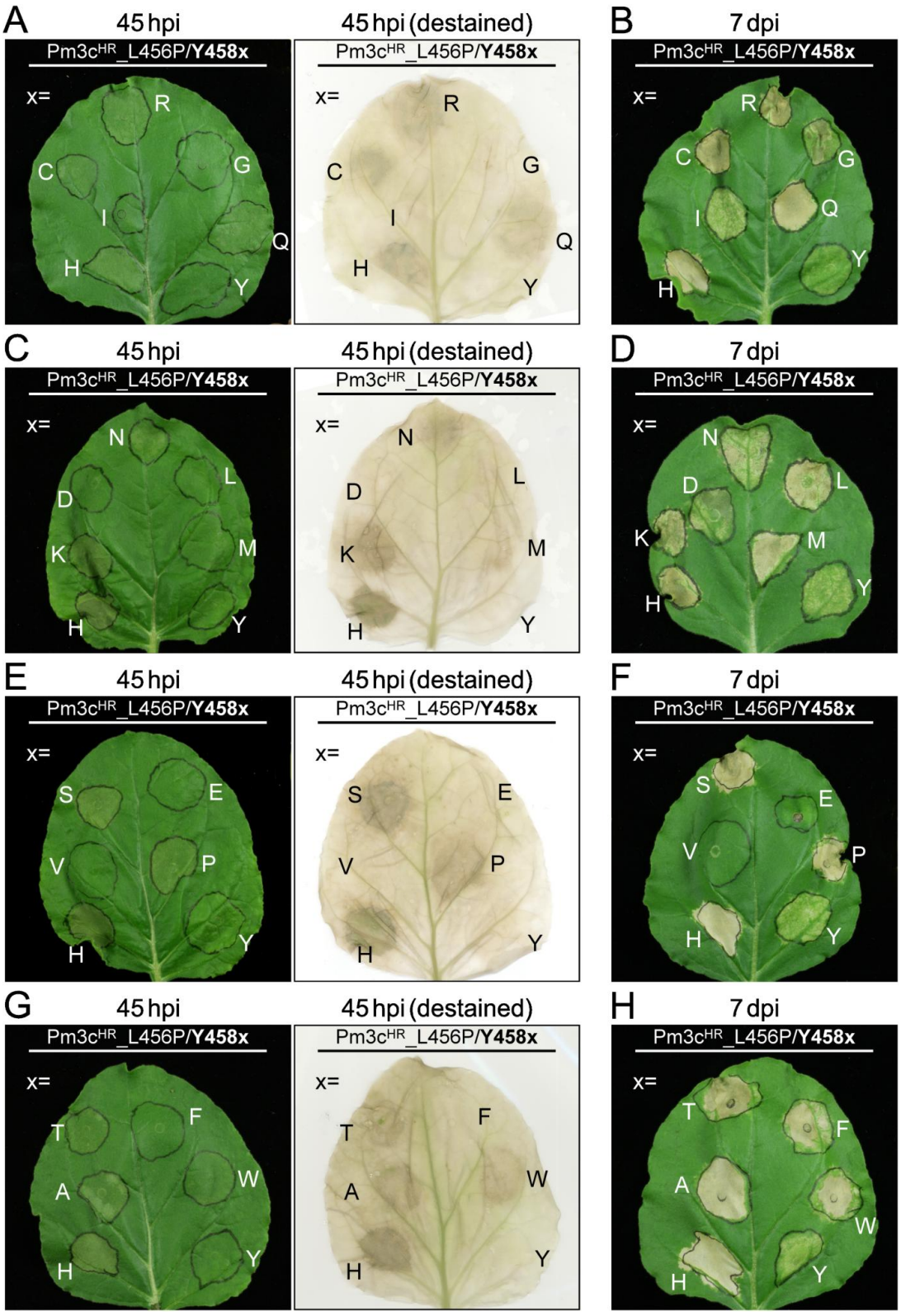

Supplementary Fig. S6 Effects of amino acid substitutions at position 458 on hypersensitive response (HR) in an autoactivated PM3C^{HR} variant carrying the L456P substitution of the strong HR-inducing L456P/Y458H variant. Examplary pictures of agroinfiltrated *Nicotiana* leaves harvested at 45 hpi (also destained in 100% ethanol) (**A/C/E/G**) and at 7 dpi (**B/D/F/H**) are shown. Infiltrated areas with the weak HR-inducing initial construct Pm3c_L456P (x=Y) and the strongest HR-inducing construct Pm3c^{HR}_L456P/Y458H (x=H) serve as references on each infiltrated leaf. Infiltrations were repeated 3 times. Due to variable phenotypes these pictures cannot be representative for all constructs. Detailed information is given in Table 1 in the main text. For the construct Pm3c^{HR}_L456P/Y458E no PM3 protein was detected.

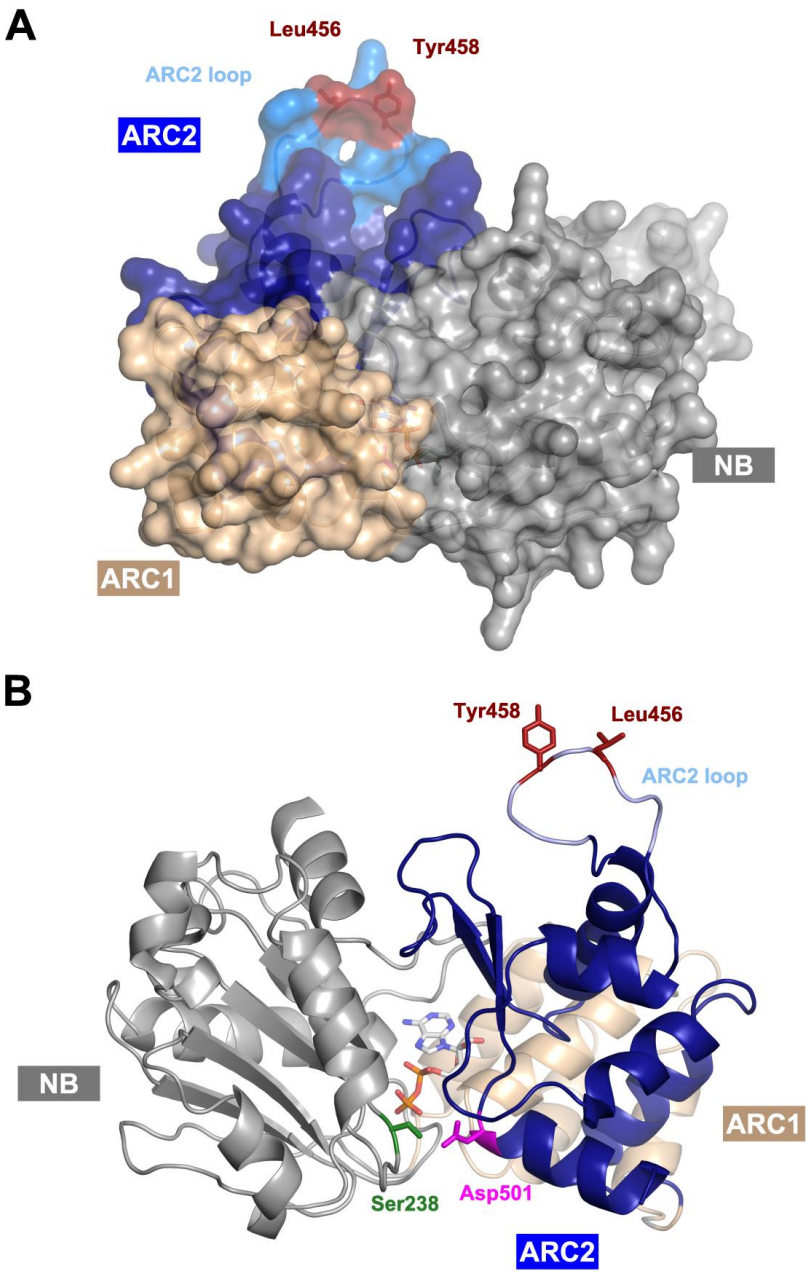

Supplementary Fig. S7 Model of the ADP bound nucleot ide binding (NB) site protein structure of PM3CS adapted from Brunner et al. (2010). **A,** A surface model in frontside view and **B,** a cartoon model in backside view is shown. The NB subdomain is colored in gray, the ARC1 subdomain in lightorange. The ARC2 subdomain is colored in blue with the ARC2 loop in lightblue and the HR modulating amino acids leucine 456 and tyrosine 458 highlighted in red with side chains. The amino acids serine 238 (green) and aspartate 501 (magenta) that were mutated to render PM3 autoactive for this study (S238F and D501V) are accentuated (B). Bound ADP is represented as sticks in CPK atom colors.

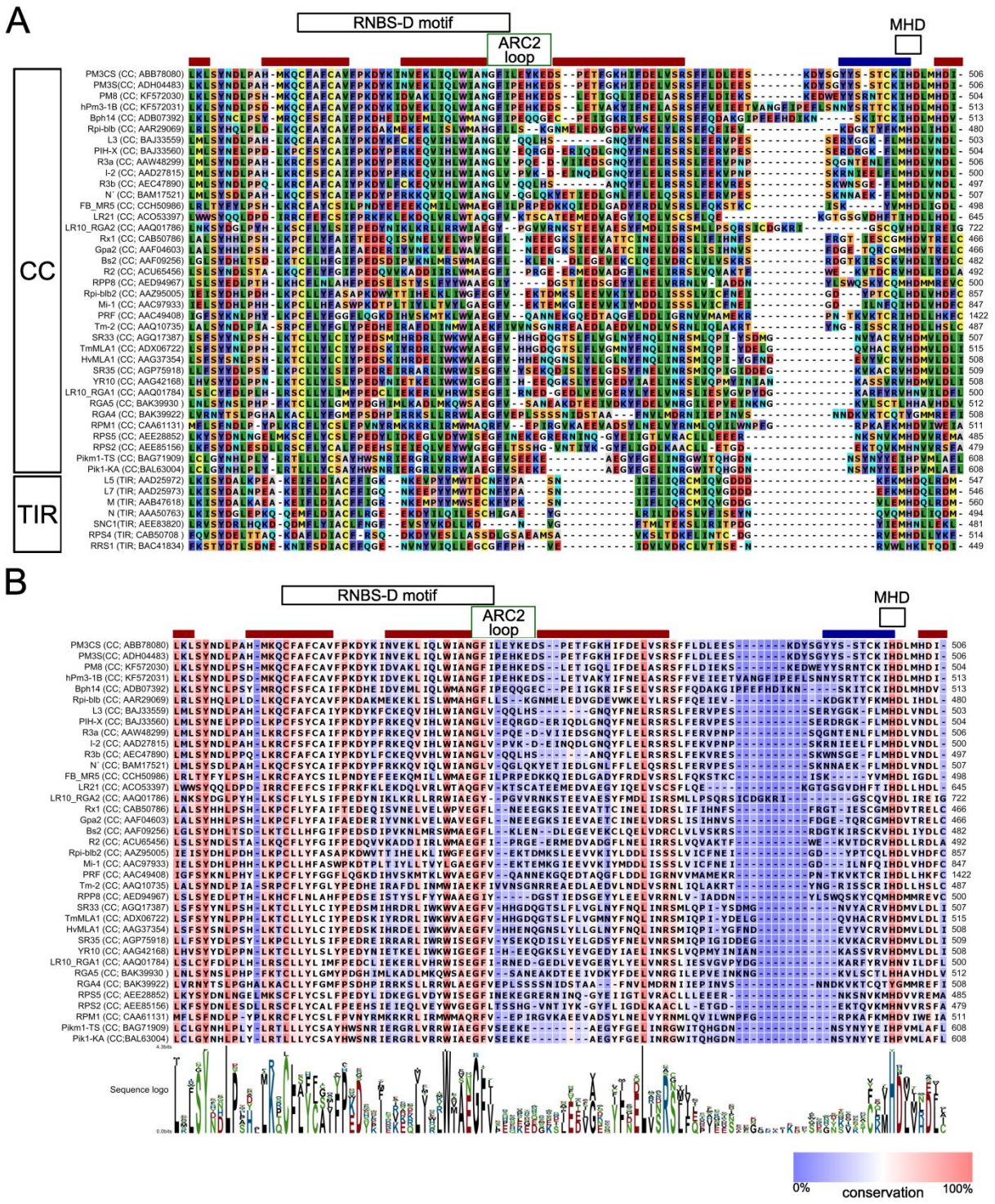

Supplementary Fig. S8 The amino acid sequence of the ARC2 loop is not found in toll interleukin 1 receptor-nucleotide binding site-leucine-rich repeat (TIR-NBS-LRR) proteins and is not conserved in coiled coil (CC)-NBS-LRR proteins except for the two amino acids overlapping with the RNBS-D-motif. **A,** Alignment of protein sequences of numerous TIR- and CC-NBS-LRR proteins with background color indicating amino acid properties according to Rasmol color code (Sayle and Milner-White 1995). **B,** Alignment of numerous CC-NBS-LRR protein sequences with background color and sequence logo indicating the conservation level of the respective amino acid position. A and B, In the top panels red (α-helix) and blue (β-sheet) bars show the predicted secondary structure for PM3CS according to the PM3-NBS-model of Brunner et al. (2010) and the green box labels the ARC2 loop for PM3CS. Black boxes mark the positions of the RNBS-D (Meyers et al. 2003) and MHD motifs.

Supplementary Table S1 List of primers used in this study.

Primer name	primer sequence 5`--> 3`
cint10R	CAGTATCTGGAAGCCACTCA
dst015	GCACATGTAAAATTCATGTTCTTATGCATGATATTGC
dst016	GCAATATCATGCATAAGAACATGAATTTTACATGTGC
dst039	CAACATGTAAAATCCACGTTCTTATGCATGATATTGC
dst040	GCAATATCATGCATAAGAACGTGGATTTTACATGTTG
dst041	ATACATGTAAAATCCACGTTCTTATGCATGATATTGC
dst042	GCAATATCATGCATAAGAACGTGGATTTTACATGTAT
dst048	CACCATGGCAGAGCTGGTGGTCAC
dst049	TCACAAATCTTCTTCAGAAATCAACTTTTGTTCGCTCCGGCAGGCCTGCCTCCGC
dst050	CACCATGGCAGAGCGGGTGGTCAC
dst051	TCAAGCATAATCTGGAACATCG
dst057	GGGGACAAGTTTGTACAAAAAAGCAGGCTATGGCAGAGCGGGTGG
dst058	CCGAGATCAGCTTCTGCTCGCTCCGGCAGGCCTGC
dst059	GGGGACCACTTTGTACAAGAAAGCTGGGTTCACAGGTCTTCCTCCGAGATCAGCTTCTGCTC
dst060	GGGGACAAGTTTGTACAAAAAAGCAGGCTATGGAAATTGAGTGGCTTCCAG
dst061	GGGGACCACTTTGTACAAGAAAGCTGGGTTCAAGCATAATCTGGAACATCGTATGGATAGCTCCGGCAGGCCTGCCTCCG
dst077	GCAAACGGCTTTATCCCAGAATACAAGGAAGATAG
dst078	CTATCTTCCTTGTATTCTGGGATAAAGCCGTTTGC
dst079	CGGCTTTATCCTAGAACACAAGGAAGATAGTCCCG
dst080	CGGGACTATCTTCCTTGTGTTCTAGGATAAAGCCG
dst081	GCTCTGGGTTTGTGTCTTTGATACCTTTGATGTG
dst082	CACATCAAAGGTATCAAAGACACAAACCCAGAGC
dst083	CTCCTTGTATTGGATGAGGTTTGGGACAACAAAG
dst084	CTTTGTTGTCCCAAACCTCATCCAATACAAGGAG
dst089	GGGGACCACTTTGTACAAGAAAGCTGGGTTCAAGCATAATCTGGAACATCG
dst097	CCGAGATCAGCTTCTGCTCCGTGGTTGTCATCCTGTTTTC
dst098	GGGGACAAGTTTGTACAAAAAAGCAGGCTATGGCGGAGCTATTGGCCAC
dst099	AACGGCTTTATCCCAGAACACAAGGAAGATAGTCC
dst100	CTATCTTCCTTGTGTTCTGGGATAAAGCCGTTTGC
dst103	TATCCATACGATGTTCCAG
dst106	CAACATGCAAAATCCATGTTCTTATGCATGATATTGC
dst107	GCAATATCATGCATAAGAACATGGATTTTGCATGTTG
dst119	GCAAATGGCTTTATCCTTGAATACAAGGAAGATAGTCTTG
dst120	ACTATCTTCCTTGTATTCAAGGATAAAGCCATTTGCGATC
dst139	CACCATGGCGGAGCTAATGGCCA
dst140	CTACTTCAAGCACATCAGCCTAC
dst150	TACTTGTAAGATCCATGTCCTTATGCATGATGTTGCAC
dst151	GCAACATCATGCATAAGGACATGGATCTTACAAGTAATC
dst153	ATGGTTTTATCCCAGAGCACCAAGGAGAGTGCCCTGAAATC
dst154	TTTCAGGGCACTCTCCTTGGTGCTCTGGGATAAAACCATTG
dst155	TGGGTTCAAGCATAATCTGGAACATCGTATGGATAACTTGGTTCCATAGTTGCAAC
dst160	ATGGCCAATGGTTTTATCCTAGAGCAACAAGGAGAGTG
dst161	CACTCTCCTTGTTGCTCTAGGATAAAACCATTGGCCAT
dst199	CCAACTATGGATTGCAAACGGCTTTATCTDSGAACACAAGGAAGATAGTCC
dst200	CCAACTATGGATTGCAAACGGCTTTATCVGCGAACACAAGGAAGATAGTCC
dst201	CCAACTATGGATTGCAAACGGCTTTATCVASGAACACAAGGAAGATAGTCC
dst202	CCAACTATGGATTGCAAACGGCTTTATCRYSGAACACAAGGAAGATAGTCC
dst203	GATAAAGCCGTTTGCAATC
dst204	ATGGATTGCAAACGGCTTTATCCCAGAADTSAAGGAAGATAGTCCCGAAAC
dst205	ATGGATTGCAAACGGCTTTATCCCAGAADGSAAGGAAGATAGTCCCGAAAC
dst206	ATGGATTGCAAACGGCTTTATCCCAGAAVAKAAGGAAGATAGTCCCGAAAC
dst207	ATGGATTGCAAACGGCTTTATCCCAGAAVCCAAGGAAGATAGTCCCGAAAC
dst208	TTCTGGGATAAAGCCGTTTG
dst211	ATGGATTGCAAACGGCTTTATCCCAGAATTTAAGGAAGATAGTCCCGAAAC
dst212	ATGGATTGCAAACGGCTTTATCCCAGAAAACAAGGAAGATAGTCCCGAAAC
dst219	GCAAATGGCTTTATCTTAGAATACAAGGAAGACAGTCTTG
dst220	ACTGTCTTCCTTGTATTCTAAGATAAAGCCATTTGCGATC
dst225	GCAAATGGCTTTATCTTAGAACACAAGGAAGATAGTCTTG
dst226	ACTATCTTCCTTGTGTTCTAAGATAAAGCCATTTGCGATC
dst227	GCAAATGGCTTTATCCCAGAGTACAAGGAAGATAGTCTTG

Supplementary Table S2 Detailed information on the cloning of the Gateway pENTR plasmids used in this study.

plasmid	cloning method	vector backbone	source plasmid	origin of source plasmid	cloning procedure	primers used
pENTR221-Pm3c-HA (gDNA)	Gateway BP cloning	pDONR221	pAHC17-Pm3c-HA (gDNA)	Brunner et al., 2012	PCR (dst057-dst089)	dst057, dst089
pENTR221-Pm3c^{HR}-HA (gDNA)	site-directed mutagenesis PCR		pENTR221-Pm3c-HA (gDNA)	this study	mutagenesis PCR (dst015-dst016)	dst015, dst016
pENTR221-Pm3c^{HR}_L456P-HA (gDNA)	site-directed mutagenesis PCR		pENTR221-Pm3c^{HR}-HA (gDNA)	this study	mutagenesis PCR (dst077-dst78)	dst077, dst078
pENTR221-Pm3c^{HR}_Y458H-HA (gDNA)	site-directed mutagenesis PCR		pENTR221-Pm3c^{HR}-HA (gDNA)	this study	mutagenesis PCR (dst079-dst80)	dst079, dst080
pENTR221-Pm3c^{HR}_L456P/Y458H-HA (gDNA)	site-directed mutagenesis PCR		pENTR221-Pm3c^{HR}_L456P-HA (gDNA)	this study	mutagenesis PCR (dst099-dst100)	dst099, dst100
pENTR221-Pm3b-HA (gDNA)	Gateway BP cloning	pDONR221	pAHC17-Pm3b	Brunner et al., 2011	PCR (dst057-dst061)	dst057, dst061
pENTR221-Pm3b^{HR}-HA (gDNA)	site-directed mutagenesis PCR		pENTR221-Pm3b-HA (gDNA)	this study	mutagenesis PCR (dst039-dst040)	dst039, dst040
pENTR221-Pm3f-HA (gDNA)	Gateway BP cloning	pDONR221	pAHC17-Pm3f-HA (gDNA)	Brunner et al., 2012	PCR (dst057-dst089)	dst057, dst089
pENTR221-Pm3f^{HR}-HA (gDNA)	site-directed mutagenesis PCR		pENTR221-Pm3f-HA (gDNA)	this study	mutagenesis PCR (dst015-dst016)	dst015, dst016
pENTR221-Pm3a-HA (gDNA)	Gateway BP cloning	pDONR221	pAHC17-Pm3a-HA (gDNA)	Brunner et al., 2012	PCR (dst057-dst089)	dst057, dst089
pENTR221-Pm3a^{HR}-HA (gDNA)	site-directed mutagenesis PCR		pENTR221-Pm3a-HA (gDNA)	this study	mutagenesis PCR (dst039-dst040)	dst039, dst040
pENTR221-Pm3a^{HR}_P456L/H458Y-HA (gDNA)	site-directed mutagenesis PCR		pENTR221-Pm3a^{HR}-HA (gDNA)	this study	mutagenesis PCR (dst119-dst120)	dst119, dst120
pENTR221-Pm3f^{HR}_L456P/Y458H-HA (gDNA)	site-directed mutagenesis PCR		pENTR221-Pm3f^{HR}-HA (gDNA)	this study	mutagenesis PCR (dst099-dst100)	dst099, dst100
pENTR221-Pm3f_L456P/Y458H-HA (gDNA)	site-directed mutagenesis PCR		pENTR221-Pm3f-HA (gDNA)	this study	mutagenesis PCR (dst099-dst100)	dst099, dst100
pENTR221-Pm3m-HA (gDNA)	Gateway BP cloning	pDONR221	pGY1-Pm3_42255	Bhullar et al., 2009	PCR (dst057-dst61)	dst057, dst061
pENTR221-Pm3m^{HR}-HA (gDNA)	site-directed mutagenesis PCR		pENTR221-Pm3m-HA (gDNA)	this study	mutagenesis PCR (dst015-dst016)	dst015, dst016
pENTR221-Pm3m^{HR}_L456P-HA	site-directed mutagenesis PCR		pENTR221-Pm3m^{HR}-HA (gDNA)	this study	mutagenesis PCR (dst077-dst078)	dst077, dst078
pENTR221-Pm3m^{HR}_Y458H-HA	site-directed mutagenesis PCR		pENTR221-Pm3m^{HR}-HA (gDNA)	this study	mutagenesis PCR (dst079-dst80)	dst079, dst080
pENTR221-Pm3s-HA (gDNA)	Gateway BP cloning	pDONR221	pGY1-Pm3_4650	Bhullar et al., 2010	PCR (dst057-dst061)	dst057, dst061
pENTR221-Pm3s^{HR}-HA (gDNA)	site-directed mutagenesis PCR		pENTR221-Pm3s-HA (gDNA)	this study	mutagenesis PCR (dst015-dst016)	dst015, dst016
pENTR-GUS	delivered as control in the kit		Gateway LR clonase II kit	life technologies, Carlsbad, CA		
pENTR221-Pm3b^{HR}_P456L/H458Y-HA (gDNA)	site-directed mutagenesis PCR		pENTR221-Pm3b^{HR}-HA (gDNA)	this study	mutagenesis PCR (dst119-dst120)	dst119, dst120
pENTR221-Pm3m_S238F-HA (gDNA)	site-directed mutagenesis PCR		pENTR221-Pm3m-HA (gDNA)	this study	mutagenesis PCR (dst081-dst82)	dst081, dst082
pENTR221-Pm3s_S238F-HA (gDNA)	site-directed mutagenesis PCR		pENTR221-Pm3s-HA (gDNA)	this study	mutagenesis PCR (dst081-dst82)	dst081, dst082
pENTR221-Pm3m_D284E-HA (gDNA)	site-directed mutagenesis PCR		pENTR221-Pm3m-HA (gDNA)	this study	mutagenesis PCR (dst083-dst084)	dst083, dst084
pENTR221-Pm3s_D284E-HA (gDNA)	site-directed mutagenesis PCR		pENTR221-Pm3s-HA (gDNA)	this study	mutagenesis PCR (dst083-dst084)	dst083, dst084
pENTR-D-Pm3CS-HA (gDNA)	Directional TOPO Cloning	pENTR-D-TOPO	pGY1-Pm3CS (gDNA)	Brunner et al., 2010	PCR (dst050-dst061), then PCR (dst050-dst051)	dst050, dst061, dst051
pENTR221-Pm3f-a_{ARC}-HA (gDNA)	Gateway BP cloning	pDONR221	pGY1-Pm3f-a_{ARC}	Brunner et al., 2010	PCR (dst057-dst061)	dst057, dst061
pENTR221-Pm3c^{HR}_**L456F/Y/C/W** /Y458H-HA (gDNA)	site-directed mutagenesis PCR		pENTR221-Pm3c^{HR}_Y458H-HA (gDNA)	this study	mutagenesis PCR (dst199-dst203)	dst199, dst203
pENTR221-Pm3c^{HR}_**L456R/S/G** /Y458H-HA (gDNA)	site-directed mutagenesis PCR		pENTR221-Pm3c^{HR}_Y458H-HA (gDNA)	this study	mutagenesis PCR (dst200-dst203)	dst200, dst203
pENTR221-Pm3c^{HR}_**L456H/Q/N/K/D/E** /Y458H-HA (gDNA)	site-directed mutagenesis PCR		pENTR221-Pm3c^{HR}_Y458H-HA (gDNA)	this study	mutagenesis PCR (dst201-dst203)	dst201, dst203
pENTR221-Pm3c^{HR}_**L456I/M/T/V/A** /Y458H-HA (gDNA)	site-directed mutagenesis PCR		pENTR221-Pm3c^{HR}_Y458H-HA (gDNA)	this study	mutagenesis PCR (dst201-dst203)	dst202, dst203
pENTR221-Pm3c^{HR}_L456P/**Y458L/I/M/V**-HA (gDNA)	site-directed mutagenesis PCR		pENTR221-Pm3c^{HR}_L456P-HA (gDNA)	this study	mutagenesis PCR (dst204-dst208)	dst204, dst208
pENTR221-Pm3c^{HR}_L456P/**Y458C/W/S/R/G**-HA (gDNA)	site-directed mutagenesis PCR		pENTR221-Pm3c^{HR}_L456P-HA (gDNA)	this study	mutagenesis PCR (dst205-dst208)	dst205, dst208
pENTR221-Pm3c^{HR}_L456P/**Y458Q/K/E/D**-HA (gDNA)	site-directed mutagenesis PCR		pENTR221-Pm3c^{HR}_L456P-HA (gDNA)	this study	mutagenesis PCR (dst206-dst208)	dst206, dst208
pENTR221-Pm3c^{HR}_L456P/**Y458P/T/A**-HA (gDNA)	site-directed mutagenesis PCR		pENTR221-Pm3c^{HR}_L456P-HA (gDNA)	this study	mutagenesis PCR (dst207-dst208)	dst207, dst208
pENTR221-Pm3c^{HR}_L456P/**Y458F**-HA (gDNA)	site-directed mutagenesis PCR		pENTR221-Pm3c^{HR}_L456P-HA (gDNA)	this study	mutagenesis PCR (dst211-dst208)	dst211, dst208
pENTR221-Pm3c^{HR}_L456P/**Y458N**-HA (gDNA)	site-directed mutagenesis PCR		pENTR221-Pm3c^{HR}_L456P-HA (gDNA)	this study	mutagenesis PCR (dst212-dst208)	dst212, dst208
pENTR-D-Pm8-myc (gDNA)	Directional TOPO Cloning	pENTR-D-TOPO	pAHC17-Pm8-myc (gDNA)	Hurni et al., 2013	PCR (dst048-dst049)	dst048, dst049
pENTR-D-Pm8^{HR}-myc (gDNA)	site-directed mutagenesis PCR		pENTR-D-Pm8-myc (gDNA)	this study	mutagenesis PCR (dst041-dst042)	dst041, dst042
pENTR-D-Pm8^{HR}_P453L/H455Y-myc (gDNA)	site-directed mutagenesis PCR		pENTR-D-Pm8^{HR}-myc (gDNA)	this study	mutagenesis PCR (dst219-dst220)	dst219, dst220
pENTR221-hPm3-1B-myc (gDNA)	Directional TOPO Cloning	pENTR-D-TOPO	genomic DNA wheat cv. Chancellor	this study	PCR (dst097-SH41), then PCR (dst098-dst059)	dst097, SH41, dst098, dst059
pENTR221-hPm3-1B^{HR}-myc (gDNA)	site-directed mutagenesis PCR		pENTR221-hPm3-1B-myc (gDNA)	this study	mutagenesis PCR (dst106-dst107)	dst106, dst107
pENTR221-hPm3-1B^{HR}_P455L-myc (gDNA)	site-directed mutagenesis PCR		pENTR221-hPm3-1B^{HR}-myc (gDNA)	this study	mutagenesis PCR (dst225-dst226)	dst225, dst226
pENTR221-hPm3-1B^{HR}_H457Y-myc (gDNA)	site-directed mutagenesis PCR		pENTR221-hPm3-1B^{HR}-myc (gDNA)	this study	mutagenesis PCR (dst227-dst228)	dst227, dst228
pENTR221-hPm3-1B^{HR}_P455L/H457Y-myc (gDNA)	site-directed mutagenesis PCR		pENTR221-hPm3-1B^{HR}-myc (gDNA)	this study	mutagenesis PCR (dst119-dst120)	dst119, dst120
pENTR-D-Bph14 (gDNA)	Directional TOPO Cloning	pENTR-D-TOPO	pCAMBIA1301-Bph14 (*Ra* , 9.6kb)	Du et al., 2009	PCR (dst139-dst140)	dst139, dst140
pENTR-D-Bph14^{HR} (gDNA)	site-directed mutagenesis PCR		pENTR-D-Bph14 (gDNA)	this study	mutagenesis PCR (dst150-dst151)	dst150, dst151
pENTR-D-Bph14^{HR}_P460L (gDNA)	site-directed mutagenesis PCR		pENTR-D-Bph14^{HR} (gDNA)	this study	mutagenesis PCR (dst160-dst161)	dst160, dst161
pENTR-D-Bph14^{HR}_Q462H (gDNA)	site-directed mutagenesis PCR		pENTR-D-Bph14^{HR} (gDNA)	this study	mutagenesis PCR (dst153-dst154)	dst153, dst154
pENTR-D-Bph14^{HR}_P460L/Q462H (gDNA)	site-directed mutagenesis PCR		pENTR-D-Bph14^{HR} (gDNA)	this study	mutagenesis PCR (dst229-dst230)	dst229, dst230
pENTR221-Pm3b_LRR-myc (cDNA)	Gateway BP cloning	pDONR221	plasmid with cDNA of Pm3b	Yahiaoui et al., 2004	PCR (dst060-dst058), then PCR (dst060-dst059)	dst060, dst058, dst059
pENTR221-Pm3b^{HR}_CC-NBS-HA	site-directed mutagenesis PCR		pENTR221-Pm3b^{HR}-HA (gDNA)	this study	mutagenesis PCR (dst103-dst155)	dst103, dst155
pENTR221-Pm3f_LRR-myc (cDNA)	Gibson Assembly		PCR (cint10R-UP81A) on pENTR221-Pm3b_LRR-myc (cDNA)	this study	PCR (R081A-SuB19) on pENTR221-Pm3f-HA (gDNA)	cint10R, UP81A, R081A, SuB19
pENTR221-Pm3f_CC-NBS-HA	site-directed mutagenesis PCR	pDONR221	pENTR221-Pm3f-HA (gDNA)	this study	mutagenesis PCR (dst103-dst155)	dst103, dst155
pENTR221-Pm3f^{HR}_CC-NBS-HA	site-directed mutagenesis PCR	pDONR221	pENTR221-Pm3f^{HR}-HA (gDNA)	this study	mutagenesis PCR (dst103-dst155)	dst103, dst155
pENTR221-Pm3f_L456P/Y458H_CC-NBS-HA	site-directed mutagenesis PCR	pDONR221	pENTR221-Pm3f_L456P/Y458H-HA (gDNA)	this study	mutagenesis PCR (dst103-dst155)	dst103, dst155
pENTR221-Pm3f^{HR}_L456P/Y458H_CC-NBS-HA	site-directed mutagenesis PCR	pDONR221	pENTR221-Pm3f^{HR}_L456P/Y458H-HA (gDNA)	this study	mutagenesis PCR (dst103-dst155)	dst103, dst155

3 Suppression among alleles encoding NB-LRR resistance proteins interferes with resistance in F1 hybrid and allele-pyramided wheat plants

Daniel Stirnweis, Samira Désiré Milani, Susanne Brunner, Gerhard Herren, Gabriele Buchmann, David Peditto, Tina Jordan, and Beat Keller*

submitted to The Plant Journal, 4 April 2014

* Author of correspondence

3.1 Summary

Developing high yielding varieties with broad-spectrum and durable disease resistance is the ultimate goal of crop breeding. In plants, immune receptors of the NB-LRR class mediate race-specific resistance against pathogen attack. This type of resistance is often rapidly overcome by newly adapted pathogen races when employed in agriculture. The stacking of different resistance genes or alleles in F1 hybrids or in pyramided lines is a promising strategy to achieve more durable resistance. Here, we identify a molecular mechanism which can negatively interfere with the allele-pyramiding approach. We show that pairwise combinations of different alleles of the powdery-mildew-resistance gene *Pm3* in F1 hybrids and stacked transgenic wheat lines can result in suppression of *Pm3*-based resistance. This effect is independent of the genetic background and solely dependent on the *Pm3* alleles. Suppression occurs at the post-translational level as neither RNA nor protein levels of the suppressed alleles are affected. Using a transient-expression system in *Nicotiana benthamiana*, the LRR domain was identified as the suppression-conferring domain. The results of this study suggest that the expression of closely related NB-LRR resistance genes or alleles in the same genotype can lead to dominant-negative interactions. These findings provide a molecular explanation for the frequently observed ineffectiveness of resistance genes introduced from the secondary gene pool into polyploid crop species and mark an important step to overcome this limitation.

3.2 Introduction

To prevent yield losses in crop production due to pathogen infestation, breeding for resistant plant genotypes is widely considered to be the most sustainable strategy. Plant breeders constantly renew the set of cultivars offered to the farmers by incorporating resistance loci from the primary, secondary, and tertiary gene pool into breeding germplasm. Molecular cloning of the underlying genetic constituents for pathogen defense has shown that many of the genes with a major resistance effect encode intracellular resistance (R) proteins with an N-terminal coiled-coil (CC) or TOLL/interleukin-1 receptor (TIR), a central nucleotide-binding (NB), and a C-terminal leucine-rich-repeat (LRR) domain (Marone et al. 2013). These proteins, designated NLR, usually provide a strong resistance that is frequently associated with a hypersensitive response (HR), a form of programmed cell death that prevents the spread especially of biotrophic pathogens. NLR proteins are specifically activated by the direct or indirect recognition of avirulence (Avr) molecules that are delivered from the pathogen into the host cell. These are mainly effector proteins that usually support the virulence of the pathogen. Co-evolution of host and pathogen populations leads to

diversification or a fast turnover at the genomic *R* and *Avr* loci, resulting in a large allelic diversity and race-specificity of the *R*-gene mediated Effector-Triggered Immunity (ETI) (Dodds and Rathjen 2010).

Thus, the use of *R*-gene based resistance in crop plants has the drawback of rapid loss of effectiveness. This is especially true for genetically uniform agricultural ecosystems that create a high selection pressure on pathogen populations. Stacking of multiple highly effective, broad-spectrum, redundantly acting *R* genes is considered a promising strategy for a more sustainable use of race-specific resistance in agriculture (Dangl et al. 2013). Due to the redundancy in recognition the pathogen will have to evolve multiple *Avr* genes simultaneously to gain virulence on such *R*-gene-pyramided plants; an unlikely event and, hence, pyramiding is expected to extend the durability of *R*-gene crop resistance (McDonald and Linde 2002).

As an alternative to the stacking of different *R* genes, different allelic variants of the same *R* gene can also be combined. For dominant *R* genes this is possible in a heterozygous form in F1 hybrids. A genetically stable combination of various alleles can be achieved by the use of transgenic approaches, for example via the cross of transgenic lines having different alleles inserted at random sites. By this approach Bieri et al. (5) selected lines expressing both the *Mla1* and *Mla6* powdery-mildew-resistance specificities from the *Mla* locus in barley. Additive resistance was also obtained when L^6 was combined with the L^2 or L^{10} alleles of a flax-rust-resistance gene in one genotype (Chen et al. 2007). These are promising examples of how, next to the genetic diversity at different loci, also the allelic diversity can be exploited for resistance improvement.

A challenge for the combination of different *R* genes or alleles is their potential functional incompatibility with the genetic background or among the stacked genes/alleles themselves. Incompatibility between resistance genes may result in autoimmunity and this hybrid necrosis sets a barrier for hybridization (Bomblies and Weigel 2007). In contrast to this immunity-activating effect, the genetic background may also lead to loss of resistance activity. This resistance-suppression phenomenon is frequently observed and results in a significant limitation for resistance breeding especially in polyploid crop species (e.g., Hanusová et al. 1996; Nelson et al. 1997; Knott 2000; McIntosh et al. 2011; Liu et al. 2013; Chen et al. 2013 and references therein). Although this is a widespread problem, the underlying molecular determinants and mechanism remained elusive.

In this study we tested the allele-pyramiding approach for *Pm3*, a coiled-coil NLR-coding gene that mediates race-specific resistance against powdery mildew (*Blumeria graminis* f. sp.

tritici, *Bgt*) in wheat and of which 17 functional alleles have so far been described (Yahiaoui et al. 2004, 2006; Srichumpa et al. 2005; Bhullar et al. 2009, 2010). We investigated the pairwise combination of five different alleles of *Pm3* in F1 hybrids and stacked transgenic lines. We show that a quantitative suppression among the *Pm3* alleles themselves frequently limits the efficiency of the resistance combination. We demonstrate that the suppression neither takes place at the transcriptional nor the translational level and that the suppression activity is delimited to the LRR domain. Our results adduce molecular evidence that non-activated alleles of NLR resistance genes can invert the dominance of their resistant counterparts which has major consequences for their use in crop resistance breeding.

3.3 Results

Different *Pm3* alleles cannot be stably combined in one genotype by classical genetics. Therefore we wanted to explore a pyramidization of transgenic *Pm3* alleles to improve powdery-mildew resistance. First, additive or non-additive action of different *Pm3* alleles were tested in the F1 progeny of crosses between lines/cultivars (cv.) that carry different alleles of *Pm3*. Wheat cv. 'Kolibri' carrying *Pm3d* or cv. 'Michigan Amber' (M. Amber) carrying *Pm3f* were crossed with the landrace 'Chul' carrying *Pm3b*. The presence of the two different *Pm3* alleles in the F1 plants was confirmed by PCR amplification of allele-specific *Pm3* markers (Tommasini et al. 2006). For leaf segment infection tests of the F1 hybrid plantlets we selected powdery-mildew isolates that differentiate the resistance specificity of the *Pm3* alleles: Isolates *Bgt* 97011 and *Bgt* 98229 are avirulent on wheat differential lines for *Pm3d* and *Pm3f* (*AvrPm3d*, *AvrPm3f*), but virulent on *Pm3b* differential lines (*avrPm3b*). In contrast, the isolates *Bgt* 07298 and *Bgt* 07201 are avirulent on *Pm3b* (*AvrPm3b*) but virulent on *Pm3d* (*avrPm3d*) or *Pm3f* (*avrPm3f*), respectively. Previous studies have shown that *Pm3a-f* alleles are dominant resistance genes (Briggle 1966; Zeller et al. 1993). Assuming additive gene action, we expected the F1 plants which carry both *Pm3* alleles in a heterozygous state to be completely resistant to all of the tested *Bgt* isolates. However, we observed low (10-37% infected leaf area for F1 Chul x Kolibri) to high (60-96% infected leaf area for F1 Chul x M. Amber) levels of infection at 7 days post infection with the isolates *Bgt* 97011 and *Bgt* 98229 (both *AvrPm3d/f*) (Figure 1a, Figure S1a and b). The F1 hybrids remained fully resistant towards the *Pm3b*-avirulent isolates *Bgt* 07298 or *Bgt* 07201. The parental cultivars of the crosses, 'Kolibri', 'M. Amber', and 'Chul', displayed complete resistance towards all matching avirulent isolates (Figure S1a and b). To investigate whether the genetic background contributes to the observed incomplete resistance in F1 hybrids we crossed *Pm3b*- (Chul/8*CC) and *Pm3f*-near isogenic lines (M. Amber/8*CC). Both lines have

cv. 'Chancellor' (CC) as the recurrent parent. F1 plants from these crosses were analyzed by infection tests. As for F1 Chul x M. Amber, we observed full resistance of the F1 Chul/8*CC x M. Amber/8*CC plants towards the *Pm3b*-avirulent isolate *Bgt* 07201 (4% infected leaf area), but also high levels of susceptibility with the *Pm3f*-avirulent isolates *Bgt* 97011 and *Bgt* 98229 (77-97% infected leaf area) (Figure 1a, Figure S1c).

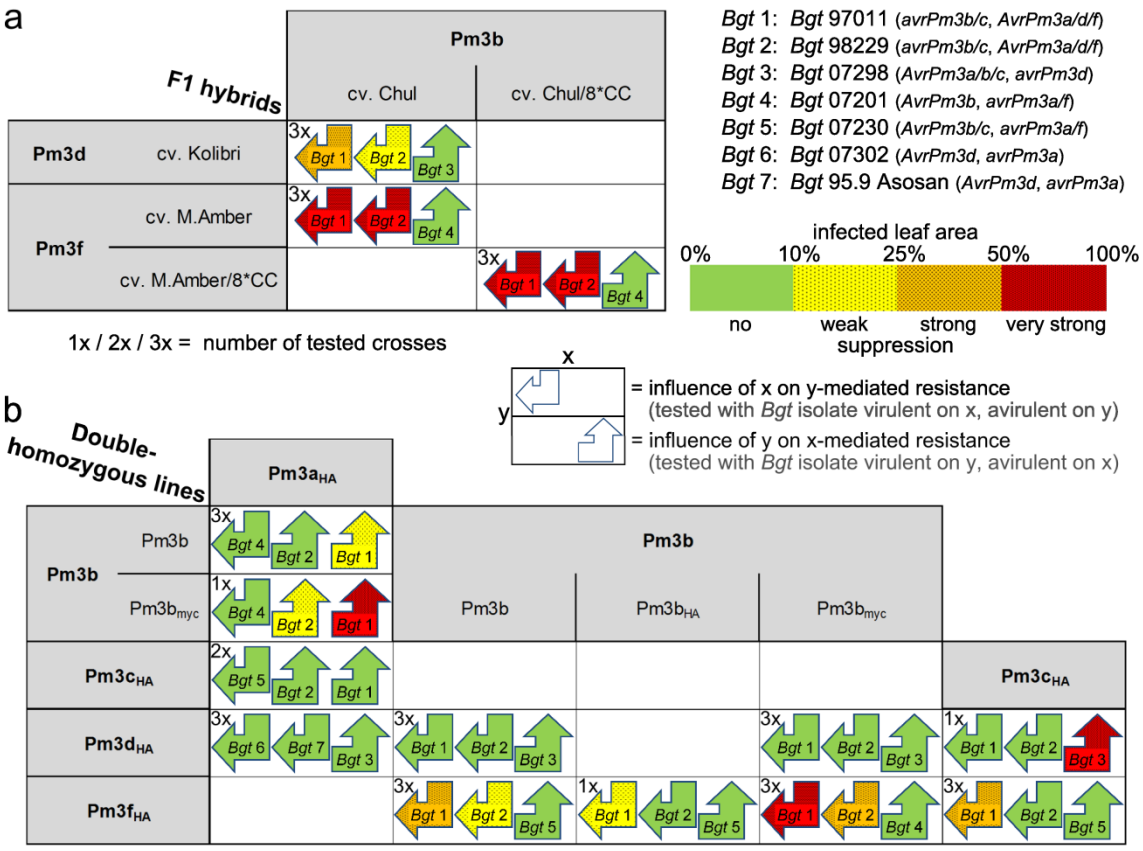

Figure 1. Suppression among *Pm3* alleles leads to incomplete resistance in F1 hybrids and in several double-homozygous transgenic *Pm3* lines.

(a) Results of leaf segment infection tests with F1 hybrids, which originate from cultivars expressing *Pm3b*, *Pm3d*, and *Pm3f*, infected with *Bgt* isolates that differentiate the parental resistance specificities. Colors of the arrows indicate mean infected leaf areas of the F1 hybrids for the tested *Bgt* isolates and the corresponding suppression levels of the F1 compared to the respective resistant parental line (light gray boxes). The direction of the arrows indicates the suppression activity of the line on the base of the arrow on the resistance activity originating from the line on the tip of the arrow. Detailed results of infection tests for all three independent crosses per hybrid combination are presented in Figure S1.
(b) Results of leaf segment infection tests with transgenic lines homozygous for two different *Pm3* alleles and differentiating *Bgt* isolates. Labeling and legend as defined in (a). Detailed results of infection tests are presented in Figure S2 and Figure S3.

Overall, these results reveal normal gene function of *Pm3b* (Briggle 1966; Yahiaoui et al. 2004) but show incomplete resistance in the investigated F1 hybrids for *Pm3d* and *Pm3f* in one or two genetic backgrounds, respectively. These data suggest that *Pm3d*- and *Pm3f*-

mediated resistance can be weakened by the quantitatively acting, negative activity of a suppressor present both in 'Chul' and in the 'Chul'-derived chromosomal regions of Chul/8*CC.

To further study if the genetic background might account for the suppressed resistance we used previously developed transgenic $Pm3a_{HA}$, Pm3b, $Pm3c_{HA}$, $Pm3d_{HA}$, and $Pm3f_{HA}$ lines. They all have the susceptible genetic background of the spring wheat line Bobwhite SH 98 26 where no *Pm3* allele is present (Brunner et al. 2011, 2012). In addition, we generated transgenic lines $Pm3b_{HA}$ and $Pm3b_{myc}$ in the same genetic background expressing the *Pm3b* allele with a C-terminally fused single hemagglutinin (HA) or c-myc (myc) epitope tag, respectively. All the lines exhibited race-specific powdery mildew resistance over multiple generations.

We used the transgenic Pm3 lines that carry a single *Pm3* allele inserted at random sites in the genome to pyramid the *Pm3* alleles in pairs in *Pm3* double-homozygous lines (Pm3x/y) that stably inherit two *Pm3* alleles. One to three independent crosses between *Pm3* lines were made and the F1 progeny was allowed to self-pollinate for three more generations (F4). The segregation of the individual *Pm3* alleles was analyzed in the F3 or F4 generations with allele-specific *Pm3* markers and double-homozygous lines were selected. For the combination of $Pm3b_{myc}$ with $Pm3f_{HA}$ we additionally selected the corresponding sister lines in the F3 generation, i.e. null segregants for $Pm3f_{HA}$ [$Pm3b_{myc}/(\Delta f_{HA})$] or $Pm3b_{myc}$ [$Pm3(\Delta b_{myc})/f_{HA}$] that are homozygous for either $Pm3b_{myc}$ or $Pm3f_{HA}$, respectively.

The powdery-mildew resistance of all double-homozygous lines was examined alongside with their parental lines (and sister lines for $Pm3b_{myc}/f_{HA}$) in infection tests with three *Bgt* isolates that differentiate the parental resistance specificities. All the parental lines and sister lines exhibited the expected resistance specificities and were either completely resistant (<3% average infected leaf area observed) or completely susceptible (>66% average infected leaf area observed) towards the tested *Bgt* isolates (Figure 2, Figure S2, Figure S3). In total, seven allele combinations were analyzed in which *Pm3b* combinations were redundantly investigated using the untagged, HA-, and myc-tagged *Pm3b*-fusion variants. Remarkably, $Pm3c_{HA}/d_{HA}$ was highly susceptible to *Bgt* 07298 (*avrPm3d* & *AvrPm3c*); $Pm3a_{HA}/b$, $Pm3a_{HA}/b_{myc}$, $Pm3b/f_{HA}$, $Pm3b_{HA}/f_{HA}$, $Pm3b_{myc}/f_{HA}$, and $Pm3c_{HA}/f_{HA}$ showed intermediate resistance or high susceptibility to *Bgt* 97011 and also in some cases lower resistance to *Bgt* 98229 (both *avrPm3b/c* & *AvrPm3a/f*) (Figure 1b, Figure S2). Here, inoculations with the isolate *Bgt* 97011 always led to a higher level of infection compared to the isolate *Bgt* 98229. This shows that the degree of susceptibility in the affected lines depends on the *Bgt* isolate used for infection. This indicates that the diverse virulence potential of different *Bgt* isolates

quantitatively influences the fungal infestation on suppressed *Pm3* lines. Summarizing these observations, we found incomplete resistance with one or two isolates in infection tests with *Pm3* double-homozygous lines of four allele combinations. In all these cases only the resistance mediated by one of the two combined *Pm3* alleles was compromised. This is consistent with the observations in the F1 hybrids of the crosses of *Pm3* cultivars (Figure 1a). From these results we infer that the incomplete dominance observed with the F1 of some *Pm3*-cultivar crosses was not due to influences of the genetic background. Instead the incomplete resistance in the F1 plants and the double-homozygous lines is based on negative epistatic effects between the *Pm3* alleles themselves. Interestingly, a reduction of *Pm3f*$_{HA}$-mediated resistance was observed in all three independent combinations of *Pm3b* with *Pm3f*, but the degree of susceptibility varied depending on the parental *Pm3b* line (e.g., Pm3b/f$_{HA}$ 22%, Pm3b$_{HA}$/f$_{HA}$ 46%, and Pm3b$_{myc}$/f$_{HA}$ 77% infected leaf area for *Bgt* 97011). Similar observations were made for the two combinations of *Pm3a* with *Pm3b* (Pm3a$_{HA}$/b, and Pm3a$_{HA}$/b$_{myc}$). Collectively, this dependence on the particular transformed construct or transgenic event shows the quantitative nature of suppression.

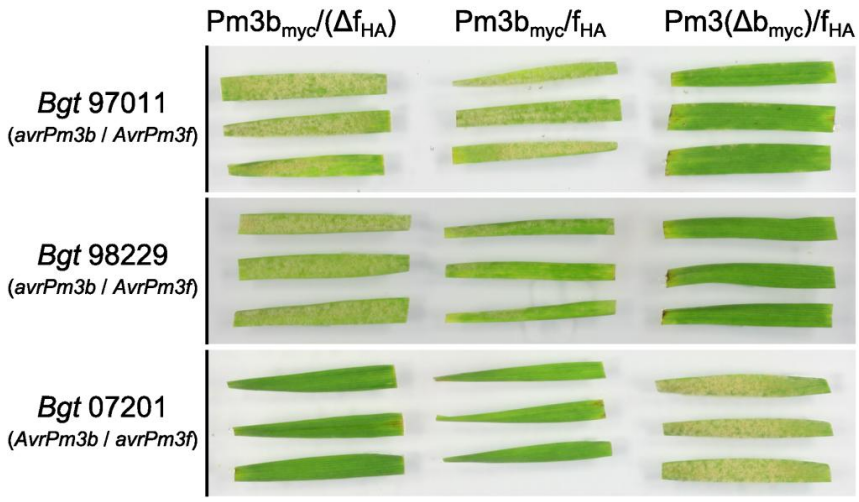

Figure 2. *Pm3f*$_{HA}$-mediated resistance is suppressed in double-homozygous Pm3b$_{myc}$/f$_{HA}$ plants and the level of fungal infestation on the suppressed plants depends on the *Bgt* isolates. Leaf segment infection tests with *Bgt* isolates 97011, 98229, and 07201 are shown. These isolates differentiate the *Pm3b*$_{myc}$- and *Pm3f*$_{HA}$-mediated resistance as shown by the resistance specificity of the Pm3b$_{myc}$/(Δf$_{HA}$) and Pm3(Δb$_{myc}$)/f$_{HA}$ sister lines. Pictures were taken at 7 days post infection.

For the combinations of *Pm3a* with *Pm3c*, *Pm3a* with *Pm3d*, and *Pm3b* with *Pm3d* we did not detect suppression: Separate infections of the respective double-homozygous lines with three *Bgt* isolates resulted in no or very little infestation (<6% average infected leaf area) (Figure 1, Figure S3). Thus, while we detected incomplete *Pm3d* resistance with the F1

Chul x Kolibri hybrids (Figure 1, Figure S1) we did not detect suppression in the Pm3b/d_{HA}, and $Pm3b_{myc}/d_{HA}$ double-transgenic lines. We explain this discrepancy by the quantitative character of suppression where the suppression may be too weak to cause an obvious loss of resistance in these combinations of *Pm3*-overexpressing transgenic lines, but may be sufficient to compromise the resistance of F1 hybrids expressing the *Pm3* alleles under native conditions. However, it is also possible that suppression is only occurring in a subset of *Pm3*-allele combinations and, therefore, does not affect the allele combinations where we observed additive resistance.

To characterize the molecular basis of the suppression effects we selected the $Pm3b_{myc}/Pm3f_{HA}$ combination for which we found strong *Pm3f* suppression and for which the different epitope tags enable allele-specific protein analyses. To test whether the *Pm3* activity is affected by transcriptional silencing we performed $Pm3f_{HA}$- and $Pm3b_{myc}$-allele-specific reverse-transcription-quantitative PCRs (RT-qPCR) with the double-homozygous lines $Pm3b_{myc}/f_{HA}$ and their sister lines from all three crosses. In two independent experiments only once and only for the second cross, we detected a minimal (2.1-fold), but significant reduction of $Pm3f_{HA}$-expression levels in $Pm3b_{myc}/f_{HA}$ lines compared to the $Pm3f_{HA}$-expressing sister lines $Pm3(\Delta b_{myc})/f_{HA}$ (Figure 3a). The only significant reduction of $Pm3b_{myc}$ expression in $Pm3b_{myc}/f_{HA}$ lines compared to the respective $Pm3b_{myc}/(\Delta f_{HA})$ sister lines was measured in the same experiment and for the same cross (2-fold reduction) (Figure S4). Given that $Pm3f_{HA}$-mediated resistance is suppressed in all $Pm3b_{myc}/f_{HA}$ lines of all three crosses and that $Pm3b_{myc}$-mediated resistance is not affected in the $Pm3b_{myc}/f_{HA}$ line where we detected a reduced expression, there is no correlation between the resistance phenotypes and differences in *Pm3* expression. Therefore, we conclude that suppression of $Pm3f_{HA}$ in the $Pm3b_{myc}/f_{HA}$ lines is not based on transcriptional silencing.

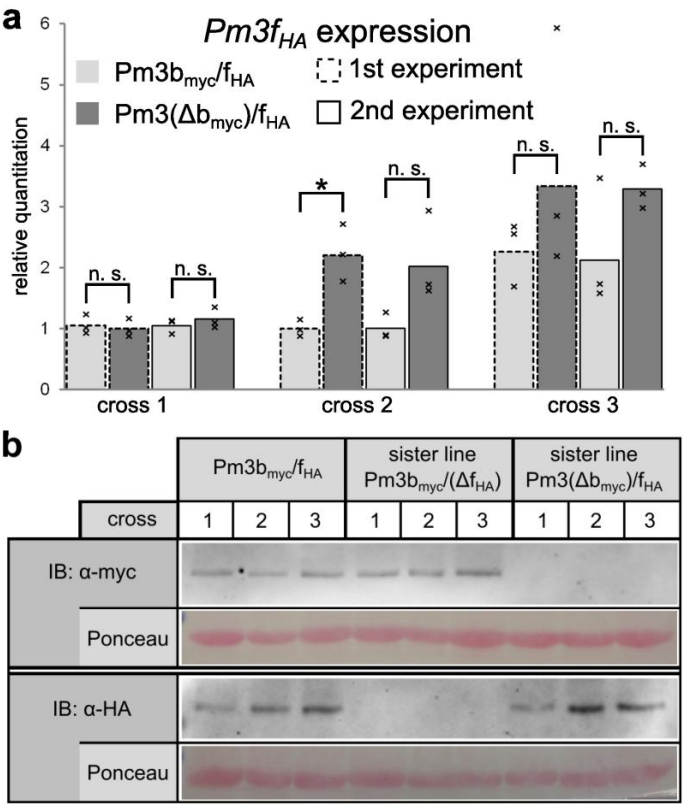

Figure 3. Suppression of *Pm3f*$_{HA}$ activity in double-homozygous Pm3b$_{myc}$/f$_{HA}$ lines does neither occur at the transcriptional nor at the translational level.

(a) RT-qPCR results for the incomplete resistant Pm3b$_{myc}$/f$_{HA}$ lines and the resistant Pm3(Δb$_{myc}$)/f$_{HA}$ sister lines show only minimal differences of *Pm3f*$_{HA}$-transcript accumulation. Mean values (represented by bars) and single data points (x) of two independent experiments each with three replicates are shown. Values are normalized to the lowest value (set to 1) within each experiment. Significant differences are indicated by asterisks (Student`s *t*-test $P<0.05$; n. s. = non significant)
(b) Immunoblot (IB) analysis of PM3B$_{myc}$ (upper panel) and PM3F$_{HA}$ protein (lower panel) in leaves of Pm3b$_{myc}$/f$_{HA}$ lines and the respective sister lines from three independent crosses. Ponceau S membrane staining of Ribulose-1,5-bis-phosphate carboxylase/oxygenase is shown as control for equal loading of total protein.

Next, we wanted to test whether post-transcriptional silencing is the cause for the suppression of *Pm3f*$_{HA}$. With immunoblots using anti-myc or anti-HA antibodies, respectively, we separately analyzed the PM3B$_{myc}$ or PM3F$_{HA}$ proteins in the double-homozygous Pm3b$_{myc}$/f$_{HA}$ lines in comparison to the sister lines. Similar band intensities indicate that similar levels of PM3B$_{myc}$ and PM3F$_{HA}$ protein are produced in the leaves of Pm3b$_{myc}$/f$_{HA}$ lines and the corresponding sister lines (Figure 3b). This suggests that the incomplete PM3F$_{HA}$-mediated resistance phenotype in Pm3b$_{myc}$/f$_{HA}$ is not correlated with a reduced amount of the PM3F$_{HA}$ resistance protein and indicates a suppression mechanism at the post-translational level.

Some coiled-coil NLR resistance proteins are known to form multimeric complexes already before pathogen perception (Ade et al. 2007; Maekawa et al. 2011). Based on these findings, we presumed that protein interactions might be important for the suppression mechanism and for this reason we analyzed whether protein complexes containing different PM3 proteins can be found in plant cells. We performed co-immunoprecipitation experiments with *Pm3b*$_{myc}$- and *Pm3f*$_{HA}$-co-infiltrated leaf material from *Nicotiana benthamiana* where we previously showed that PM3 is functional (Stirnweis et al. 2014). Here, myc-tagged PM3B$_{myc}$ co-precipitated with HA-tagged PM3F$_{HA}$ protein demonstrating that these two proteins interact (Figure 4a). No similar interaction was detected with the same analysis using primary leaves of the stable transgenic Pm3b$_{myc}$/f$_{HA}$ wheat lines. There, PM3-protein levels are very low and the immunoprecipitation and detection efficiency for PM3F$_{HA}$ or PM3B$_{myc}$, each fused with only a single epitope, may be insufficient. Using *N. benthamiana*, we also tested for the interaction of PM3F$_{HA}$ with myc-tagged hPM3-1B$_{myc}$. This protein is encoded by a homolog of *Pm3* originating from wheat homeologous chromosome 1B and has 78% similarity to the PM3B amino-acid sequence (Hurni et al. 2013). The *hPm3-1B* gene is present in cv. 'Chancellor' that was used as recurrent parent in many near-isogenic *Pm3* differential lines and is, therefore, expected to not suppress *Pm3*-mediated resistance. The detection of hPM3-1B$_{myc}$ protein in the PM3F$_{HA}$ precipitate showed that PM3F$_{HA}$ and hPM3-1B$_{myc}$ are also present in a common protein complex (Figure 4a). This indicates that protein interaction with a PM3-like protein *per se* is not sufficient for the suppression of PM3F$_{HA}$.

To examine whether the *Pm3* suppression is independent of factors from the powdery-mildew pathogen we established an assay in *Nicotiana* that allows investigating the phenotypic aspects of PM3 interactions in the absence of mildew: We performed overlapping infiltrations with *Agrobacterium tumefaciens* strains transferring either the construct under investigation or *Pm3f_D501V*$_{HA}$, a version of *Pm3f* coding for an autoactive form of the protein due to a mutation in the MHD motif. This aspartate-to-valine substitution renders many resistance proteins, including PM3, autoactive which leads to the induction of a hypersensitive response (HR) after agroinfiltration (Stirnweis et al. 2014). Hence, the programmed cell death that can be observed after agroinfiltration of *Pm3f_D501V*$_{HA}$ resembles a resistance response activated by perception of an avirulent powdery-mildew isolate. The PM3F_D501V$_{HA}$-induced cell death was completely suppressed by PM3B$_{myc}$ in the infiltration overlap at 5 days post infiltration (dpi) while the negative control GUS did not reduce the PM3F_D501V$_{HA}$-mediated HR in the overlapping infiltration zone (Figure 4b). This indicates that the suppression of PM3F by PM3B is independent of components from the powdery-mildew fungus.

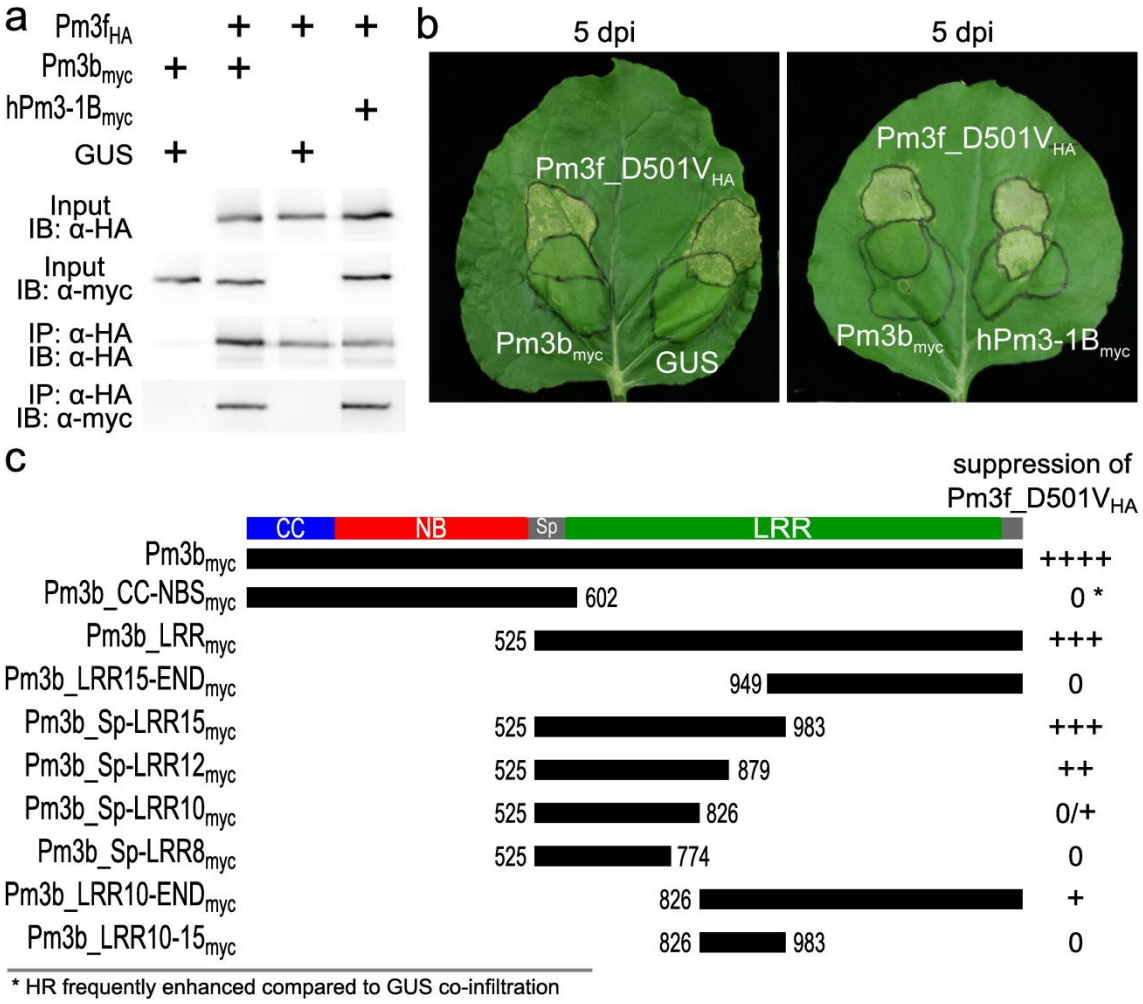

Figure 4. Agroinfiltration experiments in *Nicotiana benthamiana* reveal that PM3B$_{myc}$ and its homolog hPM3-1B$_{myc}$ physically interact with PM3F$_{HA}$, but only PM3B$_{myc}$ suppresses PM3F$_{HA}$-mediated HR via its LRR domain.

(a) Co-immunoprecipitation of c-myc-tagged PM3B or hPM3-1B with HA-tagged PM3F from co-infiltrated *N. benthamiana* leaves. Images of immunoblots (IB) before (two upper panels) and after (two lower panels) immunoprecipitation (IP) with anti-HA agarose beads are shown.
(b) Overlapping infiltrations of autoactive, HR-inducing *Pm3f_D501V$_{HA}$* (upper circles) with *Pm3b$_{myc}$*, the negative control *GUS*, and *hPM3-1B$_{myc}$* (lower circles) for the detection of phenotypic interactions in the overlap. Pictures were taken at 5 dpi.
(c) Deletion analysis for PM3B$_{myc}$ suppression activity. Constructs for PM3B$_{myc}$ fragments and Pm3f_D501V$_{HA}$ were co-infiltrated and HR suppression was scored in comparison to a co-infiltration with the negative control (GUS) at 5 dpi in at least three independent experiments with at least four replicates per experiment (0 = no HR suppression → ++++ = consistently complete HR suppression). The top row shows the PM3 domain structure with the CC (blue), NB (red), Spacer (Sp, gray) and LRR (green) domains. Black bars indicate the portion of PM3B encoded by the respective construct. Numbers give the respective positions in PM3B of the outermost amino acids of the fragments.

We also found that PM3F_D501V$_{HA}$-mediated HR was not markedly influenced in overlapping infiltrations with *hPm3-1B$_{myc}$* (Figure 4b). This is in accordance with the observation that *hPm3-1B* does not appear to interfere with *Pm3*-mediated resistance in

wheat. An immunoblot analysis of the proteins in leaf material co-infiltrated with *Pm3f_D501V$_{HA}$* and *Pm3b$_{myc}$* or *hPm3-1B$_{myc}$* and harvested at 43 hours post infiltration (hpi) shortly before the onset of HR shows that the PM3F_D501V$_{HA}$ levels did not significantly differ between infiltrations with and without active suppressor gene (Figure S5a). Overall, these results demonstrate that the *Nicotiana* system recapitulates the suppression effects observed in wheat and reveal that intrinsic protein properties make the difference between the suppressing PM3B and the non-suppressing hPM3-1B.

To investigate which part of the PM3B protein causes suppression we co-infiltrated constructs for fragments of PM3B$_{myc}$ and for PM3F_D501V$_{HA}$ in *N. benthamiana* and examined the HR at 5 dpi. *Pm3f_D501V$_{HA}$* co-infiltration with the Pm3b_CC-NBS$_{myc}$ construct comprising amino acids (aa) 1-602 of PM3B led to an HR that was at least as intense as with the GUS negative control indicating that the CC-NBS domains are not responsible for the suppression but rather enhance the PM3F_D501V$_{HA}$-induced HR (Figure 4c, Figure S6a). In contrast, the Pm3b_LRR$_{myc}$ (aa 525-1415) construct comprising the complete LRR domain very efficiently suppressed PM3F_D501V$_{HA}$-mediated HR. We split the LRR in an N-terminal (Pm3b_Sp-LRR15$_{myc}$, aa 525-983) and C-terminal part (Pm3b_LRR15-END$_{myc}$, aa 949-1415) and observed that the HR-suppression property is encoded in the N-terminal fragment. When we shortened the N-terminal fragment, co-infiltration with the construct Pm3b_Sp-LRR12$_{myc}$ (aa 525-879) still showed a strong reduction of PM3F_D501V$_{HA}$-induced HR, whereas with shorter fragments HR suppression was only rarely observed (Pm3b_Sp-LRR10$_{myc}$, aa 525-826) or not detected (Pm3b_Sp-LRR8$_{myc}$, aa 525-774) (Figure 4c, Figure S6a). This gradual loss of suppression activity from Pm3b_Sp-LRR15$_{myc}$ to Pm3b_Sp-LRR8$_{myc}$ may have its origin in the ever shorter size of the fragment or may reflect the importance of the PM3B aa 826-983 for the suppression. An observation that supports the latter hypothesis was that the Pm3b_LRR10-END$_{myc}$ construct (aa 826-1415) frequently displayed suppression in contrast to the Pm3b_LRR15-END$_{myc}$ construct. The construct Pm3b_LRR10-15$_{myc}$ (aa 826-983) was still not sufficient to suppress the PM3F_D501V$_{HA}$-induced HR. Immunoblot analysis of the protein levels in co-infiltrated *Nicotiana* leaves shortly before the onset of HR (~30 hpi for Pm3b_CC-NBS$_{myc}$) showed that PM3F_D501V$_{HA}$ abundance is not significantly altered by suppressing and non-suppressing fragments and all PM3B fragments formed stable proteins (Figure S5b). In addition, infiltrations without *Pm3f_D501V$_{HA}$* showed that none of the *Pm3b* constructs induced HR by itself (Figure S6b). In summary, we infer from the deletion analysis that the suppression activity of PM3B towards PM3F is situated in the Spacer-LRR domain and here the N-terminal half plays the major role.

3.4 Discussion

The pyramiding of resistance genes or its alleles in a single genotype by the generation of F1 hybrids or genetically stable non-segregating lines is a promising concept for the combination of gene specificities and effectiveness, and for an extension of their durability (McDonald and Linde 2002; Dangl et al. 2013). Combinations of resistance loci leading to additive gene action have been reported in a number of plant species (e.g., Liu et al. 2000; Hu et al. 2012; Zhu et al. 2012) and also the successful stacking of alleles was reported for two NLR resistance genes (Bieri et al. 2004; Chen et al. 2007). However, there are also a number of reports describing observations of weakened or lost resistance when the source of resistance is introgressed into another genetic background. This is well described for resistance breeding in polyploid crop plants where resistance loci derived from lower-ploidy species of the secondary or tertiary gene pool are often suppressed in the polyploid species or in synthetic polyploids (e.g., Hanusová et al. 1996; Nelson et al. 1997; Knott 2000; McIntosh et al. 2011; Liu et al. 2013; Chen et al. 2013 and references therein). Incomplete resistance in F1 hybrids, as seen in this study for the *Pm3* F1 hybrids, is also known (e.g., Islam et al. 1992; Wilson and McMullen 1997; Kim et al. 2012) but the causes were often attributed to gene-dosage dependency. Only few studies so far gave hints that the suppression of a resistance locus might originate from its combination with the corresponding, dominantly acting, susceptible allelic locus: For example, it was shown in *Arabidopsis thaliana* that the TIR-NLR-WRKY-resistance gene *Rrs1*, originally classified as recessive by classical genetics, behaved as a dominant gene when introduced as a transgene (Deslandes et al. 2002). A rust resistance gene of soybean showed dominance in some, but recessiveness in other crosses. There, it was found that the genetic determinant of the suppression co-segregated with the allelic, susceptible resistance locus (Garcia et al. 2011). The results of our study now demonstrate at the molecular level that incompatibility among alleles of an NLR resistance gene can cause resistance suppression.

Combining these findings with those of a companion publication (Hurni *et al.*, 2014; see accompanying manuscript), showing that rye-derived *Pm8*-mediated resistance in wheat can be suppressed by its ortholog *Pm3*, also suggests that other NLR resistance activities might be compromised by closely related NLR proteins (e.g., encoded by alleles, orthologs, homeologs, or paralogs) by the same suppression mechanism. Indeed, there are several indications that the identified mechanism how a non-functional resistance protein suppresses a resistant counterpart is of wider significance.

For instance, in hexaploid wheat Nelson *et al.* (1997) genetically mapped the suppressor of chromosome 2B-localized leaf-rust resistance gene *Lr23* to the homeologous locus on

chromosome 2D suggesting a susceptible homeolog of *Lr23* as suppressor. Furthermore, it was shown that expression of a version of the bacterial-NLR-resistance protein RPS2 that is inactivated by mutations in the CC domain has a dominant-negative effect on the wild type RPS2-mediated resistance in *Arabidopsis thaliana* (Tao et al. 2000). Moreover, the viral TIR-NLR-resistance protein N of *Nicotiana* is suppressed by co-expression of N variants inactivated by P-loop mutations, or by deletion of, or mutations in, the TIR domain (Dinesh-Kumar et al. 2000). Similar to our observation for PM3, it was also reported that cell death induced by an autoactive version of the NLR Prf can be suppressed by co-expression of its LRR in a *Nicotiana* infiltration system (Du et al. 2012). Finally, the described suppression mechanism might also be relevant for resistance proteins with an extracellular LRR (eLRR) domain. This hypothesis is based on results of Barker *et al.* (2006) showing that inactive Cf-9 variants with C-terminal deletions in the eLRR have a dominant-negative effect on the wild-type Cf-9 activity in tomato. These examples are all consistent with our findings from the deletion analysis showing that the N-terminal part of the LRR domain is the major determinant of suppression.

The results of this study present molecular evidence that *Pm3* suppression is based on dominant-negative, post-translational effects among the involved proteins. These effects are of quantitative nature as indicated by suppression differences between different *Pm3b* constructs. They are most likely independent of fungal components as suggested by the HR-suppression in the *Nicotiana* infiltration system, and could involve PM3-protein interactions. Thus, we propose the following model for the suppression by alleles: PM3 proteins form complexes, exclusively PM3-homomeric ones when only one allele is present and PM3-homomeric as well as PM3-heteromeric ones when multiple alleles are present. In contrast to homomeric complexes, heteromeric complexes might be incompatible for signaling, or even block it, thereby sequestering the active protein pool of each combined PM3 variant. This also provides an explanation of the quantitative nature of suppression where the ultimate phenotypic outcome depends on the virulence potential of the pathogen race, the individual PM3 protein level and the recognition and activation efficiency of the PM3 proteins encoded by different alleles (Stirnweis et al. 2014). This scenario also implies that the successful pyramiding of the *Pm3a* and *Pm3c*, *Pm3a* and *Pm3d*, and *Pm3b* and *Pm3d* alleles is based on limited quantitative suppression in case of an optimal combination of PM3-protein levels. The observation that hPM3-1B does not suppress PM3, even though the proteins interact as shown by co-immunoprecipitation, indicates that the inactivation of PM3-protein complexes is a complex process that possibly also depends on particular protein features which differ between PM3B and hPM3-1B.

Overall, the suppression mechanism found in this study is possibly widespread, especially in polyploid species. It can be a limiting factor for gene- or allele-pyramiding approaches as well as for the transfer of resistance genes into species where an ortholog is present. The results of this study suggest that in such cases the mutagenesis, silencing, gene editing, or replacement of the orthologous suppressor gene is a possibility to bypass the unwanted resistance suppression. The introduced *N. benthamiana* infiltration system offers an opportunity to easily verify suppression activities between cloned genes.

3.5 Experimental procedures

3.5.1 Transgenic *Pm3* lines

Five transgenic lines were previously described by Brunner et al. (Brunner et al. 2011, 2012) and were renamed in this study: $Pm3a_{HA}$ corresponds to Pm3a#1, Pm3b to Pm3b#1, $Pm3c_{HA}$ to Pm3c#1, $Pm3d_{HA}$ to Pm3d#1, and $Pm3f_{HA}$ to Pm3f#1. The cloning and transformation procedures for the $Pm3b_{myc}$ and $Pm3b_{HA}$ transgenic lines are described in Methods S1.

3.5.2 Selection of double-homozygous and sister lines

For the generation of *Pm3* double-homozygous lines up to three crosses between individual plants from two different *Pm3* transgenic lines were made. The resulting F1 progeny was allowed to self-pollinate for three more generations (F4). The segregation of the individual *Pm3* alleles was analyzed in the F3 or F4 generations with allele-specific *Pm3* markers and double-homozygous lines were selected based on segregation analysis using at least 20 individual plants per family of each line. The $Pm3b_{myc}/f_{HA}$ lines as well as the sister lines $Pm3b_{myc}/(\Delta f_{HA})$ and $Pm3(\Delta b_{myc})/f_{HA}$, null segregants for $Pm3f_{HA}$ or $Pm3b_{myc}$ that are homozygous for either $Pm3b_{myc}$ or $Pm3f_{HA}$, respectively, were selected based on marker analysis with at least 30 individuals of one family in the F3 generation.

3.5.3 *Pm3* marker

Conditions and primers for allele-specific *Pm3* markers were used as described (Tommasini et al. 2006). For the detection of the *Pm3b* and *Pm3d* alleles in the transgenic context the marker primers had to be modified: For *Pm3b* the primer sbi144 (5`-TTTAGCCCTGCCTTCATACG-3`) was combined with the primer Pm3b/R (Tommasini et

al. 2006); for *Pm3d* the primers dst003 (5`-AGATGGCAAGCAAGAGGTGT-3`) and dst004 (5`-CAAGCTTAATGCACCCACGA-3`) were used.

3.5.4 Infection tests

Powdery mildew infection tests using leaf segments were performed as previously described by Brunner et al. (2011). Box and Whisker Plots of the obtained data in Figures S1-S3 were created with the software package R (R Core Team 2013).

3.5.5 RT-qPCR analysis for detection of $Pm3f_{HA}$ and $Pm3b_{myc}$ expression

Expression of $Pm3f_{HA}$ and $Pm3b_{myc}$ was separately quantified using a reverse transcription, quantitative real-time polymerase chain reaction (RT-qPCR) assay. Per line, technical triplicates of three biological replicates each were analyzed using a CFX96 Real-Time System C1000^{TM} Thermal cycler (Bio-Rad, www.bio-rad.com). Each biological replicate consisted of three pooled first leaves of 10-day-old plants. *GAPDH* (UniGene Ta.5104) was included as reference gene. For a more detailed description see Methods S1.

3.5.6 Protein extraction and immunoblot analysis

Protein from primary leaves of wheat was detected as essentially described by Brunner et al. (2012) but using the Chemidoc XRS system (Bio-Rad) for blot development instead of x-ray film. Protein detections from *Nicotiana benthamiana* leaves at the indicated time post infiltration were performed as described by Stirnweis et al. (2014). Anti c-myc antibodies (rat monoclonal, clone JAC6, sc-56633; Santa Cruz Biotechnology, www.scbt.com) were used in 1 : 4000 dilution for the detection of c-myc tagged proteins.

3.5.7 Construction of plasmid vectors for agroinfiltrations

Complementary DNA (cDNA) was synthesized on total RNA of cv. Chul or M. Amber/8*CC with the SuperScript III RT (Life Technologies) enzyme according to the manufacturer`s protocol, *Pm3b* or *Pm3f* were amplified by PCR with primers TJ065 (5`-TTGGCGCGCCGCGGATGGCAGAGCGGGTGGTCA-3`) and TJ066 (5`-CCCCCCGGGCGGCCGCTCAGCTCCGGCAGGCC-3`) and were cloned with the StrataClone Blunt PCR Cloning Kit (Agilent Technologies, www.genomics.agilent.com). From these and from existing plasmids all genes were cloned into Gateway system

compatible entry vectors via Gateway BP Clonase II reactions (Life Technologies). Introduction of modifications and cloning of fragments were achieved by the QuikChange Site-Directed Mutagenesis Kit (Agilent Technologies). By Gateway LR reactions (Life Technologies) all resulting pENTR plasmids were recombined to the binary vector pIPKb004 (Himmelbach et al. 2007) carrying the double-enhanced cauliflower mosaic virus 35S promoter. Detailed primer and cloning information is given in Tables S2 and S3.

3.5.8 Agroinfiltrations and co-immunoprecipitation

Transient expressions of vector constructs in *N. benthamiana* leaves via *Agrobacterium tumefaciens* infiltrations and co-immunoprecipitation experiments were performed according to the protocols of Stirnweis et al. (2014). For overlapping infiltrations *A. tumefaciens* clones containing the *Pm3b*$_{myc}$, *hPm3-1B*$_{myc}$, or *GUS* constructs were infiltrated first and 1-2 h later the infiltrations of *Pm3f_D501V*$_{HA}$ were done.

3.6 Acknowledgements

We thank Serverine Hurni for her collaboration on this project. Jochen Kumlehn is acknowledged for providing the pIPKb004 vector. This work was supported by an Advanced Investigator grant from the European Research Council (ERC-2009-AdG 249996, Durable resistance) and by Swiss National Science Foundation grant 310030B_144081/1

3.7 Supporting information

3.7.1 Short legends for supporting information

Figure S1. Results of infection tests with F1 hybrids.

Figure S2. Results of infection tests with *Pm3* double-homozygous lines showing non-additive gene action.

Figure S3. Results of infection tests with *Pm3* double-homozygous lines showing additive gene action.

Figure S4. *Pm3b*$_{myc}$ expression analyses in double-homozygous Pm3b$_{myc}$/f$_{HA}$ lines and the Pm3b$_{myc}$/(Δf$_{HA}$) sister lines.

Figure S5. Immunoblot analyses of PM3 and PM3 fragments after co-infiltrations in *N. benthamiana*.

Figure S6. Pictures showing PM3F_D501V-suppression activities of PM3 fragments in *N. benthamiana* infiltrations.

Table S1. Primers used for RT-qPCR.

Table S2. Primers used for the construction of plasmid vectors for agroinfiltrations.

Table S3. Detailed information on the cloning of the Gateway pENTR plasmids.

Methods S1. Supporting information experimental procedures and references

3.7.2 Supporting information experimental procedures

Methods S1

Cloning and transformation procedures for the Pm3b$_{myc}$ and Pm3b$_{HA}$ transgenic lines

The cloning and transformation procedures for the Pm3b$_{myc}$ line were very similar to the ones described by Brunner *et al.* (2011): A genomic fragment of the *Pm3b* allele was PCR-amplified with the primers BamHI_1 (5`-TTAATTGGATCCCCAATGGCAGAGCGGGTGGTC-3`) and TJ064 (5`-CATCATGGATCCTCACAAATCTTCTTCAGAAATCAACTTTTGTTCGCTCCGGCAGGCCTGCCTCCGC-3`), the *Bam*HI-digested fragment was cloned into the *Bam*HI site of the pAHC17 vector and was verified by sequencing. From this plasmid the 6.8kb *Not*I fragment was cut out and biolistically co-transformed with a phosphomannose isomerase (PMI) selectable marker fragment into wheat cultivar ‘Bobwhite SH 98 26’ as previously described (Brunner et al. 2011).

For the development of the Pm3b$_{HA}$ transgenic line *Pm3b* and the selectable marker PMI were combined on a single plasmid. For this purpose the sequence between the matrix-associated regions (MAR) in the wheat transformation vector from Bieri et al. (2000) was replaced with a *Not*I-fragment containing the cassette with a *ubiquitin*-promoter-driven PMI selectable-marker gene from Wright et al. (2001). In addition, the *Eco*RV-flanked Gateway-system counter selection cassette from pBS-RfA (Frelet-Barrand et al. 2010) was transfered into the *Sma*I-site between the MAR2 and the PMI sequences. The genomic sequence of *Pm3b* was PCR-amplified with primers Pm3b-start-AscI (5`-TATATATAGGCGCGCCTTCCAATGGCAGAGCGGGTGGTC-3`) and Pm3-HA-stop-

NotI (5`-CATCATGCGGCCGCTCAGCTTCAAGCATAATCTGGAACATCGTATGGATAGCCACCTCCGCTCCGGCAGGCCTGCCTCCG-3`) and the corresponding *Asc*I/*Not*I-digested fragment was subcloned into a modified pENTR4 vector (Life Technologies, www.lifetechnologies.com) containing an *ubiquitin* promoter (Seeholzer et al. 2010). The HA-tagged *Pm3b* together with the *ubiquitin* promoter and the nopaline synthase terminator was then recombined into the modified wheat transformation vector described above to receive the vector pV26-2xI-MI-(ubi)-Pm3b(g)-HA. From this plasmid an 11kb fragment was excised with I-*Sce*I and biolistically transformed without additional selectable-marker fragment as previously described (Brunner et al. 2011).

RT-qPCR analysis for detection of $Pm3f_{HA}$ and $Pm3b_{myc}$ expression

Expression of $Pm3f_{HA}$ and $Pm3b_{myc}$ in $Pm3b_{myc}/f_{HA}$, $Pm3b_{myc}/(\Delta f_{HA})$, and $Pm3(\Delta b_{myc})/f_{HA}$ lines was quantified in two independent reverse transcription, quantitative real-time PCR experiments. Technical triplicates of three biological replicates were analyzed for each wheat line in each experiment. Each biological replicate consisted of three pooled primary leaves of 10-day-old seedlings. RNA was extracted using the Promega SV Total RNA Isolation System kit (Promega, www.promega.com) and quality was checked as described (Brunner et al. 2011; Risk et al. 2012). First-strand cDNA was synthesized from 600 ng total RNA using 2 µM anchored Oligo(dT)20 Primer (11822073; Fisher Scientific, www.fishersci.com), 30 ng random hexamer primers (SO142; Fisher Scientific), 0.5 mM dNTPs, 40 units M-MLV Reverse Transcriptase RNase H^- Point Mutant (M3682; Promega), 1x M-MLV-RT reaction buffer in a total volume of 12 µl. Incubation times and temperatures were adopted from the manufacturer's protocol. RT-minus controls were performed in parallel to check for DNA contamination.

Primers were designed for the $Pm3f_{HA}$ and $Pm3b_{myc}$ targets (Table S1) using Clone Manager Professional Software V 8.0 (Scientific & Educational Software, www.scied.com), GAPDH was used as reference gene as described in Travella et al. (2006).

Using a CFX96 Real-Time System C1000TM Thermal cycler (Bio-Rad) the RT-qPCR was performed with 4 µl of 16-fold diluted cDNA, forward and reverse primer according to Table S1 and 5 µl of Fast SYBR® Green Master Mix (4385612; Life Technologies) for $Pm3f_{HA}$ and *GAPDH*, or SsoFast EvaGreen® Supermix (172-5201; Bio-Rad) for $Pm3b_{myc}$ in a total reaction volume of 10 µl. Thermocycling conditions were 95°C for 20 s, followed by 40 cycles of 95°C for 3 s, then 60°C for 20 s. Specificity of the amplicons was checked by examination of dissociation curves with CFX Manager 3.1 Software (Bio-Rad). In addition,

RT-qPCR assay specificities for the two different *Pm3* alleles were confirmed by the absence of amplification products with the *Pm3f*$_{HA}$-specific primer pair on Pm3b$_{myc}$/(Δf$_{HA}$) cDNA and the *Pm3b*$_{myc}$-specific primer pair on Pm3(Δb$_{myc}$)/f$_{HA}$ cDNA. Target-specific amplification efficiencies are given in Table S1. For a description of efficiency calculation and RT-qPCR set up see Risk et al. (Risk et al. 2012). Results were checked with the CFX Manager 3.1 Software (Bio-Rad) and further analysed using the program qbasePLUS V 2.6 (Biogazelle, www.biogazelle.com).

3.7.3 Supporting information tables

Table S1. Primers used for RT-qPCR.

Target gene (UniGene)	Gene name	5'-3' Sequence		Primer concentration [nM]	PCR efficiency (E) r^2 of calibration curve Slope	Amplicon length [bp]	Reference
	Pm3f$_{HA}$	fwd	AACTGGGCAGCATCAAACG	400	E = 100%	155	this work
		rev	AGCATAATCTGGAACATCG TATGGA	400	r^2 = *0.994*		
					Slope = -3.32		
	Pm3b$_{myc}$	fwd	AACTGGGCAGCATCAAACG	400	E = 101%	169	this work
		rev	ACGGATCCTCACAAATCT	400	r^2 = *0.992*		
					Slope = -3.30		
Ta.5104	*GAPDH*	fwd	TTAGACTTGCGAAGCCAGCA	600	E = 97%	81	Travella *et al.*, 2006
		rev	AAATGCCCTTGAGGTTTCCC	600	r^2 = *0.989*		
					Slope = -3.400		

Table S2. Primers used for the construction of plasmid vectors for agroinfiltrations.

Primer name	**primer sequence 5`--> 3`**
TJ065	TTGGCGCGCCGCGGATGGCAGAGCGGGTGGTCA
TJ066	CCCCCCGGGCGGCCGCTCAGCTCCGGCAGGCC
dst015	GCACATGTAAAATTCATGTTCTTATGCATGATATTGC
dst016	GCAATATCATGCATAAGAACATGAATTTTACATGTGC
dst057	GGGGACAAGTTTGTACAAAAAAGCAGGCTATGGCAGAGCGGGTGG
dst058	CCGAGATCAGCTTCTGCTCGCTCCGGCAGGCCTGC
dst059	GGGGACCACTTTGTACAAGAAAGCTGGGTTCACAGGTCTTCCTCCGAGATCAGCTTCTGCTC
dst060	GGGGACAAGTTTGTACAAAAAAGCAGGCTATGGAAATTGAGTGGCTTCCAG
dst062	CCGAGATCAGCTTCTGCTCGTGATGCAGATACTTTGGT
dst070	GAGCAGAAGCTGATCTCGG
dst071	ACAGGTCTTCCTCCGAGATCAGCTTCTGCTCTGGTGCTTCGGGTAAATC
dst072	ATGCCAACTTTGTACAAAAAAGCAGGCTATGCAGAAATGGGATGCTGCT
dst073	CATAGCCTGCTTTTTTGTAC
dst090	ACAGGTCTTCCTCCGAGATCAGCTTCTGCTCGAAGGATGTACCACAACTG
dst101	ACAGGTCTTCCTCCGAGATCAGCTTCTGCTCGCTGTCGCCAACCTCAGT
dst102	ACAGGTCTTCCTCCGAGATCAGCTTCTGCTCTGGTGCTTCAGGTAATGC
dst109	ATGCCAACTTTGTACAAAAAAGCAGGCTATGACGTTTCCAAAACTGAAGGT

Table S3. Detailed information on the cloning of the Gateway pENTR plasmids used in this study.

Plasmid	Cloning method	Vector backbone	Source plasmid	Origin of source plasmid	Cloning procedure	Primers used
pSC-A-Pm3f_D501V (cDNA)	site-directed mutagenesis PCR		pSC-A-Pm3f (cDNA)	this study	mutagenesis PCR (dst015-dst016)	dst015, dst016
pENTR221-Pm3f_D501V-HA (cDNA)	Gateway BP cloning	pDONR221	pSC-A-Pm3f_D501V (cDNA)	this study	PCR (dst057-dst061)	dst057, dst061
pENTR221-Pm3b-myc (cDNA)	Gateway BP cloning	pDONR221	pSC-A-Pm3b (cDNA)	this study	PCR (dst057-dst058), then PCR (dst057-dst059)	dst057, dst058, dst059
pENTR221-hPm3-1B-myc (cDNA)	site-directed mutagenesis PCR		pENTR221-hPm3-1B-myc (gDNA)	Stirnweis et al., 2014	mutagenesis PCR (dst94-dst95)	dst094, dst095
pENTR221-Pm3b_CC-NBS-myc	Gateway BP cloning		pSC-A-Pm3b (cDNA)	this study	PCR (dst057-dst062), then PCR (dst057-dst059)	dst057, dst059, dst062
pENTR221-Pm3b_LRR-myc (cDNA)	Gateway BP cloning		pSC-A-Pm3b (cDNA)	this study	PCR (dst060-dst058), then PCR (dst060-dst059)	dst058, dst059, dst060
pENTR221-Pm3b_LRR15-END-myc (cDNA)	site-directed mutagenesis PCR		pENTR221-Pm3b_LRR-myc (cDNA)	this study	mutagenesis PCR (dst072-dst073)	dst072, dst073
pENTR221-Pm3b_Sp-LRR15-myc	site-directed mutagenesis PCR		pENTR221-Pm3b_LRR-myc (cDNA)	this study	mutagenesis PCR (dst070-dst071)	dst070, dst071
pENTR221-Pm3b_Sp-LRR12-myc	site-directed mutagenesis PCR		pENTR221-Pm3b_LRR-myc (cDNA)	this study	mutagenesis PCR (dst070-dst102)	dst070, dst102
pENTR221-Pm3b_Sp-LRR10-myc	site-directed mutagenesis PCR		pENTR221-Pm3b_LRR-myc (cDNA)	this study	mutagenesis PCR (dst070-dst090)	dst070, dst090
pENTR221-Pm3b_Sp-LRR8-myc	site-directed mutagenesis PCR		pENTR221-Pm3b_LRR-myc (cDNA)	this study	mutagenesis PCR (dst070-dst101)	dst070, dst101
pENTR221-Pm3b_LRR10-END-myc (cDNA)	site-directed mutagenesis PCR		pENTR221-Pm3b-myc (cDNA)	this study	mutagenesis PCR (dst109-dst073)	dst073, dst109
pENTR221-Pm3b_LRR10-15-myc	site-directed mutagenesis PCR		pENTR221-Pm3b_LRR10-END-myc (cDNA)	this study	mutagenesis PCR (dst070-dst071)	dst070, dst071
pENTR-GUS	delivered as control in the kit		Gateway LR clonase II kit	life technologies, Carlsbad, CA		
pENTR221-Pm3f-HA (gDNA)	see Stirnweis et al., 2014			Stirnweis et al., 2014		

3.7.4 Supporting information figures

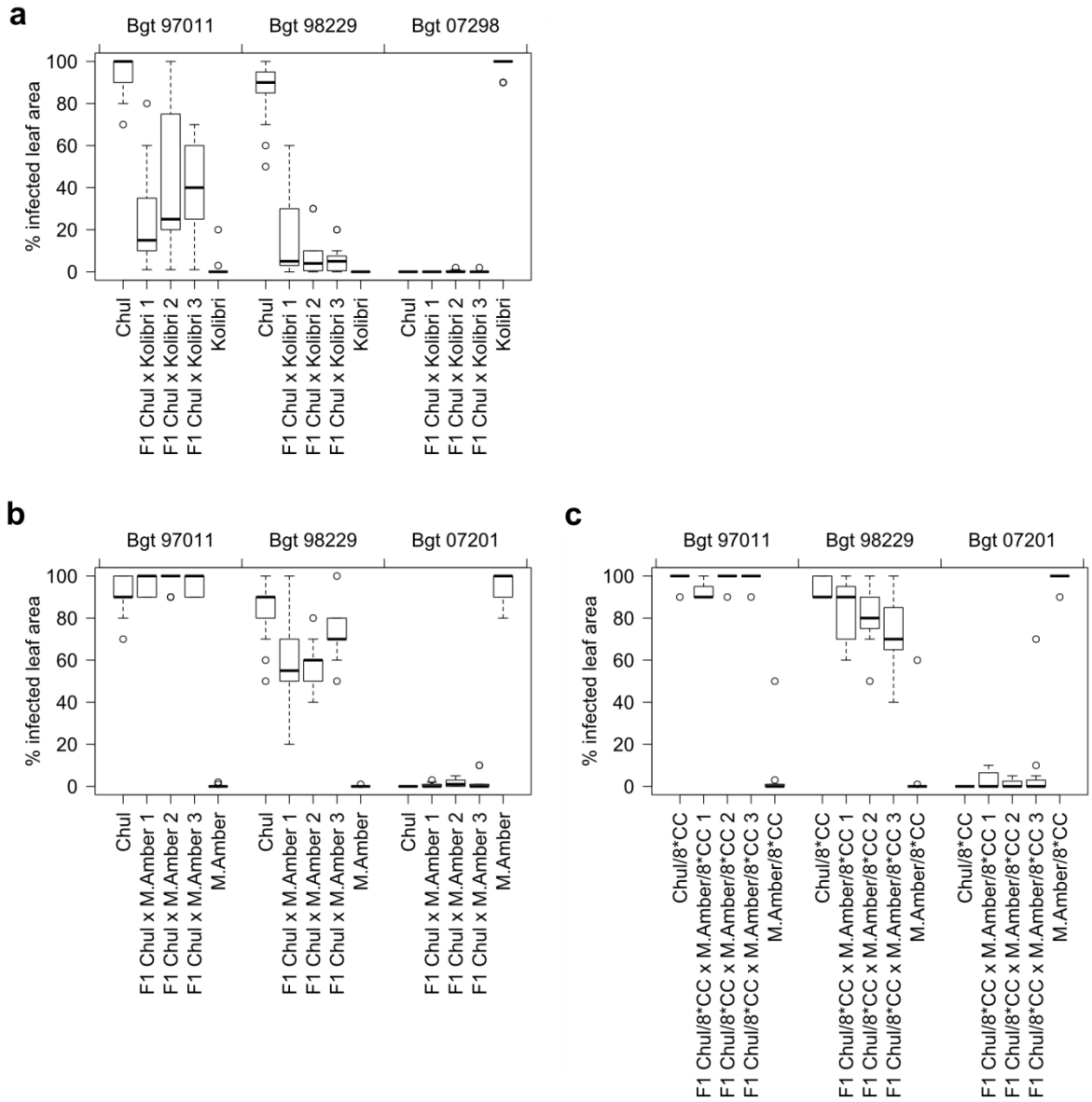

Figure S1. Incomplete resistance of F1 hybrids. Hybrids originating from parental lines expressing the *Pm3b*, *Pm3d*, or *Pm3f* allele are incompletely resistant to powdery mildew isolates that are avirulent on the *Pm3d* or *Pm3f* parental lines. Results of leaf segment infection tests with the parental lines and the F1 hybrids of three independent crosses (1-3) per line combination. Infections were done with the powdery-mildew isolates *Bgt* 97011, *Bgt* 98229 (both *avrPm3b* & *AvrPm3d/f*), *Bgt* 07201 (*AvrPm3b* & *avrPm3f*) and *Bgt* 07298 (*AvrPm3b* & *avrPm3d*). Results of infected leaf area for the combination (a) of Chul (*Pm3b*) with Kolibri (*Pm3d*), (b) of Chul (*Pm3b*) with M. Amber (*Pm3f*), and (c) of the two near-isogenic lines Chul/8*CC (*Pm3b*) and M. Amber/8*CC (*Pm3f*) are shown. Data for at least eight replicates is presented with Box and Whisker Plots and the median values are shown with black horizontal lines.

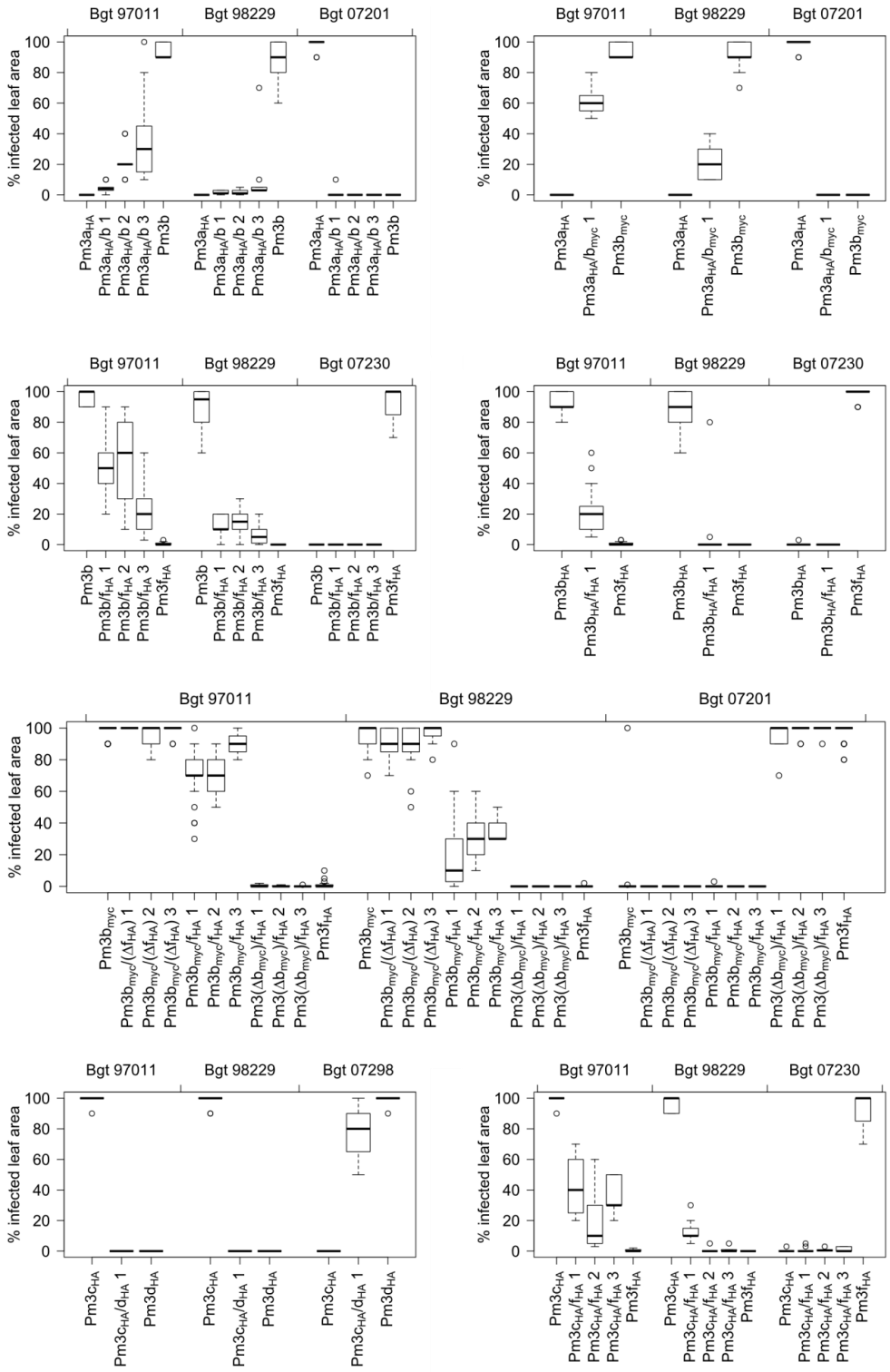

Figure S2. Non-additive gene action in double-homozygous lines for four *Pm3* allele combinations. Lines originating from crosses of transgenic lines expressing either the *Pm3a*, *Pm3b*, *Pm3c*, *Pm3d*, or *Pm3f* allele are incompletely resistant to some powdery-mildew isolates that are avirulent on one of the parental lines or of the sister lines. Results of leaf segment infection tests with the parental lines, sister lines for $Pm3b_{myc}/f_{HA}$ and the *Pm3*-double-homozygous descendants of up to three independent crosses (1-3) per line combination. Infections were done with the powdery-mildew isolates *Bgt* 97011, *Bgt* 98229 (both *AvrPm3a/d/f* & *avrPm3b/c*), *Bgt* 07201 (*AvrPm3b* & *avrPm3a/f*), *Bgt 07230* (*AvrPm3b/c* & *avrPm3f*), and *Bgt* 07298 (*AvrPm3c* & *avrPm3d*). Results of infected leaf area for combinations of *Pm3a* with *Pm3b, Pm3b* with *Pm3f, Pm3c* with *Pm3d,* and *Pm3c* with *Pm3f* are shown. Data for at least nine replicates is presented with Box and Whisker Plots and the median values are shown with black horizontal lines.

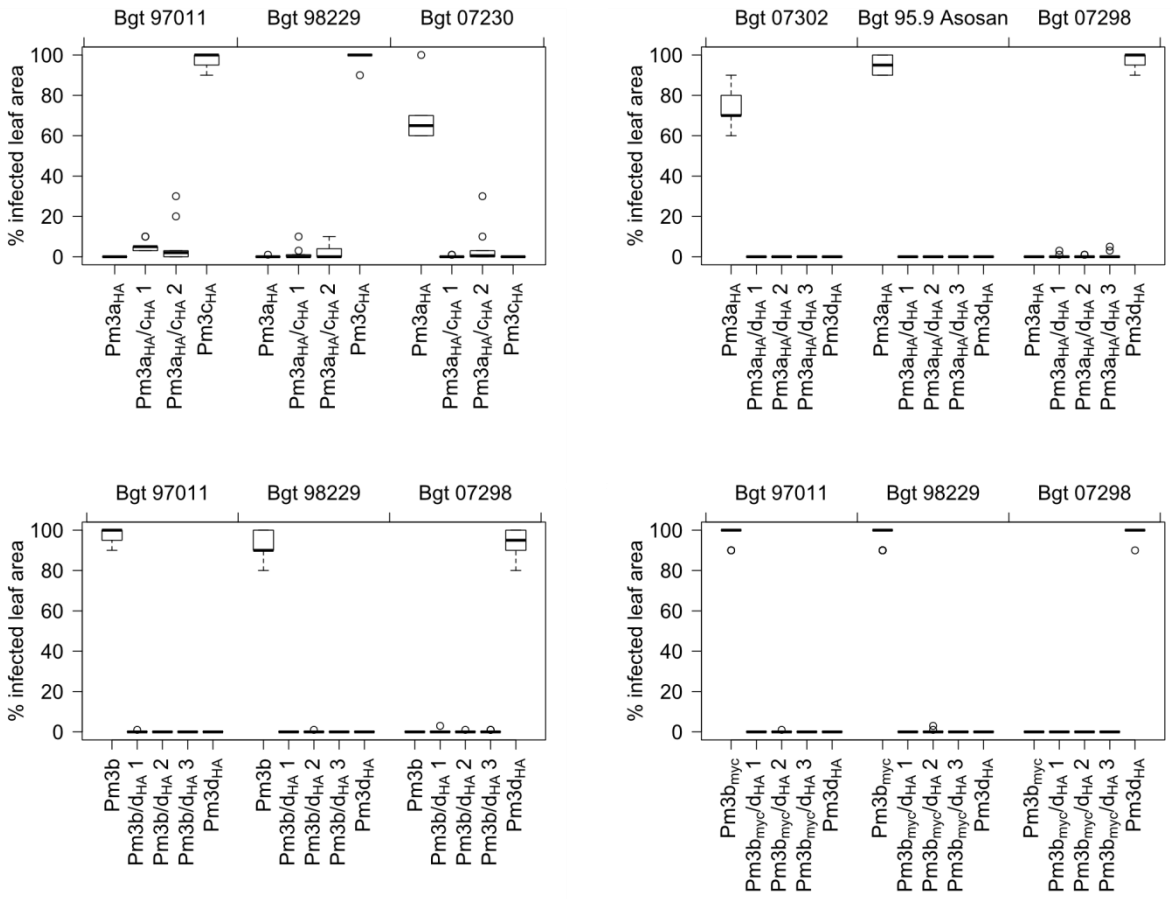

Figure S3. Additive gene action in double-homozygous lines for three *Pm3* allele combinations. Lines originating from crosses of transgenic lines expressing either the *Pm3a*, *Pm3b*, *Pm3c*, or *Pm3d* allele, additive *Pm3* gene action leads to plants resistant to powdery mildew isolates that are avirulent on either of the two parental lines. Results of leaf segment infection tests with the parental lines and the *Pm3*-double-homozygous descendants of up to three independent crosses (1-3) per line combination. Infections were done with the powdery-mildew isolates *Bgt* 97011, *Bgt* 98229 (both *AvrPm3a/d* & *avrPm3b/c*), *Bgt 07230* (*AvrPm3c* & *avrPm3a*), *Bgt* 07302, *Bgt* 95.9 Asosan (both *AvrPm3d* & *avrPm3a*), and *Bgt* 07298 (*AvrPm3a/b* & *avrPm3d*). Results of infected leaf area for combinations of *Pm3a* with *Pm3c, Pm3a* with *Pm3d,* and *Pm3b* with *Pm3d* are shown. Data for at least nine replicates are presented with Box and Whisker Plots and the median values are shown with black horizontal lines.

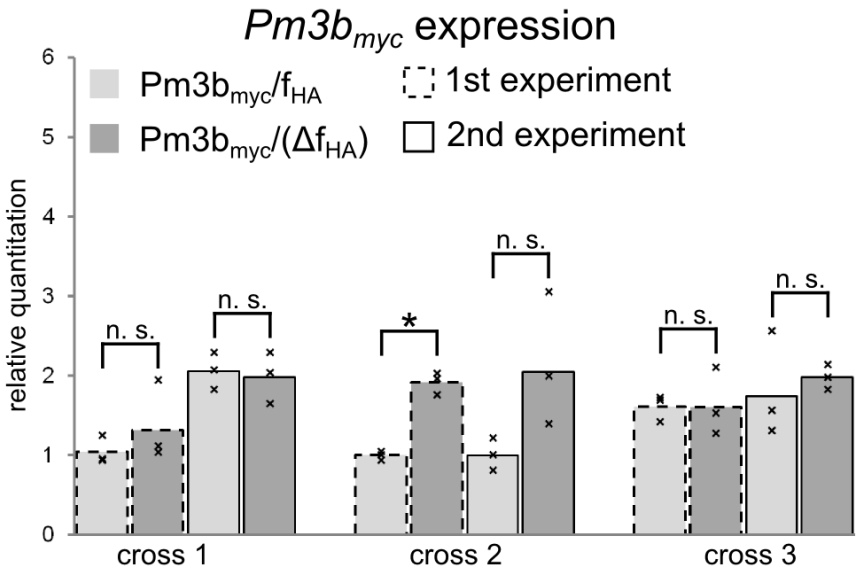

Figure S4. Double-homozygous $Pm3b_{myc}/f_{HA}$ lines and the $Pm3b_{myc}/(\Delta f_{HA})$ sister lines show no or only minimal differences of *Pm3b*$_{myc}$-transcript accumulation. Mean values (represented by bars) and single data points (x) of two independent RT-qPCR experiments each with three replicates are displayed. Values are normalized to the lowest value (set to 1) within each experiment. Significant differences are indicated by asterisks (Student`s *t*-test $P<0.05$; n. s. = non significant)

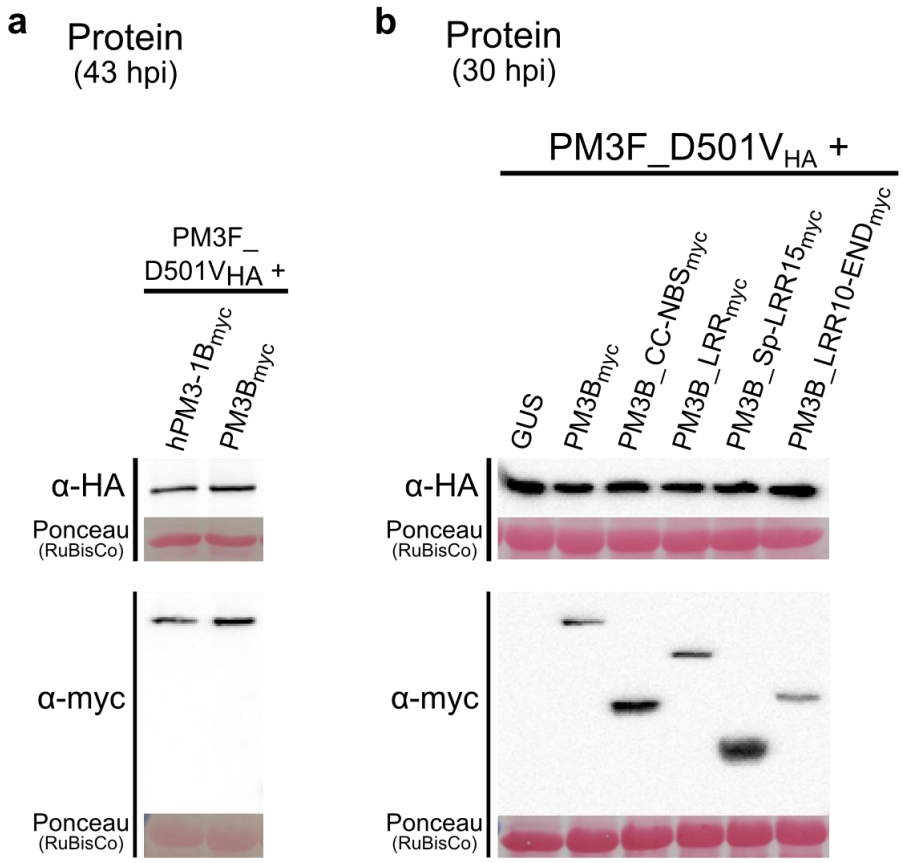

Figure S5. Suppression of PM3F_D501V$_{HA}$-induced HR by co-expression of *Pm3b* fragments is not caused by an altered PM3F_D501V$_{HA}$ protein accumulation. Figure shows protein detections after co-infiltrations of autoactive PM3F_D501V$_{HA}$ together with HR-suppressing and non-HR-suppressing fragments of PM3B$_{myc}$ or with non-HR-suppressing hPM3-1B$_{myc}$.
(a) Immunoblot analysis of PM3F_D501V$_{HA}$ (α-HA panel) and hPM3-1B$_{myc}$ or PM3B$_{myc}$ proteins (α-myc panel). Material for protein extraction was harvested before the onset of cell death from the same leaf at 43 hours post co-infiltration of *Pm3f_D501V$_{HA}$* together with the indicated constructs.
(b) Immunoblot analysis of PM3F_D501V$_{HA}$ (α-HA panel) and PM3B$_{myc}$-fragment proteins (α-myc panel). Material for protein extraction was harvested from the same leaf before the onset of cell death at 30 hours post co-infiltration of *Pm3f_D501V$_{HA}$* together with the indicated constructs. *GUS* represents the negative control for *Pm3f_D501V$_{HA}$* suppression.
Ponceau S membrane staining of Ribulose-1,5-bis-phosphate carboxylase/oxygenase (RuBisCo) is shown as control for equal loading of total protein in (a) and (b).

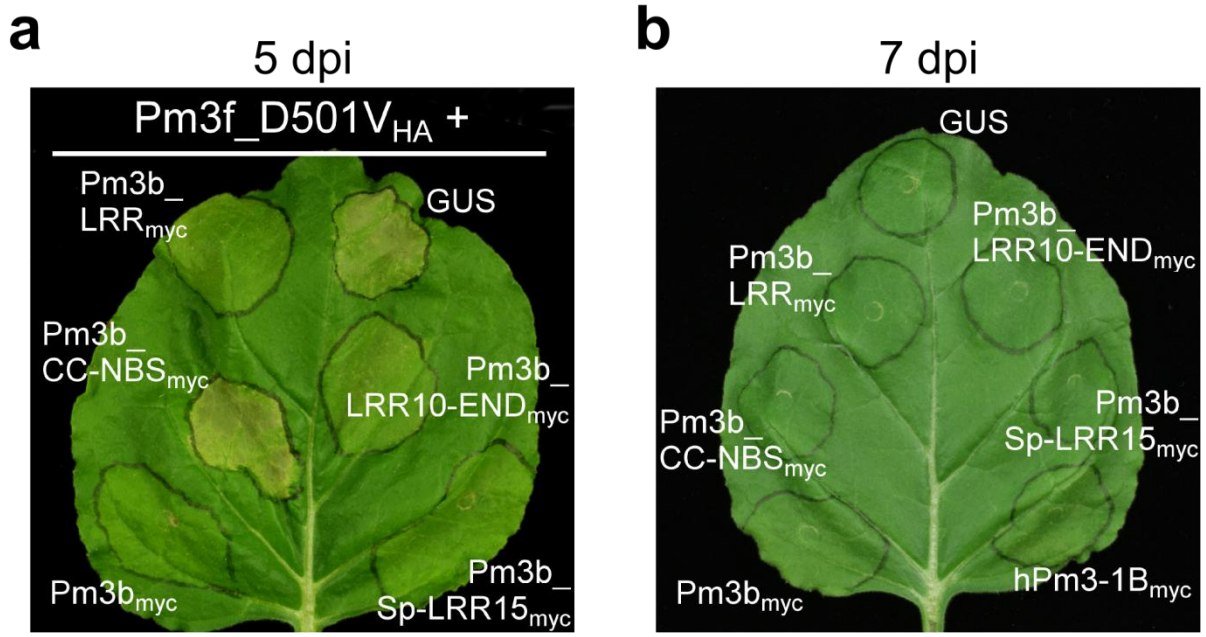

Figure S6. Cell death induction by the autoactivated PM3F_D501V$_{HA}$ is suppressed by PM3B$_{myc}$ and fragments of its LRR domain in a *Nicotiana benthamiana*-transient-expression system. Pictures of *Agrobacterium tumefaciens*-infiltrated *N. benthamiana* leaves transiently expressing different *Pm3* constructs are shown.
(a) Co-infiltration of autoactive *Pm3f_D501V$_{HA}$* with different fragments of *Pm3b$_{myc}$*. An exemplary picture taken at 5 days post infiltration (dpi) is shown. *GUS* represents the negative control for suppression. Infiltrations were repeated three times with at least three replicates. Due to variable phenotypes this picture cannot be representative for all co-infiltrations. Detailed information is given in Figure 4c in the main text.
(b) Control infiltrations of *Pm3b$_{myc}$* fragments and *hPm3-1B$_{myc}$* reveal no cell death induction by any of these constructs. A representative picture of a leaf taken at 7 dpi of the indicated constructs is shown.

4 General discussion

4.1 Both NB-LRR signaling intensity and recognition capacity contribute to resistance specificity

Whereas in earlier times the activation of resistance was normally equated with the recognition of a non-self or non-self-modified molecule, the results of chapter 2 together with recently published work by Harris and associates (2013) reveal a more complex situation. In these two studies the modification of the NB-ARC domain, a region that is obviously not involved in physical interactions with an Avr or guardee protein, modified the resistance spectrum of an NB-LRR receptor. Segretin and associates (Segretin et al. 2014) found similar gain-of-function variants. These results demonstrate that the resistance specificity of an NB-LRR receptor is dependent on its recognition specificity which has to be defined as a physical interaction, plus its activation sensitivity and signaling intensity.

Concerning the signaling intensity of CC-NB-LRR proteins, the results of chapter 2 show that the ARC2-loop sequence is a major determinant of HR amplitude and timing. The exact molecular mechanism of how the ARC2 loop is involved in this modification of signaling, whether through CC-NB-LRR internal interactions as indicated by work of Slootweg and associates (2013) or interactions with signaling components, finally remains elusive. Here, information about proteins interacting with PM3 could potentially be beneficial for a scientific investigation. Structural information of a full size CC-NB-LRR protein would also be an invaluable dataset for the understanding of mechanistic aspects of NB-LRR function, but such crystal structures will probably not be available within the next years. *In silico* structural models and docking models are not an adequate replacement for it, but still they may be a valuable source for the design of new experiments to clarify mechanistic hypotheses (Steinbrenner et al. 2012; Slootweg et al. 2013).

But for a full understanding of the activation of NB-LRR-mediated immunity it will probably be necessary to also consider interactions within larger complexes. Here, there is increasing evidence that heteromeric complexes including different NB-LRR proteins might play an important role. This inference can be drawn from numerous examples where it was shown that a pair of NB-LRR proteins was necessary to provide resistance (Ashikawa et al. 2008; Loutre et al. 2009; Narusaka et al. 2009; Cesari et al. 2013; Eitas and Dangl 2010) and from the observations that some NB-LRR R proteins rely on the presence of NB-LRR "helper" proteins for full resistance function (Grant et al. 2003; Sinapidou et al. 2004; Bonardi et al. 2011). The *in trans* suppressions between different PM3 variants and the interaction

shown for PM3F and hPM3-1B, both shown in chapter 3, add another piece of evidence for the importance of physical or functional interactions between different NB-LRR proteins.

4.2 Rational enhancement of NB-LRR resistance proteins

Disease resistance proteins of the NB-LRR type are highly sensitive immunity receptors for pathogen-derived molecules. As such they have to be tightly regulated. In the presence of the pathogen they need to be efficiently activated and trigger an adapted immune response. In the absence of a pathogen they need to stay inactive. A suboptimal regulation in any of the two aspects may be disadvantageous for the plant: On the one hand, inadequate activation or signaling after elicitor recognition can lead to only partial resistance, pathogen spread, and a spreading necrosis (Farnham and Baulcombe 2006; Komatsu et al. 2010; Nam et al. 2011). On the other hand, the presence of "leaky", misregulated immune receptors may have a tradeoff in terms of reduced fitness compared to susceptible plants (Tian et al. 2003), reduced plant growth (Todesco et al. 2010), hybrid incompatibility (Bomblies and Weigel 2007), or autoimmunity. Within these limits evolution of NB-LRR receptors takes place, constantly leading to new receptor variants adapted to new or additional *Avr* proteins. The rational enhancement of NB-LRR R proteins has to operate within the same limits to be beneficial for resistance breeding, i.e. it has to enhance resistance without negative side effects.

Though *Nicotiana*-infiltration systems are a powerful tool for functional studies with HR-inducing NB-LRR receptors, reaching this goal is not straight forward. This can be seen in the results of a LRR-random-mutagenesis study by Farnham and Baulcombe (2006) where a new Rx variant was generated that was able to detect an Avr protein from poplar mosaic virus (PopMV). But "the response to PopMV was transformed from a mild disease on plants carrying wild-type Rx to a trailing necrosis that killed the plant" (Harris et al. 2013). A second round of artificial evolution was necessary to create a useful receptor based on this initial variant (Harris et al. 2013). Another example showing the complexity of an artificial enhancement of NB-LRR proteins was recently published by Segretin and associates (2014). They successfully screened randomly-mutated R3a *Phytophthora infestans*-resistance proteins for HR induction by the previously unrecognized AVR3a^{EM} variant. However, "preliminary infection assays, conducted after transient and stable expression of the R3a+ mutants […], failed to detect increased resistance to *P. infestans* in either *N. benthamiana* or potato plants" (Segretin et al. 2014). The enlargement of the PM3F resistance spectrum by the L456P/Y458H mutations, as shown in chapter 2, appears to come without negative side effects. This might be based on the fact that information on natural variation between *Pm3* alleles was exploited and, therefore, the used mutations were already "preselected" by natural

selection. Consequently, it can be expected that the same enhancing mutations can be successfully applied to all narrow-spectrum *Pm3* proteins.

However, to ultimately clarify whether L456P/Y458H modifications in PM3F or other PM3 proteins keep their promise of being solely positive, the performance of accordingly modified wheat plants would have to be evaluated under field conditions and, here, they should be compared to the respective non-modified lines. It was shown before that the overexpression of *Pm3* alleles in transgenic wheat lines under field conditions can lead to pleiotropic effects (leaf yellowing, sterility, non-specific resistance) that are also dependent on the particular transformation event (Brunner et al. 2011, 2012). For this reason, direct comparison of, for example, lines transformed with *Pm3f* and *Pm3f_L456P/Y458H* may not be adequate to investigate the effect of L456P/Y458H modifications in the field. Instead, the comparison of a *Pm3f_L456P/Y458H* wheat line generated by genome editing with its wild-type line might be favorable. The generation of such a line might also enable the investigation of whether L456P/Y458H has a positive influence on the temperature sensitivity of narrow-spectrum PM3 proteins that was suggested by earlier work in the laboratory of Prof. Beat Keller (Krukowski 2007).

4.3 *Pm3* allele pyramiding: Possibilities, limitations, and alternatives

The pyramiding of different *R* genes is certainly an important strategy for resistance breeding in crop plants, at least for some plant-pathogen combinations (McDonald and Linde 2002). If the pyramided major resistance genes are backed up by a combination with minor, non-race-specific resistance genes, this might lead to crop varieties with durable-resistance properties even against highly aggressive and rapidly adapting pathogens. This was recently demonstrated by Rietman and associates (2012) for a *P. infestans*-resistant potato cultivar. The generation of tightly linked genetic markers for and the cloning of more and more resistance genes will further support and simplify the pyramiding of resistance genes in the future.

With the advent of transgenic approaches and the establishment of efficient screening techniques for allelic variance in *R* genes, allele pyramiding now becomes an alternative or complementary strategy to the *R*-gene pyramiding. It might potentially have some disadvantages compared to an optimal gene-pyramiding strategy (see chapter 1.3.2), but still, it theoretically largely expands the possibilities to stack sets of resistance determinants that are as diverse as possible. Nevertheless, suppression effects between alleles of NB-LRR-encoding *R* genes, as shown in chapter 3, potentially present a serious limitation for the

efficiency of the allele-pyramiding strategy. It remains to be determined whether the *Pm3*-case is rather an exception or the rule in this aspect. Examples discussed in chapter 3.4 indicate that at least the suppression mechanism might be widespread and, hence, the allele pyramiding should be carefully evaluated in the future. Therefore, the presented suppression assay in *N. benthamiana* (see chapter 3.3) could be a useful tool to easily pretest the compatibility of alleles (and genes) in future pyramiding projects.

As for the NB-LRR activity enhancement, a detailed knowledge about the mechanistic processes during NB-LRR activation would potentially help to better understand the suppression between different PM3 proteins. With the results that the LRR is the suppression conferring domain, it seems likely that a similar mechanism is responsible for *cis*- as well as *trans*-signaling regulation of NB-LRR receptors. Swapping experiments between suppressing *Pm3* and its non-suppressing homolog *hPm3-1B* are eventually a mean to further resolve the identity of the suppression-conferring protein region. Preliminary experiments with full-length gene swaps, however, were inconclusive (data not shown). With the lack of a detailed understanding of the suppression mechanism it remains difficult to prevent suppression via sequence adaptations in the genes. But maybe a careful selection of lines might anyway be sufficient to avoid non-additive gene action, at least for some allele combinations (see chapter 3.3).

Some of the pyramided *Pm3* lines will be tested in a field trial in 2014-2017 in Zürich-Affoltern, Switzerland. Regarding that the stacked *Pm3* alleles were already widely employed in wheat varieties and virulence frequencies against most of the stacked *Pm3* alleles are relatively high in Switzerland (Brunner et al. 2010), expectations for a huge durability or resistance effect in this trial should not be too high.

4.4 Consequences of possible NB-LRR suppressions

The suppression mechanism described in chapter 3 might serve as an explanation for phenomena that have so far not been understood, have possibly often been misinterpreted as gene-dosage effects or genetic incompatibility with for example signaling components, or have eventually not been published. Reports on related phenotypic observations might be underrepresented in the literature, since they represent negative results with low informative value.

As an example, the genetic transformation of an NB-LRR-encoding resistance gene into another species or variety might not lead to an actual transfer of disease resistance. This can of course have many reasons – the gene might be transcriptionally silenced, signaling

components or “helper” proteins might be missing, and so on – but it might also be caused by suppression of the transferred gene by an allele or homolog in the recipient plant. Probably, such examples are seldom investigated in detail and written reports are scarce.

From a genetic perspective suppression is not easy to detect. If an ‘actual dominant’ resistant allele in the sense that is has a gain of function compared to its susceptible allele was suppressed or partially suppressed by this dominant-negative, susceptible counterpart, the resistant allele would just appear as recessive or co-dominant allele, respectively (Garcia et al. 2011). Therefore, the suppression effect may often be hidden behind well known phenomena. But the effect becomes more obvious and probably occurs more frequently when suppression is taking places between orthologous genes from different subgenomes of a polyploid species. Results of Hurni and associates (submitted for publication) showing that the *Pm3*-ortholog *Pm8* is suppressed by *Pm3* substantiate the hypothesis. That is maybe why suppression phenomena are especially reported for polyploid species.

The finding that suppression can directly involve alleles of the same resistance gene is of special importance for hybrid breeding where dominant resistance of the parents is expected to be expressed in the F1 hybrids. Additional important crop species such as rice or wheat have started to be exploited as F1 hybrids and, therefore, an increasing relevance of the results of chapter 3 can eventually be expected in the future.

5 References

Van den Ackerveken, G., Marois, E., and Bonas, U. 1996. Recognition of the bacterial avirulence protein AvrBs3 occurs inside the host plant cell. Cell. 87:1307–1316

Ade, J., DeYoung, B. J., Golstein, C., and Innes, R. W. 2007. Indirect activation of a plant nucleotide binding site–leucine-rich repeat protein by a bacterial protease. Proc. Natl. Acad. Sci. 104:2531–2536

Alcázar, R., and Parker, J. E. 2011. The impact of temperature on balancing immune responsiveness and growth in Arabidopsis. Trends Plant Sci. 16:666–675

Ashikawa, I. 2012. Regions outside the leucine-rich repeat domain determine the distinct resistance specificities of the rice blast resistance genes *Pik* and *Pik-m*. Mol. Breed. 30:1531–1535

Ashikawa, I., Hayashi, N., Yamane, H., Kanamori, H., Wu, J., Matsumoto, T., Ono, K., and Yano, M. 2008. Two adjacent nucleotide-binding site–leucine-rich repeat class genes are required to confer *Pikm*-specific rice blast resistance. Genetics. 180:2267–2276

Axtell, M. J., McNellis, T. W., Mudgett, M. B., Hsu, C. S., and Staskawicz, B. J. 2001. Mutational analysis of the *Arabidopsis RPS2* disease resistance gene and the corresponding *Pseudomonas syringae avrRpt2* avirulence gene. Mol. Plant. Microbe Interact. 14:181–188

Bai, J., Pennill, L. A., Ning, J., Lee, S. W., Ramalingam, J., Webb, C. A., Zhao, B., Sun, Q., Nelson, J. C., Leach, J. E., and Hulbert, S. H. 2002. Diversity in nucleotide binding site–leucine-rich repeat genes in cereals. Genome Res. 12:1871–1884

Bai, S., Liu, J., Chang, C., Zhang, L., Maekawa, T., Wang, Q., Xiao, W., Liu, Y., Chai, J., Takken, F. L. W., Schulze-Lefert, P., and Shen, Q.-H. 2012. Structure-function analysis of barley NLR immune receptor MLA10 reveals its cell compartment specific activity in cell death and disease resistance. PLoS Pathog. 8

Baker, C. J., O`Neill, N. R., Keppler, L. D., and Orlandi, E. W. 1991. Early responses during plant-bacteria interactions in tobacco cell suspensions. Phytopathology. 81:1504–1507

Barker, C. L., Baillie, B. K., Hammond-Kosack, K. E., Jones, J. D. G., and Jones, D. A. 2006. Dominant-negative interference with defence signalling by truncation mutations of the tomato *Cf-9* disease resistance gene. Plant J. 46:385–399

Bella, J., Hindle, K. L., McEwan, P. A., and Lovell, S. C. 2008. The leucine-rich repeat structure. Cell. Mol. Life Sci. 65:2307–2333

Bendahmane, A., Farnham, G., Moffett, P., and Baulcombe, D. C. 2002. Constitutive gain-of-function mutants in a nucleotide binding site–leucine rich repeat protein encoded at the *Rx* locus of potato. Plant J. 32:195–204

Bendahmane, A., Querci, M., Kanyuka, K., and Baulcombe, D. C. 2000. *Agrobacterium* transient expression system as a tool for the isolation of disease resistance genes: application to the *Rx2* locus in potato. Plant J. 21:73–81

Bernoux, M., Ellis, J. G., and Dodds, P. N. 2011a. New insights in plant immunity signaling activation. Curr. Opin. Plant Biol. 14:512–518

Bernoux, M., Ve, T., Williams, S., Warren, C., Hatters, D., Valkov, E., Zhang, X., Ellis, J. G., Kobe, B., and Dodds, P. N. 2011b. Structural and functional analysis of a plant resistance protein TIR domain reveals interfaces for self-association, signaling, and autoregulation. Cell Host Microbe. 9:200–211

Bhullar, N. K., Street, K., Mackay, M., Yahiaoui, N., and Keller, B. 2009. Unlocking wheat genetic resources for the molecular identification of previously undescribed functional alleles at the *Pm3* resistance locus. Proc. Natl. Acad. Sci. 106:9519–9524

Bhullar, N. K., Zhang, Z., Wicker, T., and Keller, B. 2010. Wheat gene bank accessions as a source of new alleles of the powdery mildew resistance gene *Pm3*: a large scale allele mining project. BMC Plant Biol. 10:88

Bieri, S., Mauch, S., Shen, Q.-H., Peart, J., Devoto, A., Casais, C., Ceron, F., Schulze, S., Steinbiss, H.-H., Shirasu, K., and Schulze-Lefert, P. 2004. RAR1 positively controls steady state levels of barley MLA resistance proteins and enables sufficient MLA6 Accumulation for effective resistance. Plant Cell. 16:3480–3495

Bieri, S., Potrykus, I., and Fütterer, J. 2000. Expression of active barley seed ribosome-inactivating protein in transgenic wheat. Theor. Appl. Genet. 100:755–763

Van der Biezen, E. A., and Jones, J. D. G. 1998. The NB-ARC domain: a novel signalling motif shared by plant resistance gene products and regulators of cell death in animals. Curr. Biol. 8:R226–R228

Boller, T., and Felix, G. 2009. A renaissance of elicitors: Perception of microbe-associated molecular patterns and danger signals by pattern-recognition receptors. Annu. Rev. Plant Biol. 60:379–406

Bomblies, K., and Weigel, D. 2007. Hybrid necrosis: autoimmunity as a potential gene-flow barrier in plant species. Nat Rev Genet. 8:382–393

Bonardi, V., Tang, S., Stallmann, A., Roberts, M., Cherkis, K., and Dangl, J. L. 2011. Expanded functions for a family of plant intracellular immune receptors beyond specific recognition of pathogen effectors. Proc. Natl. Acad. Sci. 108:16463–16468

Bowen, K. L., Everts, K. L., and Leath, S. 1991. Reduction in yield of winter wheat in North Carolina due to powdery mildew and leaf rust. Phytopathology. 81:503–511

Braun, U. 2011. The current systematics and taxonomy of the powdery mildews (Erysiphales): an overview. Mycoscience. 52:210–212

Briggle, L. W. 1966. Three loci in wheat involving resistance to *Erysiphe graminis* f. sp. *tritici*. Crop Sci. 6:461

Brunner, S., Hurni, S., Herren, G., Kalinina, O., von Burg, S., Zeller, S. L., Schmid, B., Winzeler, M., and Keller, B. 2011. Transgenic *Pm3b* wheat lines show resistance to powdery mildew in the field. Plant Biotechnol. J. 9:897–910

Brunner, S., Hurni, S., Streckeisen, P., Mayr, G., Albrecht, M., Yahiaoui, N., and Keller, B. 2010. Intragenic allele pyramiding combines different specificities of wheat *Pm3* resistance alleles. Plant J. 64:433–445

Brunner, S., Stirnweis, D., Diaz Quijano, C., Buesing, G., Herren, G., Parlange, F., Barret, P., Tassy, C., Sautter, C., Winzeler, M., and Keller, B. 2012. Transgenic *Pm3* multilines of wheat show increased powdery mildew resistance in the field. Plant Biotechnol. J. 10:398–409

Cao, A., Xing, L., Wang, X., Yang, X., Wang, W., Sun, Y., Qian, C., Ni, J., Chen, Y., Liu, D., Wang, X., and Chen, P. 2011. Serine/threonine kinase gene Stpk-V, a key member of powdery mildew resistance gene Pm21, confers powdery mildew resistance in wheat. Proc. Natl. Acad. Sci. 108:7727 –7732

Caplan, J. L., Mamillapalli, P., Burch-Smith, T. M., Czymmek, K., and Dinesh-Kumar, S. P. 2008. Chloroplastic protein NRIP1 mediates innate immune receptor recognition of a viral effector. Cell. 132:449–462

Cesari, S., Thilliez, G., Ribot, C., Chalvon, V., Michel, C., Jauneau, A., Rivas, S., Alaux, L., Kanzaki, H., Okuyama, Y., Morel, J.-B., Fournier, E., Tharreau, D., Terauchi, R., and Kroj, T. 2013. The rice resistance protein pair RGA4/RGA5 recognizes the *Magnaporthe oryzae* effectors AVR-Pia and AVR_1-CO_{39} by direct binding. Plant Cell. 25:1463–1481

Chang, C., Yu, D., Jiao, J., Jing, S., Schulze-Lefert, P., and Shen, Q.-H. 2013. Barley MLA immune receptors directly interfere with antagonistically acting transcription factors to initiate disease resistance signaling. Plant Cell. 25:1158–1173

Charmet, G. 2011. Wheat domestication: Lessons for the future. C. R. Biol. 334:212–220

Chen, W., Liu, T., and Gao, L. 2013. Suppression of stripe rust and leaf rust resistances in interspecific crosses of wheat. Euphytica. 192:339–346

Chen, Y., Singh, S., Rashid, K., Dribnenki, P., and Green, A. 2007. Pyramiding of alleles with different rust resistance specificities in *Linum usitatissimum* L. Mol. Breed. 21:419–430

Collier, S. M., Hamel, L.-P., and Moffett, P. 2011. Cell death mediated by the N-terminal domains of a unique and highly conserved class of NB-LRR protein. Mol. Plant. Microbe Interact. 24:918–931

Cong, L., Ran, F. A., Cox, D., Lin, S., Barretto, R., Habib, N., Hsu, P. D., Wu, X., Jiang, W., Marraffini, L. A., and Zhang, F. 2013. Multiplex genome engineering using CRISPR/Cas systems. Science. 339:819–823

Dangl, J. L., Horvath, D. M., and Staskawicz, B. J. 2013. Pivoting the plant immune system from dissection to deployment. Science. 341:746–751

Deslandes, L., Olivier, J., Theulières, F., Hirsch, J., Feng, D. X., Bittner-Eddy, P., Beynon, J., and Marco, Y. 2002. Resistance to *Ralstonia solanacearum* in *Arabidopsis thaliana* is conferred by the recessive *RRS1-R* gene, a member of a novel family of resistance genes. Proc. Natl. Acad. Sci. 99:2404–2409

Dinesh-Kumar, S. P., Tham, W.-H., and Baker, B. J. 2000. Structure–function analysis of the tobacco mosaic virus resistance gene *N*. Proc. Natl. Acad. Sci. 97:14789–14794

Dodds, P. N., Lawrence, G. J., Catanzariti, A.-M., Ayliffe, M. A., and Ellis, J. G. 2004. The *Melampsora lini AvrL567* avirulence genes are expressed in haustoria and their products are recognized inside plant cells. Plant Cell. 16:755–768

Dodds, P. N., Lawrence, G. J., Catanzariti, A.-M., Teh, T., Wang, C.-I. A., Ayliffe, M. A., Kobe, B., and Ellis, J. G. 2006. Direct protein interaction underlies gene-for-gene specificity and coevolution of the flax resistance genes and flax rust avirulence genes. Proc. Natl. Acad. Sci. 103:8888–8893

Dodds, P. N., and Rathjen, J. P. 2010. Plant immunity: towards an integrated view of plant–pathogen interactions. Nat. Rev. Genet. 11:539–548

Du, B., Zhang, W., Liu, B., Hu, J., Wei, Z., Shi, Z., He, R., Zhu, L., Chen, R., Han, B., and He, G. 2009. Identification and characterization of *Bph14*, a gene conferring resistance to brown planthopper in rice. Proc. Natl. Acad. Sci. 106:22163–22168

Du, X., Miao, M., Ma, X., Liu, Y., Kuhl, J. C., Martin, G. B., and Xiao, F. 2012. Plant programmed cell death caused by an autoactive form of Prf is suppressed by co-expression of the Prf LRR domain. Mol. Plant. 5:1058–1067

Eitas, T. K., and Dangl, J. L. 2010. NB-LRR proteins: pairs, pieces, perception, partners, and pathways. Curr. Opin. Plant Biol. 13:472–477

Ellis, J., Dodds, P., and Pryor, T. 2000. Structure, function and evolution of plant disease resistance genes. Curr. Opin. Plant Biol. 3:278–284

Ellis, J. G., Lawrence, G. J., Luck, J. E., and Dodds, P. N. 1999. Identification of regions in alleles of the flax rust resistance gene *L* that determine differences in gene-for-gene specificity. Plant Cell. 11:495–506

Everts, K. L., and Leath, S. 1992. Effect of early season powdery mildew on development, survival, and yield contribution of tillers of winter wheat. Phytopathol. USA.

Everts, K. L., Leath, S., and Finney, P. L. 2001. Impact of powdery mildew and leaf rust on milling and baking quality of soft red winter wheat. Plant Dis. 85:423–429

Farnham, G., and Baulcombe, D. C. 2006. Artificial evolution extends the spectrum of viruses that are targeted by a disease-resistance gene from potato. Proc. Natl. Acad. Sci. 103:18828–18833

Frelet-Barrand, A., Boutigny, S., Moyet, L., Deniaud, A., Seigneurin-Berny, D., Salvi, D., Bernaudat, F., Richaud, P., Pebay-Peyroula, E., Joyard, J., and Rolland, N. 2010. *Lactococcus lactis*, an alternative system for functional expression of peripheral and intrinsic *Arabidopsis* membrane proteins. PLoS ONE. 5:e8746

Frost, D., Way, H., Howles, P., Luck, J., Manners, J., Hardham, A., Finnegan, J., and Ellis, J. 2004. Tobacco transgenic for the flax rust resistance gene *L* expresses allele-specific activation of defense responses. Mol. Plant. Microbe Interact. 17:224–232

Gao, Z., Chung, E.-H., Eitas, T. K., and Dangl, J. L. 2011. Plant intracellular innate immune receptor Resistance to *Pseudomonas syringae pv. maculicola* 1 (RPM1) is activated at, and functions on, the plasma membrane. Proc. Natl. Acad. Sci. 108:7619 –7624

Garcia, A., Calvo, É. S., Kiihl, R. A. de S., and Souto, E. R. de. 2011. Evidence of a susceptible allele inverting the dominance of rust resistance in soybean. Crop Sci. 51:32–40

Glawe, D. A. 2008. The powdery mildews: A review of the world's most familiar (yet poorly known) plant pathogens. Annu. Rev. Phytopathol. 46:27–51

Grant, J. J., Chini, A., Basu, D., and Loake, G. J. 2003. Targeted activation tagging of the *Arabidopsis NBS-LRR* gene, *ADR1* , conveys resistance to virulent pathogens. Mol. Plant. Microbe Interact. 16:669–680

Gutierrez, J. R., Balmuth, A. L., Ntoukakis, V., Mucyn, T. S., Gimenez-Ibanez, S., Jones, A. M. E., and Rathjen, J. P. 2010. Prf immune complexes of tomato are oligomeric and contain multiple Pto-like kinases that diversify effector recognition. Plant J. 61:507–518

Hanusová, R., Hsam, S. L. K., Bartos, P., and Zeller, F. J. 1996. Suppression of powdery mildew resistance gene *Pm8* in *Triticum aestivum* L. (common wheat) cultivars carrying wheat-rye tranlocation T1BL·1RS. Heredity. 77:383–387

Harris, C. J., Slootweg, E. J., Goverse, A., and Baulcombe, D. C. 2013. Stepwise artificial evolution of a plant disease resistance gene. Proc. Natl. Acad. Sci. 110:21189–21194

Himmelbach, A., Zierold, U., Hensel, G., Riechen, J., Douchkov, D., Schweizer, P., and Kumlehn, J. 2007. A set of modular binary vectors for transformation of cereals. Plant Physiol. 145:1192–1200

Hogenhout, S. A., Van der Hoorn, R. A. L., Terauchi, R., and Kamoun, S. 2009. Emerging concepts in effector biology of plant-associated organisms. Mol. Plant. Microbe Interact. 22:115–122

Van der Hoorn, R. A. L., Laurent, F., Roth, R., and De Wit, P. J. G. M. 2000. Agroinfiltration is a versatile tool that facilitates comparative analyses of *Avr*9/*Cf-9*-induced and *Avr*4/*Cf-4*-induced necrosis. Mol. Plant. Microbe Interact. 13:439–446

Van der Hoorn, R. A. L. van der, and Kamoun, S. 2008. From guard to decoy: A new model for perception of plant pathogen effectors. Plant Cell. 20:2009–2017

Houterman, P. M., Ma, L., van Ooijen, G., de Vroomen, M. J., Cornelissen, B. J. C., Takken, F. L. W., and Rep, M. 2009. The effector protein Avr2 of the xylem-colonizing fungus *Fusarium oxysporum* activates the tomato resistance protein I-2 intracellularly. Plant J. 58:970–978

Hu, J., Li, X., Wu, C., Yang, C., Hua, H., Gao, G., Xiao, J., and He, Y. 2012. Pyramiding and evaluation of the brown planthopper resistance genes *Bph14* and *Bph15* in hybrid rice. Mol. Breed. 29:61–69

Hurni, S., Brunner, S., Buchmann, G., Herren, G., Jordan, T., Krukowski, P., Wicker, T., Yahiaoui, N., Mago, R., and Keller, B. 2013. Rye *Pm8* and wheat *Pm3* are orthologous genes and show evolutionary conservation of resistance function against powdery mildew. Plant J. 76:957–969

Islam, M. R., Jahoor, A., and Fischbeck, G. 1992. Analysis of powdery mildew reactions of barley F1 plants involving different *M1a* alleles. Physiol. Mol. Plant Pathol. 40:353–358

Jones, J. D. G., and Dangl, J. L. 2006. The plant immune system. Nature. 444:323–329

Kim, H.-J., Lee, H.-R., Jo, K.-R., Mortazavian, S. M. M., Huigen, D. J., Evenhuis, B., Kessel, G., Visser, R. G. F., Jacobsen, E., and Vossen, J. H. 2012. Broad spectrum late blight resistance in potato differential set plants Ma*R8* and Ma*R9* is conferred by multiple stacked *R* genes. Theor. Appl. Genet. 124:923–935

Knott, D. R. 2000. Inheritance of resistance to stem rust in Medea durum wheat and the role of suppressors. Crop Sci. 40:98

Kobe, B., and Kajava, A. V. 2001. The leucine-rich repeat as a protein recognition motif. Curr. Opin. Struct. Biol. 11:725–732

Komatsu, K., Hashimoto, M., Ozeki, J., Yamaji, Y., Maejima, K., Senshu, H., Himeno, M., Okano, Y., Kagiwada, S., and Namba, S. 2010. Viral-Induced Systemic Necrosis in Plants Involves Both Programmed Cell Death and the Inhibition of Viral Multiplication, Which Are Regulated by Independent Pathways. Mol. Plant. Microbe Interact. 23:283–293

Koncz, C., and Schell, J. 1986. The promoter of TL-DNA gene *5* controls the tissue-specific expression of chimaeric genes carried by a novel type of *Agrobacterium* binary vector. Mol. Gen. Genet. MGG. 204:383–396

Krasileva, K. V., Dahlbeck, D., and Staskawicz, B. J. 2010. Activation of an *Arabidopsis* resistance protein is specified by the in planta association of its leucine-rich repeat domain with the cognate oomycete effector. Plant Cell. 22:2444–2458

Krattinger, S. G., Lagudah, E. S., Spielmeyer, W., Singh, R. P., Huerta-Espino, J., McFadden, H., Bossolini, E., Selter, L. L., and Keller, B. 2009. A putative ABC transporter confers durable resistance to multiple fungal pathogens in wheat. Science. 323:1360 – 1363

Krukowski, P. 2007. Master thesis: Genetic and molecular analysis of *Pm3*, *Pm8* and *Pm17* based powdery mildew resistance in wheat.

Laemmli, U. K. 1970. Cleavage of structural proteins during the assembly of the head of bacteriophage T4. Nature. 227:680–685

Leister, R. T., Dahlbeck, D., Day, B., Li, Y., Chesnokova, O., and Staskawicz, B. J. 2005. Molecular genetic evidence for the role of *SGT1* in the intramolecular complementation of Bs2 protein activity in *Nicotiana benthamiana*. Plant Cell. 17:1268–1278

Li, T., Liu, B., Spalding, M. H., Weeks, D. P., and Yang, B. 2012. High-efficiency TALEN-based gene editing produces disease-resistant rice. Nat. Biotechnol. 30:390–392

Liu, J., Liu, D., Tao, W., Li, W., Wang, S., Chen, P., Cheng, S., and Gao, D. 2000. Molecular marker-facilitated pyramiding of different genes for powdery mildew resistance in wheat. Plant Breed. 119:21–24

Liu, W., Danilova, T. V., Rouse, M. N., Bowden, R. L., Friebe, B., Gill, B. S., and Pumphrey, M. O. 2013. Development and characterization of a compensating wheat-*Thinopyrum intermedium* Robertsonian translocation with *Sr44* resistance to stem rust (Ug99). Theor. Appl. Genet. 126:1167–1177

Lopez-Gomez, M., Sandal, N., Stougaard, J., and Boller, T. 2012. Interplay of flg22-induced defence responses and nodulation in Lotus japonicus. J. Exp. Bot. 63:393–401

Loutre, C., Wicker, T., Travella, S., Galli, P., Scofield, S., Fahima, T., Feuillet, C., and Keller, B. 2009. Two different CC-NBS-LRR genes are required for Lr10-mediated leaf rust resistance in tetraploid and hexaploid wheat. Plant J. 60:1043–1054

Luck, J. E., Lawrence, G. J., Dodds, P. N., Shepherd, K. W., and Ellis, J. G. 2000. Regions outside of the leucine-rich repeats of flax rust resistance proteins play a role in specificity determination. Plant Cell. 12:1367–1378

Luo, Y., Caldwell, K. S., Wroblewski, T., Wright, M. E., and Michelmore, R. W. 2009. Proteolysis of a negative regulator of innate immunity is dependent on resistance genes in tomato and *Nicotiana benthamiana* and induced by multiple bacterial effectors. Plant Cell. 21:2458 –2472

Ma, L., Lukasik, E., Gawehns, F., and Takken, F. L. W. 2012. The use of agroinfiltration for transient expression of plant resistance and fungal effector proteins in *Nicotiana benthamiana* leaves. Pages 61–74 in: Plant Fungal Pathogens, Methods in Molecular Biology. M.D. Bolton and B.P.H.J. Thomma, eds. Humana Press.

Mackey, D., Holt III, B. F., Wiig, A., and Dangl, J. L. 2002. RIN4 interacts with *Pseudomonas syringae* type III effector molecules and is required for RPM1-mediated resistance in *Arabidopsis*. Cell. 108:743–754

Maekawa, T., Cheng, W., Spiridon, L. N., Töller, A., Lukasik, E., Saijo, Y., Liu, P., Shen, Q.-H., Micluta, M. A., Somssich, I. E., Takken, F. L. W., Petrescu, A.-J., Chai, J., and Schulze-Lefert, P. 2011. Coiled-coil domain-dependent homodimerization of intracellular barley immune receptors defines a minimal functional module for triggering cell death. Cell Host Microbe. 9:187–199

Mahfouz, M. M., Li, L., Shamimuzzaman, M., Wibowo, A., Fang, X., and Zhu, J.-K. 2011. De novo-engineered transcription activator-like effector (TALE) hybrid nuclease with novel DNA binding specificity creates double-strand breaks. Proc. Natl. Acad. Sci. 108:2623–2628

Mali, P., Yang, L., Esvelt, K. M., Aach, J., Guell, M., DiCarlo, J. E., Norville, J. E., and Church, G. M. 2013. RNA-Guided Human Genome Engineering via Cas9. Science. 339:823–826

Manyangarirwa, W., Turnbull, M., McCutcheon, G. S., and Smith, J. P. 2006. Gene pyramiding as a Bt resistance management strategy: How sustainable is this strategy? Afr. J. Biotechnol. 5:781–785

Marone, D., Russo, M., Laidò, G., De Leonardis, A., and Mastrangelo, A. 2013. Plant nucleotide binding site–leucine-rich repeat (NBS-LRR) genes: active guardians in host defense responses. Int. J. Mol. Sci. 14:7302–7326

McDonald, B. A., and Linde, C. 2002. Pathogen population genetics, evolutionary potential, and durable resistance. Annu. Rev. Phytopathol. 40:349–379

McDowell, J. M., Dhandaydham, M., Long, T. A., Aarts, M. G. M., Goff, S., Holub, E. B., and Dangl, J. L. 1998. Intragenic recombination and diversifying selection contribute to the evolution of downy mildew resistance at the *RPP8* locus of Arabidopsis. Plant Cell. 10:1861–1874

McIntosh, R. A. 2013. A catalogue of gene symbols for wheat. Pages 1197–1255 in: Proc. XII Int. Wheat Genet. Symp., Yokohama, Japan,

McIntosh, R. A., Zhang, P., Cowger, C., Parks, R., Lagudah, E. S., and Hoxha, S. 2011. Rye-derived powdery mildew resistance gene *Pm8* in wheat is suppressed by the *Pm3* locus. Theor. Appl. Genet. 123:359–367

Mestre, P., and Baulcombe, D. C. 2006. Elicitor-mediated oligomerization of the tobacco N disease resistance protein. Plant Cell. 18:491–501

Meyers, B. C., Kozik, A., Griego, A., Kuang, H., and Michelmore, R. W. 2003. Genome-wide analysis of NBS-LRR–encoding genes in *Arabidopsis*. Plant Cell. 15:809–834

Meyers, B. C., Shen, K. A., Rohani, P., Gaut, B. S., and Michelmore, R. W. 1998. Receptor-like genes in the major resistance locus of lettuce are subject to divergent selection. Plant Cell. 10:1833–1846

Moffett, P., Farnham, G., Peart, J., and Baulcombe, D. C. 2002. Interaction between domains of a plant NBS-LRR protein in disease resistance-related cell death. EMBO J. 21:4511–4519

Mucyn, T. S., Clemente, A., Andriotis, V. M. E., Balmuth, A. L., Oldroyd, G. E. D., Staskawicz, B. J., and Rathjen, J. P. 2006. The tomato NBARC-LRR protein Prf interacts with Pto kinase in vivo to regulate specific plant immunity. Plant Cell. 18:2792–2806

Mundt, C. C. 2002. Use of multiline cultivars and cultivar mixtures for disease management. Annu. Rev. Phytopathol. 40:381–410

Nam, M., Koh, S., Kim, S. U., Domier, L. L., Jeon, J. H., Kim, H. G., Lee, S.-H., Bent, A. F., and Moon, J. S. 2011. *Arabidopsis TTR1* causes LRR-dependent lethal systemic necrosis, rather than systemic acquired resistance, to Tobacco ringspot virus. Mol. Cells. 32:421–429

Narusaka, M., Shirasu, K., Noutoshi, Y., Kubo, Y., Shiraishi, T., Iwabuchi, M., and Narusaka, Y. 2009. *RRS1* and *RPS4* provide a dual *Resistance*-gene system against fungal and bacterial pathogens. Plant J. 60:218–226

Nelson, J., Singh, R., Autrique, J., and Sorrells, M. 1997. Mapping genes conferring and suppressing leaf rust resistance in wheat. Crop Sci. 37:1928–1935

Oerke, E.-C. 2006. Crop losses to pests. J. Agric. Sci. 144:31–43

Oh, C.-S., and Martin, G. B. 2011. Effector-triggered immunity mediated by the Pto kinase. Trends Plant Sci. 16:132–140

Van Ooijen, G., Mayr, G., Albrecht, M., Cornelissen, B. J. C., and Takken, F. L. W. 2008a. Transcomplementation, but not physical association of the CC-NB-ARC and LRR

domains of tomato R protein Mi-1.2 is altered by mutations in the ARC2 subdomain. Mol. Plant. 1:401–410

Van Ooijen, G., Mayr, G., Kasiem, M. M. A., Albrecht, M., Cornelissen, B. J. C., and Takken, F. L. W. 2008b. Structure–function analysis of the NB-ARC domain of plant disease resistance proteins. J. Exp. Bot. 59:1383 –1397

Padmanabhan, M., Cournoyer, P., and Dinesh-Kumar, S. P. 2009. The leucine-rich repeat domain in plant innate immunity: a wealth of possibilities. Cell. Microbiol. 11:191–198

Pan, Q., Wendel, J., and Fluhr, R. 2000. Divergent evolution of plant NBS-LRR resistance gene homologues in dicot and cereal genomes. J. Mol. Evol. 50:203–213

Periyannan, S., Moore, J., Ayliffe, M., Bansal, U., Wang, X., Huang, L., Deal, K., Luo, M., Kong, X., Bariana, H., Mago, R., McIntosh, R., Dodds, P., Dvorak, J., and Lagudah, E. 2013. The gene *Sr33*, an ortholog of barley *Mla* genes, encodes resistance to wheat stem rust race Ug99. Science. 341:786–788

Qi, D., DeYoung, B. J., and Innes, R. W. 2012. Structure-function analysis of the coiled-coil and leucine-rich repeat domains of the RPS5 disease resistance protein. Plant Physiol. 158:1819–1832

Qi, D., and Innes, R. W. 2013. Recent advances in plant NLR structure, function, localization, and signaling. Front. Immunol. 4

R Core Team. 2013. *R: A language and environment for statistical computing*. R Foundation for Statistical Computing, Vienna, Austria.

Rafiqi, M., Bernoux, M., Ellis, J. G., and Dodds, P. N. 2009. In the trenches of plant pathogen recognition: Role of NB-LRR proteins. Semin. Cell Dev. Biol. 20:1017–1024

Rairdan, G. J., Collier, S. M., Sacco, M. A., Baldwin, T. T., Boettrich, T., and Moffett, P. 2008. The coiled-coil and nucleotide binding domains of the potato Rx disease resistance protein function in pathogen recognition and signaling. Plant Cell. 20:739–751

Rairdan, G. J., and Moffett, P. 2006. Distinct domains in the ARC region of the potato resistance protein Rx mediate LRR binding and inhibition of activation. Plant Cell. 18:2082–2093

Rietman, H., Bijsterbosch, G., Cano, L. M., Lee, H.-R., Vossen, J. H., Jacobsen, E., Visser, R. G. F., Kamoun, S., and Vleeshouwers, V. G. A. A. 2012. Qualitative and quantitative late blight resistance in the potato cultivar Sarpo Mira is determined by the perception of five distinct RXLR effectors. Mol. Plant. Microbe Interact. 25:910–919

Risk, J. M., Selter, L. L., Krattinger, S. G., Viccars, L. A., Richardson, T. M., Buesing, G., Herren, G., Lagudah, E. S., and Keller, B. 2012. Functional variability of the *Lr34* durable resistance gene in transgenic wheat. Plant Biotechnol. J. 10:477–487

Roush, R. T. 1998. Two–toxin strategies for management of insecticidal transgenic crops: can pyramiding succeed where pesticide mixtures have not? Philos. Trans. R. Soc. Lond. B. Biol. Sci. 353:1777–1786

Sacco, M. A., Mansoor, S., and Moffett, P. 2007. A RanGAP protein physically interacts with the NB-LRR protein Rx, and is required for Rx-mediated viral resistance. Plant J. 52:82–93

Sayle, R. A., and Milner-White, E. J. 1995. RASMOL: biomolecular graphics for all. Trends Biochem. Sci. 20:374–376

Schweizer, P., Pokorny, J., Abderhalden, O., and Dudler, R. 1999. A transient assay system for the functional assessment of defense-related genes in wheat. Mol. Plant. Microbe Interact. 12:647–654

Seeholzer, S., Tsuchimatsu, T., Jordan, T., Bieri, S., Pajonk, S., Yang, W., Jahoor, A., Shimizu, K. K., Keller, B., and Schulze-Lefert, P. 2010. Diversity at the *Mla* powdery mildew resistance locus from cultivated barley reveals sites of positive selection. Mol. Plant. Microbe Interact. 23:497–509

Segretin, M. E., Pais, M., Franceschetti, M., Chaparro-Garcia, A., Bos, J. I., Banfield, M. J., and Kamoun, S. 2014. Single amino acid mutations in the potato immune receptor R3a expand response to *Phytophthora* effectors. Mol. Plant. Microbe Interact. Posted online on 28 Mar 2014, First Look

Shen, Q.-H., Saijo, Y., Mauch, S., Biskup, C., Bieri, S., Keller, B., Seki, H., Ulker, B., Somssich, I. E., and Schulze-Lefert, P. 2007. Nuclear activity of MLA immune receptors links isolate-specific and basal disease-resistance responses. Science. 315:1098–1103

Shtienberg, D. 1992. Effects of foliar diseases on gas exchange processes: a comparative study. Phytopathology. 82

Sinapidou, E., Williams, K., Nott, L., Bahkt, S., Tör, M., Crute, I., Bittner-Eddy, P., and Beynon, J. 2004. Two TIR:NB:LRR genes are required to specify resistance to Peronospora parasitica isolate Cala2 in Arabidopsis. Plant J. 38:898–909

Singh, R. P., Hodson, D. P., Huerta-Espino, J., Jin, Y., Bhavani, S., Njau, P., Herrera-Foessel, S., Singh, P. K., Singh, S., and Govindan, V. 2011. The emergence of Ug99 races of the stem rust fungus is a threat to world wheat production. Annu. Rev. Phytopathol. 49:465–481

Slootweg, E. J., Spiridon, L. N., Roosien, J., Butterbach, P., Pomp, R., Westerhof, L., Wilbers, R., Bakker, E., Bakker, J., Petrescu, A.-J., Smant, G., and Goverse, A. 2013. Structural determinants at the interface of the ARC2 and leucine-rich repeat domains control the activation of the plant immune receptors Rx1 and Gpa2. Plant Physiol. 162:1510–1528

Srichumpa, P., Brunner, S., Keller, B., and Yahiaoui, N. 2005. Allelic series of four powdery mildew resistance genes at the *Pm3* locus in hexaploid bread wheat. Plant Physiol. 139:885–895

Steinbrenner, A. D., Goritschnig, S., Krasileva, K. V., Schreiber, K. J., and Staskawicz, B. J. 2012. Effector recognition and activation of the *Arabidopsis thaliana* NLR innate immune receptors. Cold Spring Harb. Symp. Quant. Biol. 77:249–257

Stirnweis, D., Milani, S. D., Jordan, T., Keller, B., and Brunner, S. 2014. Substitutions of two amino acids in the nucleotide-binding site domain of a resistance protein enhance the hypersensitive response and enlarge the PM3F resistance spectrum in wheat. Mol. Plant. Microbe Interact. 27:265–276

Strange, R. N., and Scott, P. R. 2005. Plant disease: A threat to global food security. Annu. Rev. Phytopathol. 43:83–116

Stukenbrock, E. H., and McDonald, B. A. 2008. The origins of plant pathogens in agro-ecosystems. Annu. Rev. Phytopathol. 46:75–100

Swiderski, M. R., Birker, D., and Jones, J. D. G. 2009. The TIR domain of TIR-NB-LRR resistance proteins is a signaling domain involved in cell death induction. Mol. Plant. Microbe Interact. 22:157–165

Takken, F. L., Albrecht, M., and Tameling, W. I. 2006. Resistance proteins: molecular switches of plant defence. Curr. Opin. Plant Biol. 9:383–390

Takken, F. L., and Goverse, A. 2012. How to build a pathogen detector: structural basis of NB-LRR function. Curr. Opin. Plant Biol. 15:375–384

Tameling, W. I. L., and Baulcombe, D. C. 2007. Physical association of the NB-LRR resistance protein Rx with a Ran GTPase–activating protein is required for extreme resistance to *Potato virus X*. Plant Cell. 19:1682–1694

Tameling, W. I. L., Elzinga, S. D. J., Darmin, P. S., Vossen, J. H., Takken, F. L. W., Haring, M. A., and Cornelissen, B. J. C. 2002. The tomato *R* gene products I-2 and Mi-1 are functional ATP binding proteins with ATPase activity. Plant Cell. 14:2929–2939

Tameling, W. I. L., Nooijen, C., Ludwig, N., Boter, M., Slootweg, E., Goverse, A., Shirasu, K., and Joosten, M. H. A. J. 2010. RanGAP2 mediates nucleocytoplasmic partitioning of the NB-LRR immune receptor Rx in the Solanaceae, thereby dictating Rx function. Plant Cell. 22:4176 –4194

Tameling, W. I. L., Vossen, J. H., Albrecht, M., Lengauer, T., Berden, J. A., Haring, M. A., Cornelissen, B. J. C., and Takken, F. L. W. 2006. Mutations in the NB-ARC domain of I-2 that impair ATP hydrolysis cause autoactivation. Plant Physiol. 140:1233–1245

Tang, X., Frederick, R. D., Zhou, J., Halterman, D. A., Jia, Y., and Martin, G. B. 1996. Initiation of plant disease resistance by physical interaction of AvrPto and Pto kinase. Science. 274:2060–2063

Tao, Y., Yuan, F., Leister, R. T., Ausubel, F. M., and Katagiri, F. 2000. Mutational analysis of the Arabidopsis nucleotide binding site–leucine-rich repeat resistance gene *RPS2*. Plant Cell. 12:2541–2554

Thomma, B. P. H. J., Nürnberger, T., and Joosten, M. H. A. J. 2011. Of PAMPs and effectors: The blurred PTI-ETI dichotomy. Plant Cell. 23:4–15

Tian, D., Traw, M. B., Chen, J. Q., Kreitman, M., and Bergelson, J. 2003. Fitness costs of R-gene-mediated resistance in *Arabidopsis thaliana*. Nature. 423:74–77

Todesco, M., Balasubramanian, S., Hu, T. T., Traw, M. B., Horton, M., Epple, P., Kuhns, C., Sureshkumar, S., Schwartz, C., Lanz, C., Laitinen, R. A. E., Huang, Y., Chory, J., Lipka, V., Borevitz, J. O., Dangl, J. L., Bergelson, J., Nordborg, M., and Weigel, D. 2010. Natural allelic variation underlying a major fitness trade-off in *Arabidopsis thaliana*. Nature. 465:632–636

Tomita, R., Sekine, K.-T., Mizumoto, H., Sakamoto, M., Murai, J., Kiba, A., Hikichi, Y., Suzuki, K., and Kobayashi, K. 2011. Genetic basis for the hierarchical interaction between *Tobamovirus* spp. and *L* resistance gene alleles from different pepper species. Mol. Plant. Microbe Interact. 24:108–117

Tommasini, L., Yahiaoui, N., Srichumpa, P., and Keller, B. 2006. Development of functional markers specific for seven *Pm3* resistance alleles and their validation in the bread wheat gene pool. Theor. Appl. Genet. 114:165–175

Tornero, P., Chao, R. A., Luthin, W. N., Goff, S. A., and Dangl, J. L. 2002. Large-scale structure-function analysis of the *Arabidopsis* RPM1 disease resistance protein. Plant Cell. 14:435–450

Travella, S., Klimm, T. E., and Keller, B. 2006. RNA interference-based gene silencing as an efficient tool for functional genomics in hexaploid bread wheat. Plant Physiol. 142:6–20

Ueda, H., Yamaguchi, Y., and Sano, H. 2006. Direct interaction between the tobacco mosaic virus helicase domain and the ATP-bound resistance protein, N factor during the hypersensitive response in tobacco plants. Plant Mol. Biol. 61:31–45

Voinnet, O., Rivas, S., Mestre, P., and Baulcombe, D. 2003. An enhanced transient expression system in plants based on suppression of gene silencing by the p19 protein of tomato bushy stunt virus. Plant J. 33:949–956

Weaver, M., Swiderski, M. R., Li, Y., and Jones, J. D. G. 2006. The *Arabidopsis thaliana* TIR-NB-LRR R-protein, RPP1A; protein localization and constitutive activation of defence by truncated alleles in tobacco and Arabidopsis. Plant J. 47:829–840

Weiberg, A., Wang, M., Lin, F.-M., Zhao, H., Zhang, Z., Kaloshian, I., Huang, H.-D., and Jin, H. 2013. Fungal small RNAs suppress plant immunity by hijacking host RNA interference pathways. Science. 342:118–123

Wicker, T., Yahiaoui, N., and Keller, B. 2007a. Contrasting rates of evolution in *Pm3* loci from three wheat species and rice. Genetics. 177:1207–1216

Wicker, T., Yahiaoui, N., and Keller, B. 2007b. Illegitimate recombination is a major evolutionary mechanism for initiating size variation in plant resistance genes. Plant J. 51:631–641

Williams, S. J., Sornaraj, P., deCourcy-Ireland, E., Menz, R. I., Kobe, B., Ellis, J. G., Dodds, P. N., and Anderson, P. A. 2011. An autoactive mutant of the M flax rust resistance protein has a preference for binding ATP, whereas wild-type M protein binds ADP. Mol. Plant. Microbe Interact. 24:897–906

Wilson, W. A., and McMullen, M. S. 1997. Dosage dependent genetic suppression of oat crown rust resistance gene *Pc-62*. Crop Sci. 37:1699

Wright, M., Dawson, J., Dunder, E., Suttie, J., Reed, J., Kramer, C., Chang, Y., Novitzky, R., Wang, H., and Artim-Moore, L. 2001. Efficient biolistic transformation of maize (*Zea mays* L.) and wheat (*Triticum aestivum* L.) using the phosphomannose isomerase gene, *pmi*, as the selectable marker. Plant Cell Rep. 20:429–436

Wulff, B. B., Horvath, D. M., and Ward, E. R. 2011. Improving immunity in crops: new tactics in an old game. Curr. Opin. Plant Biol. 14:468–476

Yahiaoui, N., Brunner, S., and Keller, B. 2006. Rapid generation of new powdery mildew resistance genes after wheat domestication. Plant J. 47:85–98

Yahiaoui, N., Kaur, N., and Keller, B. 2009. Independent evolution of functional *Pm3* resistance genes in wild tetraploid wheat and domesticated bread wheat. Plant J. 57:846–856

Yahiaoui, N., Srichumpa, P., Dudler, R., and Keller, B. 2004. Genome analysis at different ploidy levels allows cloning of the powdery mildew resistance gene *Pm3b* from hexaploid wheat. Plant J. 37:528–538

Zeller, F. J., Lutz, J., and Stephan, U. 1993. Chromosome location of genes for resistance to powdery mildew in common wheat (*Triticum aestivum* L.) 1. *Mlk* and other alleles at the *Pm3* locus. Euphytica. 68:223–229

Zhang, Z., Henderson, C., Perfect, E., Carver, T. L. W., Thomas, B. J., Skamnioti, P., and Gurr, S. J. 2005. Of genes and genomes, needles and haystacks: *Blumeria graminis* and functionality. Mol. Plant Pathol. 6:561–575

Zhou, T., Wang, Y., Chen, J.-Q., Araki, H., Jing, Z., Jiang, K., Shen, J., and Tian, D. 2004. Genome-wide identification of NBS genes in *japonica* rice reveals significant expansion of divergent non-TIR NBS-LRR genes. Mol. Genet. Genomics. 271:402–415

Zhu, S., Li, Y., Vossen, J. H., Visser, R. G. F., and Jacobsen, E. 2012. Functional stacking of three resistance genes against *Phytophthora infestans* in potato. Transgenic Res. 21:89–99

Zhu, Z., Xu, F., Zhang, Y., Cheng, Y. T., Wiermer, M., Li, X., and Zhang, Y. 2010. Arabidopsis resistance protein SNC1 activates immune responses through association with a transcriptional corepressor. Proc. Natl. Acad. Sci. 107:13960–13965

6 Acknowledgements

I would like to thank …

… Beat Keller for giving me the opportunity to work on this interesting research, for providing an excellently equipped working environment, for the freedom to adapt my research according to my own interest, for the opportunity to visit conferences like the MPMI meeting, and for keeping his door open.

… Christoph Ringli and Prof. Gruissem for being part of my PhD committee.

… Susanne Brunner and Tina Jordan for their guidance and mentoring, their ideas, their excellently documented groundwork, their patience during project discussions, their open mindedness and critical questions, their effort beyond the regular working hours, their recognition for my work, and the fun in the lab.

… my master student Samira Milani for her outstanding effort and hard work that she invested in the projects, for the recognition of my teaching, and for her friendly character.

… Severine Hurni for being such a nice and very cooperative labmate for so many years, for sharing her knowledge, plants and cakes with me, and for not always taking me too serious.

… Gabi Buchmann und Geri Herren for running the lab so smoothly, for their excellent technical support, for teaching me wheat transformation, for the opportunity to rely on their qRT-PCR and first aid skills and for their support in general.

… Bea Senger (and her headband magnifier) for showing me how to cross and for all her effort to keep tons of my plants happy in the greenhouse.

… David Peditto for his effort in the projects and a box full of bloting membranes.

… my master student Michela Ruinelli for a fun time in the lab, for her patience on a difficult, not so promising project, and for teaching me about the real value of some roots.

… Roi Ben David for many interesting scientific discussions and the enthusiasm, drive and sounds that he brought to the lab.

… Luzia Guyer for discussions on protein expression.

… Edith Schlagenhauf for the weekly sequencing, Christian Frey for gardening and Agnesza Lleshaj for lab support.

… all current and former lab members for sharing their knowledge and skills with me, for joyful, frustrating and exciting moments in the lab, and for becoming friends.

… my friends and family for their everyday support. Thank you Lisa!